SAMANDA LÓPEZ PEÑA

GENOME-EDITING FOR GLUFOSINATE TOLERANCE IN MICRO-TOM TOMATO (*Solanum lycopersicum*)

LAVRAS – MG
2025

SAMANDA LÓPEZ PEÑA

CHARACTERIZATION AND GENOME-EDITING FOR GLUFOSINATE TOLERANCE IN MICRO-TOM TOMATO (*Solanum lycopersicum*)

Thesis submitted to the Federal University of Lavras, in partial fulfillment of the requirements of the Graduate Program in Plant Biotechnology, concentration in Plant Biotechnology, for the award of the doctoral degree.

Advisor
Prof. DSc. Luciano Vilela Paiva

Co-Advisor
DSc. Renan Terassi Pinto

LAVRAS – MG
2025

Ficha Catalográfica elaborada pelo Sistema de Geração de Ficha Catalográfica da Biblioteca Universitária da UFLA, com dados informados pelo(a) próprio(a) autor(a).

Peña, Samanda López.
Genome-editing for glufosinate tolerance in micro-tom tomato (Solanum lycopersicum) / Samanda López Peña. - 2025.
131 p.

Orientador: Luciano Vilela Paiva
Coorientador: Renan Terassi Pinto

Tese (Doutorado) - Universidade Federal de Lavras, 2025.
Bibliografia.

1. Genetic editing of Solanum lycopersicum. 2. CRISPR-Cas9. 3. Ammonium glufosinate resistance. 4. Characterization of the SPL and ARF gene families in tomato. 5. Protein–DNA interaction modeling via AlphaFold3. I. Vilela Paiva, Luciano . II. Terassi Pinto, Renan . III. Universidade Federal de Lavras. IV. Título.

SAMANDA LÓPEZ PEÑA

GENOME-EDITING FOR GLUFOSINATE TOLERANCE IN MICRO-TOM TOMATO (*Solanum lycopersicum*)

Thesis submitted to the Federal University of Lavras, in partial fulfillment of the requirements of the Graduate Program in Plant Biotechnology, concentration in Plant Biotechnology, for the award of the doctoral degree.

APPROVED on December 10, 2025.

DSc. Luciano Vilela Paiva	UFLA
DSc. Welison Andrade Pereira	UFLA
DSc. Sebastião Marcio de Azevedo	UFLA
DSc. Evandro Novaes	UFLA
DSc. Pedro Augusto Braga	UFV

gov.br Documento assinado digitalmente
LUCIANO VILELA PAIVA
Data: 24/02/2026 15:45:02-0300
Verifique em https://validar.iti.gov.br

Advisor
Prof. DSc. Luciano Vilela Paiva

Co-Advisor
DSc. Renan Terassi Pinto

LAVRAS – MG
2025

ACKNOWLEDGMENTS

I wish to express my deepest gratitude, first and foremost, to my parents and brother, who have been the fundamental pillar of my life. Throughout this journey, their unwavering faith in my abilities and their constant support have guided my every step, encouraging me especially in moments of greatest challenge and vulnerability. The values they instilled in me—marked by integrity, commitment, and a strong sense of responsibility—allowed me to cultivate the courage and perseverance needed to face and overcome the adversities inherent to academic and personal life. Their example and dedication have been the quiet driving force that pushed me to give my best day after day, not only to achieve my own dreams, but also to give back to them, even if only in part, for the sacrifice and love with which they made it possible for me to go as far as I had hoped.

I also extend my special appreciation to the Coordenação de Aperfeiçoamento de Pessoal de Nível Superior (CAPES), whose financial support was essential for the continuity of my academic training, as well as to the Universidade Federal de Lavras, a place where I was able to consolidate my scientific knowledge and develop my professional vocation around research.

My gratitude is directed, in a very special way, to Professor Luciano, my advisor, who not only taught me the principles of scientific rigor but also played a key role in strengthening my character as a researcher. His guidance and teachings continually encouraged me to explore my capacity for analysis, problem-solving, and creativity—skills that were essential for the development and completion of this work, as well as for my personal and professional growth.

I am likewise deeply grateful to Dr. Renan Pinto for his constant support throughout my training period. His guidance and accompaniment were decisive not only in the academic sphere, but also on a human level; his encouragement in difficult moments served as a fundamental guide and support in my decision-making and in overcoming the challenges I faced.

I cannot fail to mention the affection and support of the LCBM group, with whom I shared long days of work, learning, and sincere friendships. This team, which in many moments became a family, was characterized by camaraderie, solidarity, and a genuine concern for the well-being and progress of all its members. They remain in my memory as a reminder that success is never achieved in isolation, but is always sustained by the hands and hearts of those who wish to see us grow.

I am deeply grateful to Nathalia Lima Reskalla, Paola Fajardo, Viviana Ramirez Ríos, and Robert Delgado, who offered me a home and a refuge where I could always find words of

encouragement and emotional support. Their confidence in my abilities and their constant companionship were essential in helping me not lose sight of the strength I often thought I had lost.

Finally, I express my sincere appreciation to all the people who, directly or indirectly, contributed to the completion of this work. To each and every one of you, my eternal gratitude.

RESUMO

Este estudo desenvolveu uma estratégia abrangente para enfrentar essa limitação por meio de edição genômica precisa, fundamentada em três componentes complementares: caracterização experimental da sensibilidade de *Micro-Tom* ao glufosinato, identificação bioinformática de genes candidatos à edição e validação experimental da transformação genética.No primeiro capítulo, a sensibilidade de *Micro-Tom* a aplicações foliares de glufosinato foi caracterizada sistematicamente em condições controladas de casa de vegetação. As plantas foram expostas a cinco concentrações do herbicida (0, 0,5, 1,0, 2,0 e 3,0 $g \cdot L^{-1}$) e foram avaliadas respostas fenotípicas (sintomas visuais) e fisiológicas (atividade de catalase). Os resultados revelaram uma clara relação dose–resposta, na qual mesmo a dose mais baixa (25% da dose recomendada) levou à mortalidade completa em dez dias, indicando ausência de margem segura de tolerância. A atividade de catalase exibiu um padrão bifásico (indução inicial de 52% seguida de esgotamento), ressaltando a insuficiência dos mecanismos de defesa endógenos do cultivar.
No segundo capítulo, análises bioinformáticas integradas (BLASTP recíproco, inferência filogenética e modelagem estrutural com AlphaFold3) identificaram sete candidatos ortólogos em tomate dos genes de arroz *OsARF18* e *OsSPL10*, que atuam como repressores transcricionais dos genes de glutamina sintetase (*GS1* e *GS2*), modulando assim a resistência ao glufosinato. A avaliação multifatorial classificou *Solyc11g069500* (ortólogo de *OsARF18*) e *Solyc10g018780* (ortólogo de *OsSPL10*) como os alvos de edição mais promissores, apresentando arquitetura gênica conservada, um conjunto completo de domínios funcionais essenciais e padrões densos de sítios de ligação nos promotores.No terceiro capítulo, a transformação genética foi validada experimentalmente via *Agrobacterium tumefaciens*, alcançando uma eficiência de transformação de 13,3% com vetores CRISPR–Cas9 montados por Golden Gate (60% de eficiência de clonagem), e o protocolo de regeneração foi otimizado mediante substituição da citocinina, resultando na regeneração bem-sucedida de aproximadamente 20 explantes.Coletivamente, esses achados posicionam *Solyc11g069500* e *Solyc10g018780* como candidatos viáveis para estratégias futuras de edição genômica destinadas a conferir resistência ao glufosinato no tomate, contornando as limitações dos enfoques transgênicos convencionais e contribuindo de forma relevante para a segurança alimentar global e a agricultura sustentável.

Palavras-chave: Glutamina sintetase; tolerância a herbicidas; bioinformática; transformação genética.

ABSTRACT

This study developed a comprehensive strategy to address this limitation through precise genome editing, grounded in three complementary components: experimental characterization of Micro-Tom sensitivity to glufosinate, bioinformatic identification of candidate genes for editing, and experimental validation of genetic transformation. In the first chapter, Micro-Tom sensitivity to foliar glufosinate applications was systematically characterized under controlled greenhouse conditions. Plants were exposed to five herbicide concentrations (0, 0.5, 1.0, 2.0, and 3.0 g L^{-1}), and phenotypic (visual symptoms) and physiological (catalase activity) responses were evaluated. Results revealed a pronounced dose–response relationship, in which even the lowest dose (25% of the recommended rate) led to complete mortality by ten days, indicating the absence of any safety margin of tolerance. Catalase activity displayed a biphasic pattern (an initial 52% induction followed by depletion), highlighting the insufficiency of the cultivar's endogenous defense mechanisms. In the second chapter, integrated bioinformatic analyses (reciprocal BLASTP, phylogenetic analyses, and structural modeling with AlphaFold 3) identified seven tomato ortholog candidates of rice genes (OsARF18 and OsSPL10) that act as transcriptional repressors of glutamine synthetase genes (GS1 and GS2), thereby modulating glufosinate resistance. Multifactorial evaluation ranked Solyc11g069500 (OsARF18 ortholog) and Solyc10g018780 (OsSPL10 ortholog) as the most promising editing targets, exhibiting conserved gene architecture, a full complement of essential functional domains, and dense patterns of promoter binding sites. In the third chapter, genetic transformation was experimentally validated via *Agrobacterium tumefaciens*, achieving a transformation efficiency of 13.3% with Golden Gate–assembled CRISPR–Cas9 vectors (60% cloning efficiency) and optimizing the regeneration protocol through cytokinin replacement, yielding successful regeneration of approximately 20 explants. Collectively, these findings position Solyc11g069500 and Solyc10g018780 as viable genes for future genome-editing strategies aimed at conferring glufosinate resistance in tomato, circumventing the limitations of conventional transgenic approaches and contributing meaningfully to global food security and sustainable agriculture.

Keywords: Glutamine synthetase; herbicide tolerance; bioinformatics; genetic transformation.

IMPACT INDICATORS

Este trabalho representa uma contribuição importante para o conhecimento científico e tecnológico sobre a interação entre o tomate e o glufosinato, ao fornecer uma caracterização exaustiva e inédita da sensibilidade fenotípica e fisiológica do cultivar Micro-Tom a diferentes doses deste herbicida, demonstrando a ausência de uma margem segura de tolerância sob exposição foliar, mesmo nas doses mais baixas — um achado crucial para o manejo agronômico e para prevenir danos decorrentes da deriva de pulverização ou manuseio involuntário em sistemas de produção comerciais. O estudo estabelece referências quantitativas para o início dos sintomas de fitotoxicidade e para a cinética da resposta antioxidante, fornecendo uma base sólida para o desenho racional de protocolos de aplicação e manejo seguro do glufosinato no tomate.Além disso, a abordagem bioinformática possibilitou a primeira identificação e caracterização em tomate dos ortólogos dos genes de arroz *OsARF18* e *OsSPL10*, representando um avanço relevante na transferência de conhecimento interespecífico e na ampliação do repertório genético útil para engenharia de tolerância a herbicidas, posicionando *Solyc11g069500* e *Solyc10g018780* como alvos prioritários para edição genômica de precisão. Ademais, a validação experimental bem-sucedida da transformação genética mediada por *Agrobacterium tumefaciens* utilizando vetores CRISPR-Cas9, juntamente com a otimização do protocolo de regeneração de plantas, estabelece bases metodológicas reproduzíveis para o desenvolvimento de variedades de tomate tolerantes ao glufosinato, marcando um marco inovador no melhoramento biotecnológico. Consequentemente, este trabalho impacta diretamente a segurança alimentar e a sustentabilidade agrícola ao propor soluções tecnologicamente viáveis para ampliar opções de controle efetivo de plantas daninhas em culturas solanáceas, reduzir a dependência de práticas manuais ou mecânicas e fortalecer a resiliência dos sistemas produtivos frente ao surgimento de plantas daninhas resistentes. Por fim, a estratégia multidisciplinar adotada acelera a incorporação de tecnologias de edição genética em programas de melhoramento, promove a convergência entre pesquisa básica e aplicações práticas, e contribui para posicionar a biotecnologia como um pilar da agricultura moderna, servindo também como modelo replicável para o estudo e aprimoramento de outras culturas de relevância global.

INDICADORES DE IMPACTO

This work represents an important contribution to scientific and technological knowledge on the interaction between tomato and glufosinate, as it provides an exhaustive and unprecedented characterization of the phenotypic and physiological sensitivity of the Micro-Tom cultivar to different doses of this herbicide, demonstrating the absence of a safe tolerance margin under foliar exposure even at the lowest doses—a key finding for agronomic management and for preventing damage resulting from spray drift or unintentional handling in commercial production systems. The study establishes quantitative references for the onset of phytotoxicity symptoms and for antioxidant-response kinetics, providing a solid basis for the rational design of application protocols and the safe management of glufosinate in tomato. In addition, the bioinformatic approach enabled the first identification and characterization in tomato of orthologs of the rice genes OsARF18 and OsSPL10, representing a relevant advance in interspecific knowledge transfer and in expanding the genetic repertoire useful for engineering herbicide tolerance, positioning Solyc11g069500 and Solyc10g018780 as priority targets for precision genome editing. Furthermore, the successful experimental validation of *Agrobacterium tumefaciens*-mediated genetic transformation using CRISPR-Cas9 vectors and the optimization of the plant-regeneration protocol lay reproducible methodological foundations for developing glufosinate-tolerant tomato varieties, marking an innovative milestone in biotechnological breeding. Consequently, this work directly impacts food security and agricultural sustainability by proposing technologically viable solutions to broaden options for effective weed control in solanaceous crops, reduce reliance on manual or mechanical practices, and strengthen the resilience of production systems against the emergence of resistant weeds. Finally, the multidisciplinary strategy adopted accelerates the incorporation of gene-editing technologies into breeding programs, promotes convergence between basic research and practical applications, and helps position biotechnology as a pillar of modern agriculture and as a replicable model for the study and improvement of other globally relevant crops.

LIST OF ILLUSTRATIONS

SUMMARY

LIST OF ABBREVIATIONS

ARF - Auxin Response Factors

BSA - Bovine Serum Albumin

CRD – Completely randomized design

DAA - Days after application

GS – Glutamine synthetase

HAA - Hours after application

ROS - Reactive Oxygen Species

SPL - SQUAMOSA Promoter-Binding Protein-Like factors

PAT – Phosphinothricin Acetyl Transferase

NADPH - Nicotinamide Adenine Dinucleotide Phosphate

EDTA - Ethylenediaminetetraacetic acid

FIRST PART

1 INTRODUCTION

Tomato (*Solanum lycopersicum L.*) represents one of the most economically and nutritionally significant vegetables worldwide, establishing itself as a strategic crop for global food security. In 2024, the global tomato market was valued at approximately USD 181.21 billion, with projections reaching USD 316.98 billion by 2033, reflecting a compound annual growth rate (CAGR) of 6.41% (Market Data Forecast, 2025). Beyond its commercial importance, tomato constitutes an essential source of nutritional and bioactive compounds crucial for human health, including vitamins, minerals, fiber, and carotenoids (Rellini et al., 2024). Among these compounds, lycopene—the main carotenoid present in tomato fruits—has been widely documented in scientific literature for its antioxidant properties, exhibiting a singlet oxygen-quenching capacity twice that of β-carotene and ten times higher than that of α-tocopherol (Gerenu & Cela, 2024). Lycopene has been associated with the prevention of chronic-degenerative diseases such as cancer, cardiovascular dysfunction, and cognitive decline, thus reinforcing the importance of tomato in preventive health diets.

Despite the relevance of tomato in agricultural production, crop productivity is severely constrained by agroecological factors, with weed interference being one of the most critical determinants. Weeds represent biotic stress factors that substantially limit agricultural yields worldwide, causing considerable economic losses (Sondhia & Mishra, 2024). They compete aggressively with tomato plants for essential resources—water, nutrients, light, and space—leading to yield reductions that vary according to the weed species, infestation density, and the crop's phenological stage (de Oliveira et al., 2023). In the absence of control strategies, potential tomato yields can be reduced by 30% to 60% of their maximum productivity, leading to significant economic losses that compromise the viability of commercial production systems. The severity of weed competition is particularly critical during early vegetative growth, requiring the implementation of robust and efficient integrated weed management protocols.

To mitigate the negative impact of weed competition, glufosinate ammonium—a non-selective, broad-spectrum herbicide—has become increasingly relevant in integrated weed management systems. This herbicide acts by specifically inhibiting the enzyme glutamine synthetase (GS), a key catalytic enzyme mediating the assimilation of inorganic ammonium in plant nitrogen metabolism (Takano et al., 2024). Inhibition of GS results in the accumulation of phytotoxic ammonium in plant tissues, causing membrane integrity loss, photosynthesis

cessation, and eventual plant death. The herbicidal spectrum of glufosinate is particularly effective against annual broadleaf and grass weeds that have developed resistance to other herbicides, including species such as Amaranthus, Lolium, Conyza, and Malva, making it a strategic tool in contexts of multiple herbicide resistance (Takano et al., 2024). However, there remains a pronounced gap in scientific knowledge specifically characterizing tomato sensitivity to glufosinate. A comprehensive review of existing literature reveals a significant asymmetry: whereas the phytotoxicity of other herbicides—particularly glyphosate and auxinic compounds—has been widely documented in tomato, information regarding the physiological response of tomato to glufosinate remains extremely limited. Available studies show major methodological limitations, as they have primarily focused on directed applications avoiding direct foliar contact, without assessing the inherent sensitivity of the crop to unintentional or accidental exposure (de Oliveira et al., 2023). Previous research has shown that tomato is highly sensitive to herbicides in general, being subject to severe damage from sublethal doses of glyphosate and auxinic herbicides, which may cause symptoms such as necrosis of meristematic tissues, leaf distortion, and fruit deformation (College of Agricultural and Life Sciences [CALS], 2024). This inherent sensitivity highlights the urgency of defining specific tolerance thresholds for glufosinate in tomato, a crucial step toward optimizing weed control strategies while minimizing the risk of damage from accidental drift.

In the context of plant biotechnology, CRISPR-Cas9 technology has catalyzed a revolution in modern plant breeding, enabling genomic modifications with high precision, efficiency, and gene specificity. Unlike conventional breeding protocols that require decades to introgress desirable traits, CRISPR-Cas9-mediated genome editing enables equivalent modifications in significantly shorter timeframes, typically within a few years. Plants edited via CRISPR-Cas9, particularly those carrying small nucleotide deletions or point mutations without permanent integration of foreign genomic sequences, are regulated as non-transgenic in multiple jurisdictions, since these modifications result from endogenous alteration of existing host genome sequences (Office of the Gene Technology Regulator [OGTR], 2025). This categorization offers a significantly more favorable regulatory framework compared to conventional transgenic crops, broadening the prospects for public and commercial acceptance in developed markets.

Recent studies have identified candidate genes in rice (*Oryza sativa*) that confer glufosinate resistance through molecular mechanisms conserved across plant species. Specifically, the functional loss of OsARF18—encoding an auxin response factor—represses the expression of glutamine synthetase genes (OsGS1;1 and OsGS1;2), increasing GS activity

and conferring resistance to glufosinate concentrations up to 10 g L^{-1}, while simultaneously enhancing tolerance to salt and drought stress (Xia et al., 2023). Similarly, the functional loss of OsSPL10—encoding a SQUAMOSA promoter-binding-like (SPL) transcription factor—acts as a negative regulator of glufosinate resistance via transcriptional repression of OsGS genes, conferring tolerance to herbicide concentrations up to 10 g L^{-1} and increasing tolerance to multiple abiotic stresses (Xia et al., 2023). The identification of functional orthologs of these genes in tomato enables the rational design of targeted gene-editing strategies to generate tomato germplasm with glufosinate-conferred resistance, representing an innovative strategy that transcends the limitations of traditional transgenic approaches based on the introduction of foreign bacterial genes.

Consequently, the present study developed an integrated research strategy encompassing three complementary components: (1) a systematic characterization of the sensitivity of the Micro-Tom cultivar—a model plant widely used in functional genomics due to its dwarf phenotype, short life cycle, and ease of genetic transformation—to foliar-applied glufosinate under controlled greenhouse conditions, evaluating both visual and physiological phenotypic responses using biochemical markers; (2) bioinformatic identification of tomato candidate genes modulating glufosinate resistance through integrated phylogenetic analysis, structural modeling using AlphaFold 3, and multifactorial evaluation of functional conservation with rice orthologs; and (3) experimental validation of genetic transformation using Agrobacterium tumefaciens and CRISPR-Cas9 vectors. This multidimensional approach seeks to bridge the current knowledge gap in tomato–glufosinate interaction, providing a rigorous scientific foundation that contributes both to the refinement of safe agronomic practices and to the rational development of tolerant varieties through precision plant biotechnology within the contemporary framework of sustainable agriculture, where efficient integration of weed control tools constitutes an essential strategy to maximize productivity while minimizing environmental impact.

REFERENCES

AUSTRALIAN OFFICE OF THE GENE TECHNOLOGY REGULATOR (OGTR). (2025). **Status of gene editing and other new technologies**. *Department of Climate Change, Energy, Environment and Water.* https://www.ogtr.gov.au/sites/default/files/2025-02/status_of_gene_editing_and_other_new_technologies_feb_2025.pdf

COLLEGE OF AGRICULTURAL AND LIFE SCIENCES (CALS). (2024). **Herbicide damage in tomatoes.** *University of Florida Extension Publications*. Southwest Florida Research and Education Center.

DE OLIVEIRA, C., MACHADO, B. B., RIBEIRO, R. V., & MARQUES JUNIOR, J. (2023). **Weed interference and herbicide selectivity in horticultural crops**. *Pest Management Science,* 79(12), 4823–4835. https://doi.org/10.1002/ps.7565

DE OLIVEIRA, T. R., SERAFIM, A. D., BRELAND, B., MILLER, A., BENETON, K., SINGH, V., ... & TSENG, T. M. (2023). **An integrated weed management approach in tomato using soil steaming, mulching, and winter cover crops**. *Frontiers in Agronomy*, 5, 1075726. https://doi.org/10.3389/fagro.2023.1075726

GERENU, A., & CELA, V. (2024). **Lycopene: A potent antioxidant with multiple health benefits**. *Nutrients*, 13(6), 1516–1532. https://doi.org/10.3390/nu13061516

KUMAR, S., SHARMA, N., SAINI, P., GAUTAM, A., SINGH, B., & KAUR, J. (2024). **Weed management challenges in modern agriculture**. *Science of The Total Environment*, 910, 168501. https://doi.org/10.1016/j.scitotenv.2024.168501

MARKET DATA FORECAST. (2025). **Tomato market size, share, trends & growth report, 2033**. *Market Data Forecast.* https://www.marketdataforecast.com/market-reports/tomato-market

RELLINI, P., MARCHETTI, S., ROSSI, G., & CASADIO, R. (2024). **Nutritional and bioactive compounds in tomato fruits.** *Journal of Agricultural and Food Chemistry*, 72(15), 8234–8251. https://doi.org/10.1021/acs.jafc.3c08401

STRAITS RESEARCH. (2025). **Tomato market size, share, and forecast by 2033**. Retrieved from https://www.straitsresearch.com/

SONDHIA, S., & MISHRA, S. (2024**). Crop-weed competition and herbicide bioefficacy**. *Indian Journal of Weed Science*, 56(4), 391–403.

TAKANO, H. K., WESTRA, P., PRESTON, C., BEFFA, R., & DAYAN, F. E. (2024**). The mechanism of action of glufosinate: Understanding rapid injury responses in plants.** *Pest Management Science*, 80(2), 524–535. https://doi.org/10.1002/ps.7651

TAKANO, H. Y., BRAZ, G. B. P., PALMA-TENAGO, M., DAYAN, F. E., & MATALLO, M. B. (2024). **Mechanisms of glufosinate herbicide resistance and control strategies for resistant weeds.** *Pesticide Biochemistry and Physiology*, 195, 105–118. https://doi.org/10.1016/j.pestbp.2024.105835

WORLD PROCESSING TOMATO COUNCIL (WPTC). (2024). **2024 post season global tomato crop update**. *Morning Star Company.* https://www.morningstarco.com/2024-post-season-global-tomato-crop-update/

XIA, J. Q., ET AL. (2023). **Knockout of OsSPL10 confers enhanced glufosinate ammonium herbicide tolerance and abiotic stress resistance in rice.** *Plant Biotechnology Journal,* 21(5), 987–1005. https://doi.org/10.1111/pbi.14006

SECOND PART - CHAPTERS

CHAPTER 1 - CHARACTERIZATION OF GLUFOSINATE SENSITIVITY IN *Solanum lycopersicum* CV. MICRO-TOM

ABSTRACT

Tomato (*Solanum lycopersicum* L.) is a strategic horticultural crop whose productivity is constrained by weed interference, necessitating herbicides as a key tool within integrated pest management programs. Glufosinate-ammonium is a non-selective, broad-spectrum herbicide; however, there is a notable lack of scientific evidence specifically characterizing tomato sensitivity to this compound, particularly regarding quantitative tolerance thresholds under direct foliar exposure. This knowledge gap significantly hinders the development of safe management strategies for commercial production systems. The objective of this study was to systematically characterize the sensitivity of the Micro-Tom cultivar to foliar glufosinate applications under controlled greenhouse conditions, assessing both phenotypic and physiological responses. Micro-Tom plants at the four fully expanded true-leaf stage were exposed to five glufosinate concentrations (0, 0.5, 1.0, 2.0, and 3.0 g L^{-1}), corresponding to 0%, 25%, 50%, 100%, and 150% of the recommended rate. Phenotypic response was evaluated by visual assessment of symptoms (chlorosis, necrosis, wilting), quantified on a 0–100% severity scale at five time points (3, 5, 7, and 10 days post-application). In parallel, catalase specific activity was determined by UV–Vis spectrophotometry in leaf samples collected at 1, 2, 6, and 12 hours post-application. Results showed a pronounced dose–response relationship, with all glufosinate concentrations inducing quantifiable damage. Even the lowest dose (0.5 g L^{-1}; 25% of the recommended rate) caused wilting and loss of leaf turgor by three days post-application, with complete mortality by ten days, indicating the absence of any safety margin for unintended foliar exposure. The kinetics of symptom development were consistent across doses—progressive leaf yellowing (3 days), plant collapse (6–7 days), and terminal necrosis (10 days). The antioxidant response, measured as catalase activity, displayed a biphasic pattern characterized by rapid induction at 1 hour post-application (a 52% increase relative to the control), followed by a relative decline between 2 and 12 hours, revealing the insufficiency of the cultivar's defense mechanisms to counteract glufosinate-induced oxidative stress. The lack of a safety tolerance margin in Micro-Tom has critical implications for agricultural management—demanding application protocols that minimize herbicide drift—as well as for breeding programs aimed at developing tolerant varieties via genome editing or conventional selection.

Keywords: *Solanum lycopersicum*; glufosinate-ammonium; herbicide sensitivity; phytotoxicity; oxidative stress; catalase; herbicide tolerance; integrated pest management.

1 INTRODUCTION

Tomato (*Solanum lycopersicum L.*) ranks among the most consequential horticultural crops worldwide, owing to its nutritional significance as well as its economic value and production volume (Zsögön et al., 2017; Klapproth et al., 2018). Global demand is sustained by diversified uses, encompassing fresh consumption and industrial processing into a wide range of value-added products (Straits Research, 2024). The scale of the international tomato market reflects this importance, with an estimated value of USD 200–204 billion in 2024 and projections of sustained growth over the next decade (Straits Research, 2024; Mordor Intelligence, 2025).

Despite its strategic role in global agri-food trade flows, tomato cultivation faces significant agroecological constraints that substantially limit productivity (Klapproth et al., 2018). Among these limiting factors, weed interference ranks among the most severe, both in terms of economic impact and management complexity (Singh et al., 2022). Weeds compete aggressively with tomato plants for essential resources (water, nutrients, light, and space) resulting in yield losses that vary considerably as a function of multiple variables, including the taxonomic identity of the weed species, the infestation density, and the crop's phenological stage at the time competition occurs (Singh et al., 2022).

To mitigate the negative impact of weed competition, the strategic use of effective herbicides constitutes a fundamental agronomic tool (Singh et al., 2022). Glufosinate-ammonium has become established as a non-selective, broad-spectrum herbicide in tomato weed-management systems (Russo et al., 2022), both in conventional cultivars and in transgenic lines that express resistance (Ahmad et al., 2023). This compound, classified as Group 10 (glutamine synthetase inhibitors) (HRAC/WSSA Classification, 2024), acts through the specific inhibition of glutamine synthetase (GS), a key catalytic enzyme that mediates the assimilation of inorganic ammonium into plant nitrogen metabolism (Takano et al., 2021). Inhibition of GS leads to the accumulation of phytotoxic ammonium in plant tissues, triggering loss of membrane integrity, cessation of photosynthesis, and plant death (Takano et al., 2021). The herbicidal spectrum of glufosinate is particularly valuable for controlling annual broadleaf and grass weeds, including species that have evolved resistance to glyphosate, such as Amaranthus, Lolium, Conyza, and Malva (Krähmer et al., 2024; BASF Agriculture, 2023).

Despite the widespread adoption of glufosinate in agricultural systems and its documented efficacy in weed control (Singh et al., 2022), there is a marked paucity of scientific evidence specifically characterizing tomato sensitivity to this herbicide. A comprehensive

review of the scientific literature reveals a pronounced asymmetry, whereas the phytotoxicity of other herbicides (glyphosate and auxinic compounds) has been extensively documented in tomato (Ibrahim et al., 2022; Kolberg et al., 2023), the information available on the crop's physiological response to glufosinate remains extremely limited (Russo et al., 2022).

This knowledge gap stands in marked contrast to the abundant information available for large-scale crops such as soybean, maize, and canola, in which glufosinate tolerance has been thoroughly characterized in both conventional varieties and transgenic lines expressing the bar gene (Krähmer et al., 2024; ISAAA, 2017). Consequently, a rigorous characterization of tomato sensitivity to glufosinate constitutes a priority research objective.

Accurate information on tomato sensitivity to glufosinate is critically relevant across multiple applied contexts. From an agricultural standpoint, establishing quantitative tolerance thresholds would enable the optimization of weed-management strategies in commercial production systems, minimizing the risk of injury from accidental drift or miscalibrated directed applications. Characterizing phytotoxic dose ranges would facilitate the design of safe and efficient application protocols, protecting growers economic investments and ensuring optimal yields.

2 MATERIALS AND METHODS

Experimental trials were conducted at the Universidade Federal de Lavras, located in Lavras, Minas Gerais, Brazil. Evaluations were performed under controlled greenhouse conditions with standardized environmental parameters to characterize variation in the phenotypic and physiological responses of the plant material to glufosinate via enzymatic analyses, thereby enabling a more detailed determination of the response to treatment.

2.1 Phenotypic analysis

2.1.1 Plant Material and Grow conditions

Micro-Tom tomato plants were obtained from seeds provided by the Department of Horticulture at the Universidade Federal de Lavras. Seeds were germinated in 128-cell trays (8×16 matrix configuration) containing a substrate:perlite mixture at a volumetric ratio of 3:1 (v/v). Monitoring seedling development allowed identification of the optimal transplanting time: once seedlings reached the stage of 1–2 fully expanded true leaves (approximately 14–16 days after sowing), individuals of uniform vigor and homogeneous size were selected, totaling 16 seedlings per experimental lot. The selected seedlings were transplanted into individual pots with a 1 L capacity, filled with a clay-loam soil and commercial substrate mixture at a 1:2 ratio (v/v), amended with a slow-release granular fertilizer (N–P–K) applied at a rate of 2 g per pot.

Thermal conditions were set to a daytime temperature of 25 ± 2 °C during the light (photoperiod) phase and a nighttime temperature of 18 ± 2 °C during the dark phase. The light regime comprised a 12-h photoperiod. Irrigation was applied daily in amounts sufficient to maintain the substrate at field capacity, avoiding waterlogging that could compromise root health. Deliberately, no plant-protection products (pesticides, fungicides, or bactericides) were applied throughout the cultivation period prior to the treatments, thereby permitting an unconfounded evaluation of herbicide-induced phytotoxicity symptoms.

Plants were evaluated and processed once they reached a consistent developmental stage: approximately three weeks post-transplanting, at which point they exhibited four fully expanded true leaves, no reproductive structures (flower buds or inflorescences), and a plant height of approximately 15–20 cm. This phenological stage was selected as the standard for the experimental treatments, ensuring biological homogeneity of the plant material and comparability across replicates.

2.1.2 Experimental design

The experiment was arranged in a completely randomized design (CRD), with glufosinate-ammonium concentration as the treatment factor. Five herbicide concentrations were included: a positive control (distilled water + Tween) and four glufosinate doses equivalent to 25% (0.5 g L^{-1}), 50% (1.0 g L^{-1}), 100% (2.0 g L^{-1}), and 150% (3.0 g L^{-1}) of the recommended field rate for broadleaf weed control. Each treatment comprised five biological replicates, totaling 25 plants, which were randomly repositioned within the greenhouse on each evaluation day to minimize positional effects (light or temperature gradients).

2.1.3 Herbicide preparation and application

Glufosinate-ammonium concentrations were selected based on agronomic field-use recommendations and a review of the specialized literature (Krenchinski et al., 2019). The standard reference rate corresponds to 2.0 g L^{-1}, a concentration typically recommended for post-emergence weed control in commercial tomato crops. On this basis, six treatments were established: (i) a negative control (distilled water without herbicide); (ii–iii) sub-recommended doses (0.5 and 1.0 g L^{-1}, equivalent to 25% and 50% of the standard rate, respectively); (iv) the standard dose (2.0 g L^{-1}); and (v) a supra-recommended dose (3.0 g L^{-1}, equivalent to 150% of the standard rate). This dose structure enabled a comparative assessment of tomato sensitivity across a range of herbicide concentrations (Krenchinski et al., 2019).

Each treatment solution was prepared from the commercial herbicide FACINATE (95% glufosinate-ammonium, technical active ingredient) diluted in distilled water to the specified concentrations. A nonionic surfactant, Tween 80, was added to all spray solutions—including the control treatment—at a concentration of 0.1% (v/v). This surfactant addition was implemented to enhance wettability, coverage, and adhesion of the solution on the leaf surface, thereby aligning the experimental conditions with standard agricultural practice. The control treatment consisted specifically of distilled water with 0.1% (v/v) Tween 20 and no herbicide, enabling discrimination between phytotoxicity attributable to glufosinate and potential effects arising from mechanical or water stress caused solely by the application.

Foliar applications for all treatments were performed when plants reached three weeks post-transplanting, coinciding with the stage of four fully expanded true leaves. All treatments were applied simultaneously on the same day, ensuring uniform environmental conditions during application within the greenhouse. A pressure handheld sprayer was used, dedicated exclusively to each application cycle to prevent cross-contamination among treatments.

Applications were performed during morning hours under minimal air movement, a condition that promotes homogeneous coverage of the solution on the leaf surface and minimizes herbicide spray drift. Each plant was treated individually according to its assigned dose, with spray applications made to foliar saturation (approximately 1.3 mL of solution per plant). During application, the sprayer was agitated at regular intervals to maintain suspension homogeneity, a procedure that is particularly critical in low-concentration treatments where sedimentation could compromise dose uniformity.

Following herbicide application, pots were returned to the greenhouse while maintaining the random arrangement specified by the experimental design, thereby ensuring spatial randomization of the plant material. A critical constraint was implemented to ensure optimal herbicide uptake: during the first 24 h post-application, routine irrigation was withheld and plants were protected from precipitation or accidental leaf wash-off. This precaution allowed complete absorption of glufosinate through the leaf cuticle without dilution or wash-off of the spray solution. During the application procedure, the absence of excessive runoff of the solution into the substrate was verified, confirming that the dose was contained within the foliar tissues.

2.1.4 Evaluation of the herbicide response

Sensitivity of Micro-Tom tomato plants to glufosinate was assessed using a standardized protocol based on visual observations and photographic documentation at defined post-application intervals. Evaluations were conducted at five time points: 3, 5, 6, 7, and 10 days after application (DAA) of the herbicide. This temporal distribution enabled a detailed characterization of the kinetics of phytotoxic symptom development, from early manifestations through to terminal expression of herbicide injury. At each evaluation date, all plants were photographed individually using a smartphone digital camera positioned at a fixed distance of 0.5 m from the foliage.

At each evaluation, the presence and nature of phytotoxic symptoms were recorded, including: (i) foliar chlorosis (tissue yellowing), (ii) foliar necrosis (tissue death and darkening), (iii) wilting or tissue flaccidity, and (iv) malformations or morphological distortions. Foliar injury severity for each plant was quantified using a visual percentage scale of 0 to 100, where 0% denotes the complete absence of symptoms (healthy plant), 10–30% represents mild injury with limited chlorotic or necrotic spotting, 40–60% indicates moderate injury with multiple leaf areas affected, 70–90% reflects severe injury with most of the foliage compromised, and 100% represents total plant death. This scale was applied by estimating the percentage of leaf area

exhibiting chlorotic or necrotic symptoms. Digital photographs served as visual references to ensure consistency in severity scoring across successive evaluations.

To minimize experimental bias, all severity assessments were conducted in a blinded manner with respect to treatment assignments: the evaluator was unaware of the glufosinate concentration assigned to each plant during scoring. This experimental blinding substantially reduces the likelihood of observational bias and ensures objectivity in the visual appraisal of phytotoxic symptoms. In cases of ambiguity in classification, digital images were used as references to establish a consensus final rating. Foliar injury severity data were recorded for all plants at each evaluation date, generating a time-resolved response matrix that enabled characterization of injury progression and the tomato crop's dose–response relationship to glufosinate.

2.2 Physiological analysis

2.2.1 Plant Material

In addition to the phenotypic evaluation performed on whole plants, a second experimental batch of tomato (*Solanum lycopersicum* L.), cultivar Micro-Tom, was established for physiological analyses, adhering to the same greenhouse conditions and plant-material collection parameters—as well as the plant developmental stage—previously described.

2.2.2 Experimental design

The experiment was arranged as a completely randomized design (CRD) with a 4 × 2 factorial structure. The first experimental factor was sampling time post-herbicide application, set at four levels: 1, 2, 6, and 12 hours after application (HAA). The second factor was treatment type, with two levels: application of glufosinate-ammonium versus a positive control without herbicide. Each time–treatment combination was assigned four biological replicates, yielding a total of 32 experimental units (4 times × 2 treatments × 4 replicates).

Each biological replicate consisted of two individual plants grown in adjacent pots within the greenhouse (Figure 1). Following herbicide application, at the harvest time corresponding to each sampling time point, leaf tissue was collected from both plants in the replicate. Leaf material from the two individuals was combined *in situ* to constitute a single homogenized biological sample representative of the replicate. This biological pooling procedure increased the homogeneity of the plant material and reduced inherent within-

replicate variability, thereby improving the statistical robustness of subsequent physiological analyses (Kwiatkowski et al., 2016; Hao et al., 2025). Leaf samples were either processed immediately or snap-frozen in liquid nitrogen and stored at −80 °C for later analyses.

Figure 1 – Diagram of the procedure for obtaining the plant extract used for catalase analysis. Representation of one of the collection time points, applicable to all other sampling times.

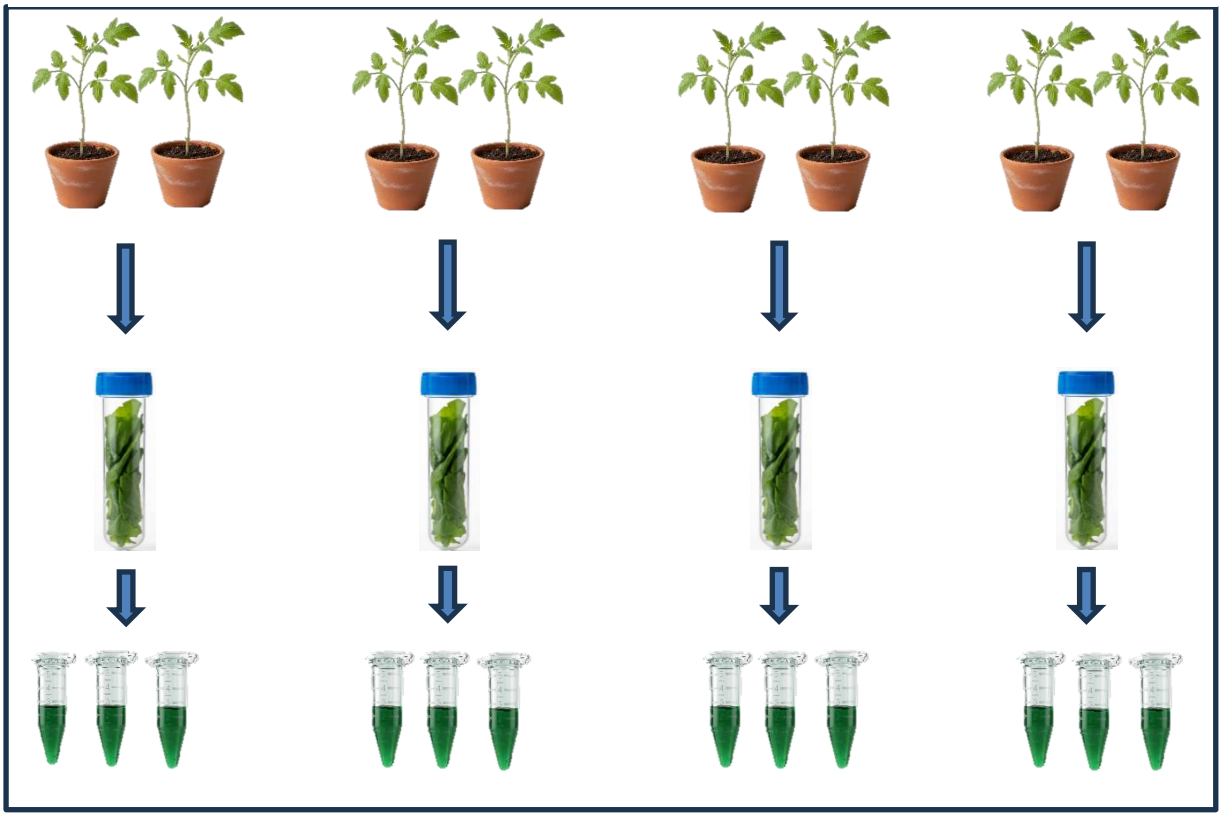

Source: Author (2025).

2.2.3 Herbicide preparation and application

The herbicide solution was prepared from the commercial product FACINATE (technical-grade glufosinate-ammonium, 95% active ingredient) diluted in sterile distilled water to a concentration of 0.5 g L^{-1} active ingredient (Thermo Fisher Scientific, 2025). This concentration represents 25% of the standard recommended field rate (2.0 g L^{-1}). A nonionic surfactant, Tween 20, was added to all spray solutions—both herbicide and control—at 0.2% (v/v) to enhance wettability, coverage, and penetration through the leaf cuticle, thereby aligning the experimental conditions with standard agricultural practice (Croda Agriculture, 2025). The control solution consisted of sterile distilled water supplemented with 0.2% (v/v) Tween 20 without herbicide, enabling discrimination between phytotoxic effects specifically attributable to glufosinate and any stress arising solely from foliar application.

Foliar applications were carried out during morning hours (6:00 a.m.). A calibrated, pressure handheld sprayer was used to deliver approximately 1.3 mL of solution per plant. Application was performed as four consecutive sprays until complete foliar saturation was achieved, ensuring homogeneous coverage without excessive runoff onto the substrate. All applications were conducted under minimal air movement within the greenhouse, thereby minimizing spray drift and maximizing deposition of the herbicide on the target leaf surface.

2.2.4 Collection and preservation of plant tissue

Leaf tissue was collected at five post-application time points: 1, 2, 6, and 12 hours after application (HDA) of the herbicide. At each sampling time, four glufosinate-treated replicates and four control replicates were processed simultaneously, thereby maintaining temporal synchronization between treatments and ensuring comparability of physiological states at the time of analysis. This structure enabled characterization of the temporal kinetics of the physiological response to the herbicide across the experimental time window.

For each biological replicate, the four fully expanded true leaves from both plants constituting the replicate (n = 2 plants per replicate) were harvested. The collection included the entire leaf blade with petiole, and the material was immediately combined *in situ* to form a single homogenized biological sample per replicate. The combined leaf tissue was transferred to pre-identified and labeled 50 mL Falcon-type tubes. Immediately after harvest, samples were immersed in liquid nitrogen (N_2) to instantaneously halt all metabolic and enzymatic activity, thereby preventing degradation of bioactive compounds and proteins during storage. Following liquid-nitrogen freezing, samples were transferred to ultra–low-temperature freezers at −80 °C, where they remained until biochemical analysis of catalase enzyme activity.

2.2.5 Determination of catalase (CAT) enzymatic activity

Catalase (EC 1.11.1.6) activity was quantified by UV–Vis spectrophotometry based on kinetic monitoring of hydrogen peroxide (H_2O_2) decomposition. The assay relies on the enzyme's catalytic capacity to disproportionate H_2O_2 into water and molecular oxygen, a reaction that can be tracked spectrophotometrically via the decrease in absorbance at 240 nm, the characteristic wavelength at which H_2O_2 absorbs (Hadwan, 2024). This methodology was adapted from the protocol of Mengutay et al. (2013) and optimized for ELISA microplates. Total protein concentration in each extract was determined using the Bradford method (Kielkopf et al., 2020) with bovine serum albumin (BSA) as the protein standard. All assays were performed in technical triplicate for each biological sample.

For preparation of the enzymatic extract, approximately 200 mg of frozen leaf tissue were ground in a mortar pre-chilled by immersion in liquid nitrogen until a uniform, homogeneous powder was obtained. The resulting powder was transferred to 2 mL microcentrifuge tubes, and 1.5 mL of 100 mM potassium phosphate extraction buffer (pH 7.0) supplemented with (i) 0.1 mM EDTA, (ii) 10 mM ascorbic acid, and (iii) 1% (w/v) polyvinylpyrrolidone (PVP) was added. This buffer composition stabilizes enzymatic proteins and prevents oxidation of phenolic compounds that could interfere with the analysis (Verde et al., 2021; Kurakula & Agu, 2020).

Samples were vortex-homogenized for 30 s, kept on ice for 10 min to facilitate extraction, and subsequently centrifuged at 12,000 × g for 10 min at 4 °C. The supernatant was carefully collected, aliquoted, and kept on ice as the enzymatic extract for subsequent catalase activity assays and total protein quantification.

Catalase activity was determined in 1 cm pathlength quartz cuvettes using a UV–Vis spectrophotometer equipped with temperature control set to 30 °C. The reaction mixture consisted of (i) 100 µL of 100 mM potassium phosphate buffer (pH 7.0), (ii) 10 µL of the enzymatic extract prepared as described above, and (iii) H_2O_2 to initiate the reaction. The reaction was started by rapidly adding 10 µL of 250 mM H_2O_2, yielding a stated final cuvette concentration of 12.5 mM, followed by gentle mixing by inverting the cuvette. The decrease in absorbance at 240 nm was monitored over 3 min, with readings recorded every 15 s using the spectrophotometer's kinetic program.

Catalase activity was calculated using the molar extinction coefficient of H_2O_2 (ε_{240} = 39.4 $M^{-1}\cdot cm^{-1}$) according to the following equation:

$$Actividad\ CAT = \frac{\Delta A_{240} \times V_t}{\varepsilon \times l \times V_e \times t}$$

Where:

- **ΔA_{240}/min** = change in absorbance per minute at 240 nm
- **V_t** = total reaction mixture volume (180 µL)
- **ε_{240}** = molar extinction coefficient of H_2O_2 (39.4 $M^{-1}\cdot cm^{-1}$)
- **l** = optical path length (1 cm)
- **V_e** = volume of enzymatic extract (10 µL or 0.010 mL)

One unit of catalase activity (U) is defined as the amount of enzyme required to decompose 1 μmol of H_2O_2 per minute under the assay conditions (30 °C, pH 7.0) (Sigma-Aldrich, 2024).

Total protein content in the enzymatic extracts was determined using the Bradford method (1976) with BSA as the reference protein standard. Appropriately diluted enzymatic extract (10 μL) was mixed with 200 μL of Bradford reagent (Coomassie Brilliant Blue G-250) in 96-well microplates. After a 5-min incubation at room temperature, absorbance was measured at 595 nm using a microplate reader. Protein concentration was determined by interpolation from a BSA standard curve (range: 0.05–0.5 mg mL^{-1}) prepared in the same extraction buffer used for sample preparation.

Catalase specific activity was expressed as units of activity per milligram of total protein (U mg^{-1} protein), which normalizes for variation in protein content among samples and enables valid comparisons across treatments and sampling times. Specific activity values were calculated for each biological replicate (based on the mean of technical triplicates) and used for subsequent statistical analyses.

3 RESULTS AND DISCUSSION

3.1 Visual symptomatology and temporal progression of symptoms

The temporal assessment of the phytotoxic response of the tomato cultivar Micro-Tom to foliar application of glufosinate revealed symptom-development kinetics clearly dependent on both the applied concentration and post-application time. This time- and dose-dependent progression was evident at all assessment stages and was characterized by the sequential manifestation of specific symptoms.

During the early evaluations, the loss of one plant in the 0.5 $g \cdot L^{-1}$ treatment was documented and attributed to mechanical damage unrelated to the phytotoxic effect of glufosinate. At the first evaluation (3 days after application, DAA) (Figure 2), wilting and loss of turgor were documented in terminal regions of the foliage across all glufosinate treatments, with this symptomatology being more pronounced at 0.5 $g \cdot L^{-1}$. Injury symptoms such as chlorosis and wilting usually occur within 3–5 days after glufosinate application, followed by necrosis in 1–2 weeks. By contrast, plants in the control group (treated solely with distilled water and Tween 20 surfactant) maintained full vigor without morphological or functional alterations.

Figure 2 – Sensitivity curve after 3 days of glufosinate application at concentrations of 0.5 g/L, 1.0 g/L, 2.0 g/L, and 3.0 g/L.

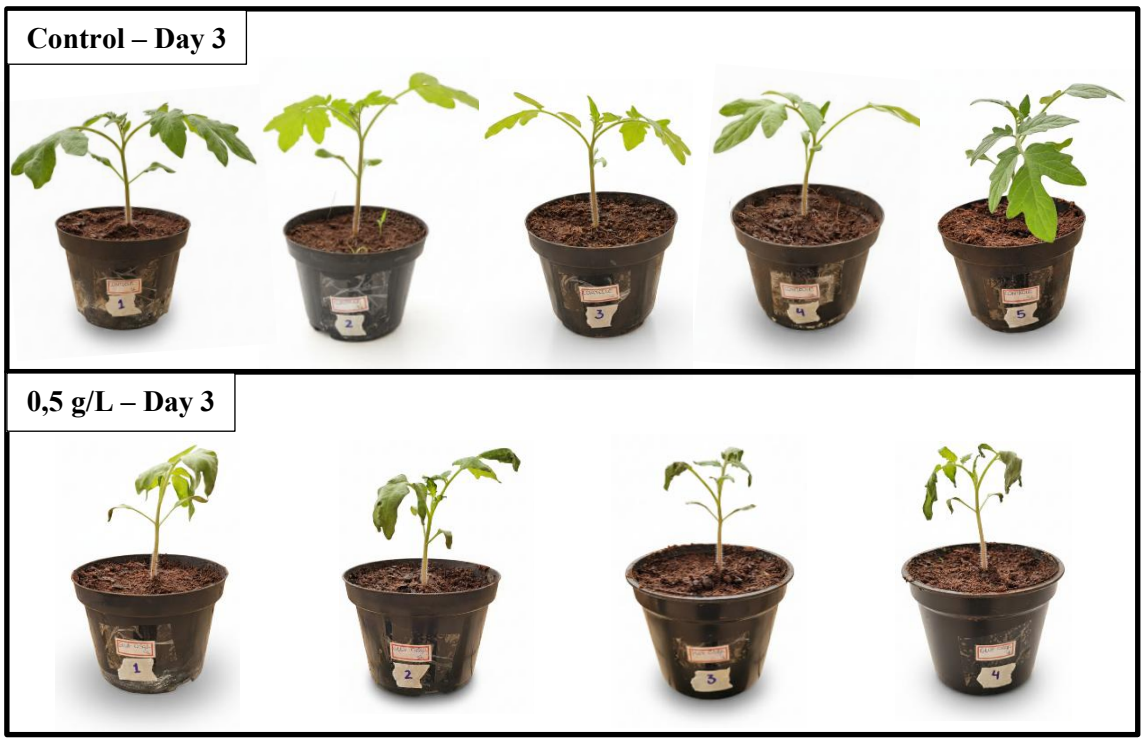

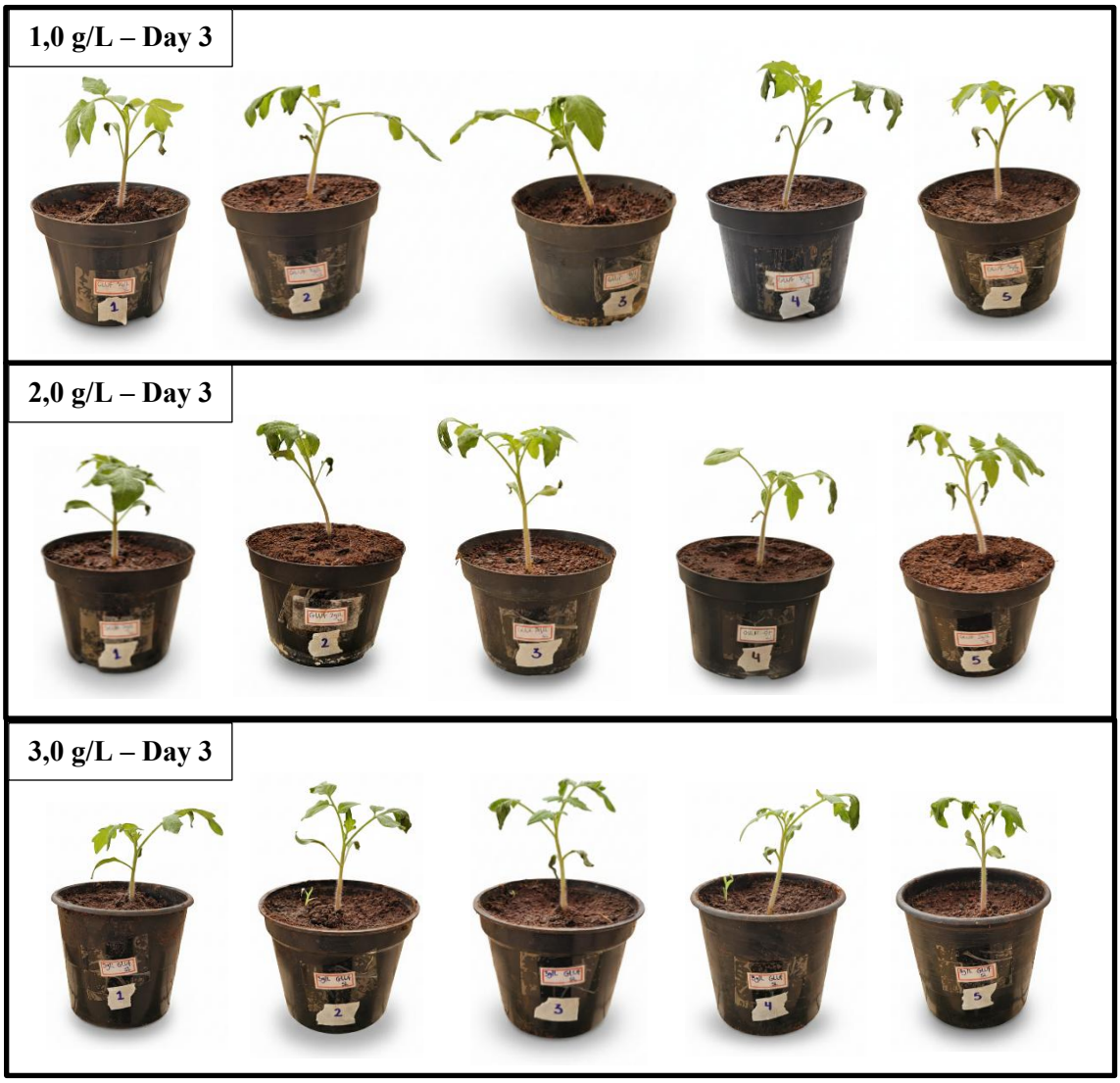

Source: Author (2025).

At 5 days after application (DDA) (Figure 3), a marked escalation in the severity of phytotoxic symptoms was observed. Across all glufosinate concentrations, foliar chlorosis (tissue yellowing) appeared, accompanied by foliar necrosis (tissue darkening and death) and persistent wilting in the upper foliar regions. The presentation of these symptoms showed clear dose-dependent variation.

Figure 3 - Sensitivity curve after 5 days of glufosinate application at concentrations of 0.5 g/L, 1.0 g/L, 2.0 g/L, and 3.0 g/L.

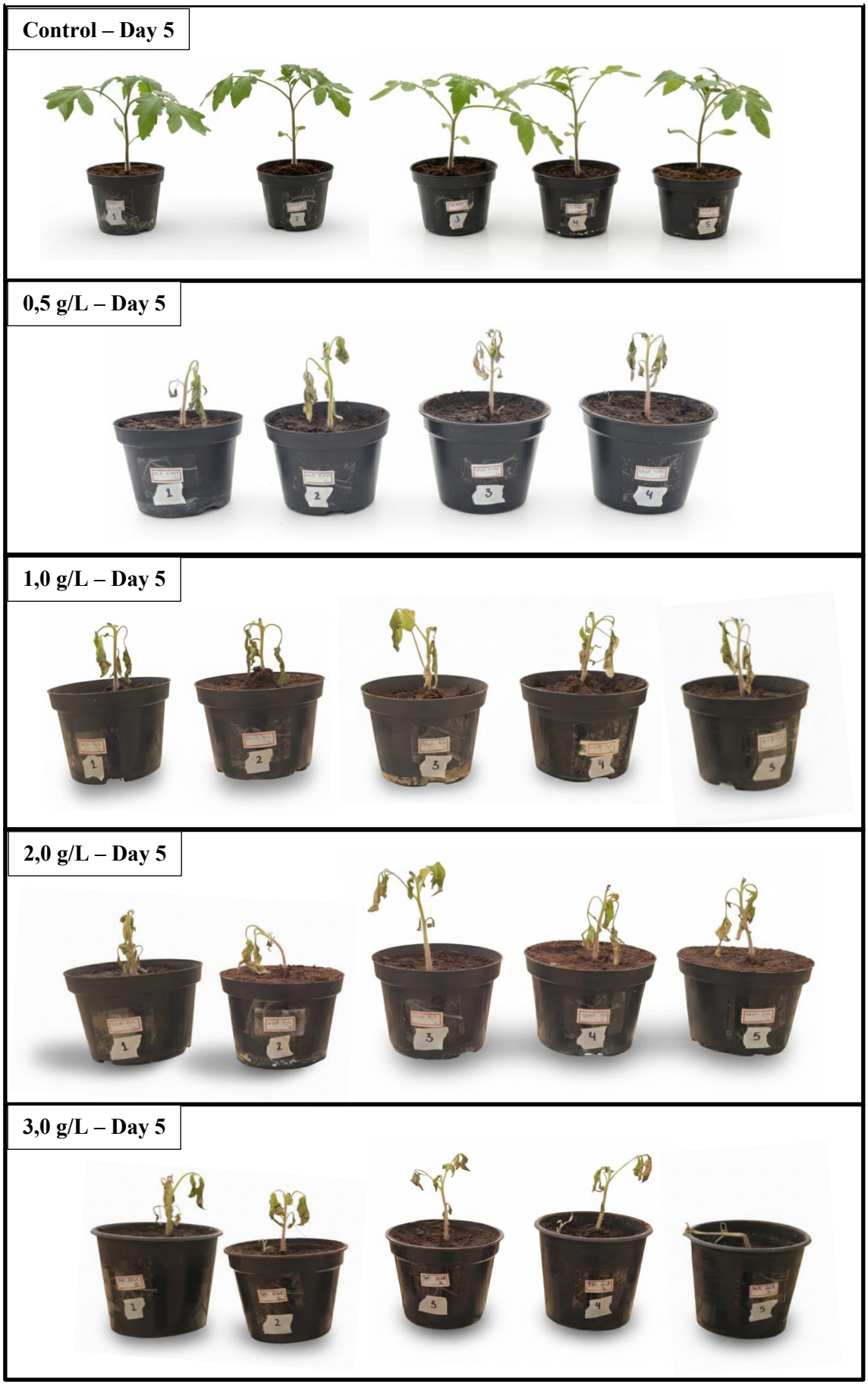

Source: Author (2025).

At 7 DDA (Figure 4), the symptomatology was essentially similar to that on day six, with the exception of the 3.0 g/L treatment, in which all plants exhibited complete foliar necrosis. The 0.5 and 1.0 g/L treatments continued to show a variable picture, with some plants in a prostrate state but retaining residual viability. The 2.0 g/L treatment showed complete plant prostration, although total tissue necrosis had not been reached.

Figure 4 - Sensitivity curve after 7 days of glufosinate application at concentrations of 0.5 g/L, 1.0 g/L, 2.0 g/L, and 3.0 g/L.

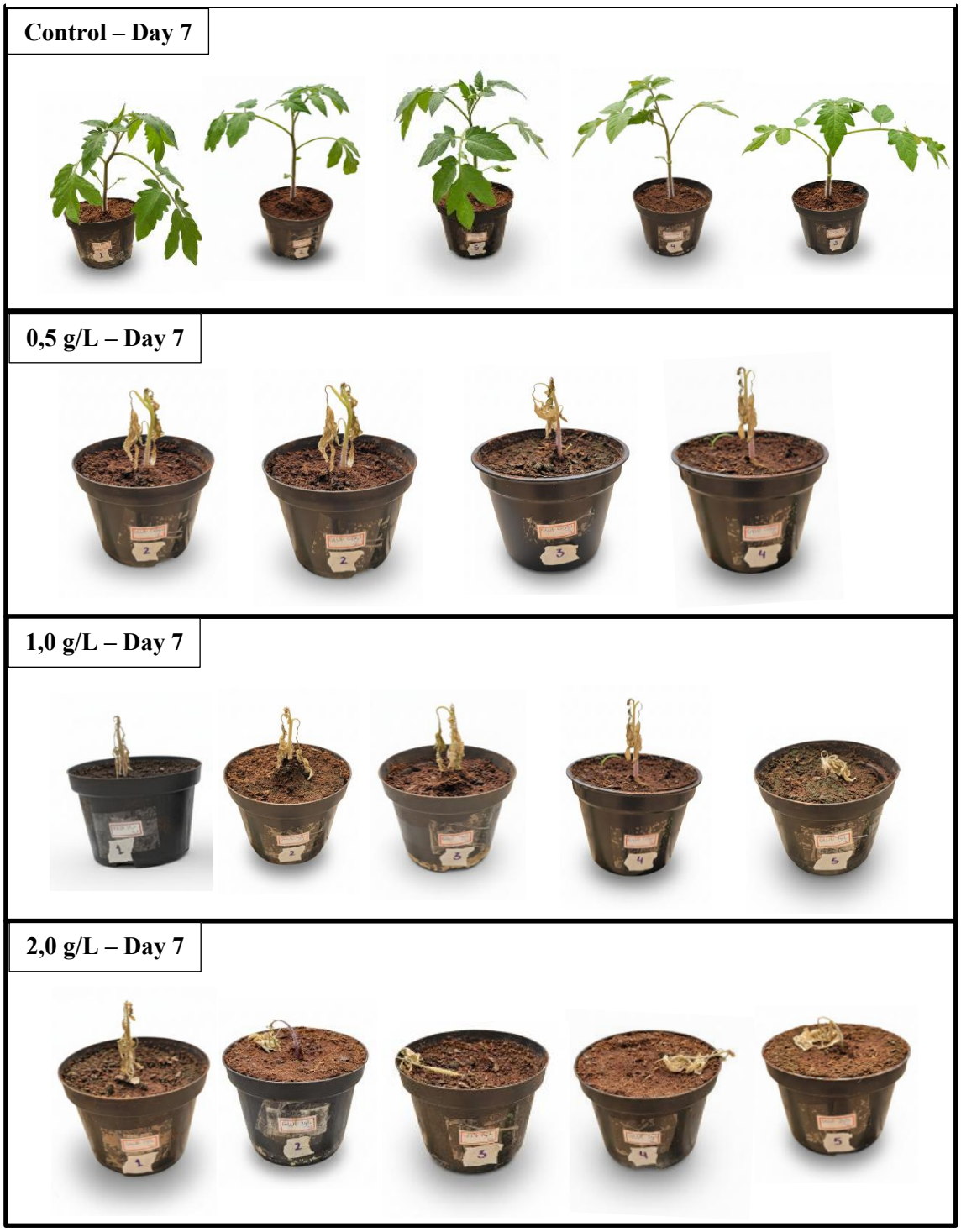

Source: Author (2025).

By the tenth day after application (Figure 5), complete plant death was recorded in all glufosinate treatments. The 1.0, 2.0, and 3.0 g/L treatments displayed features of terminal senescence: fully desiccated leaves, advanced generalized yellowing, and complete horizontal prostration, indicating terminal dehydration and the biological impossibility of recovery.

Figure 5 - Sensitivity curve after 10 days of glufosinate application at concentrations of 0.5 g/L, 1.0 g/L, 2.0 g/L, and 3.0 g/L.

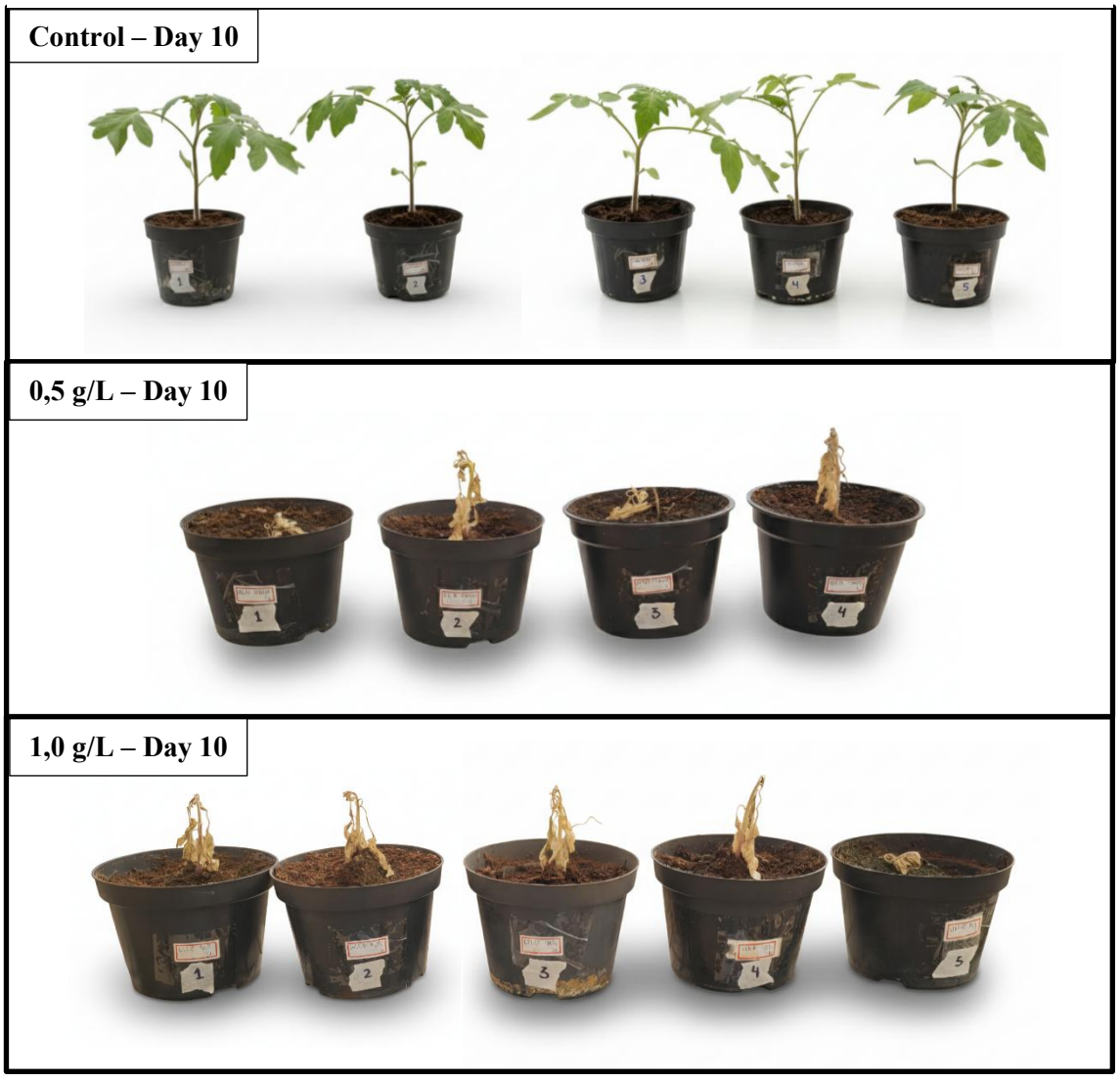

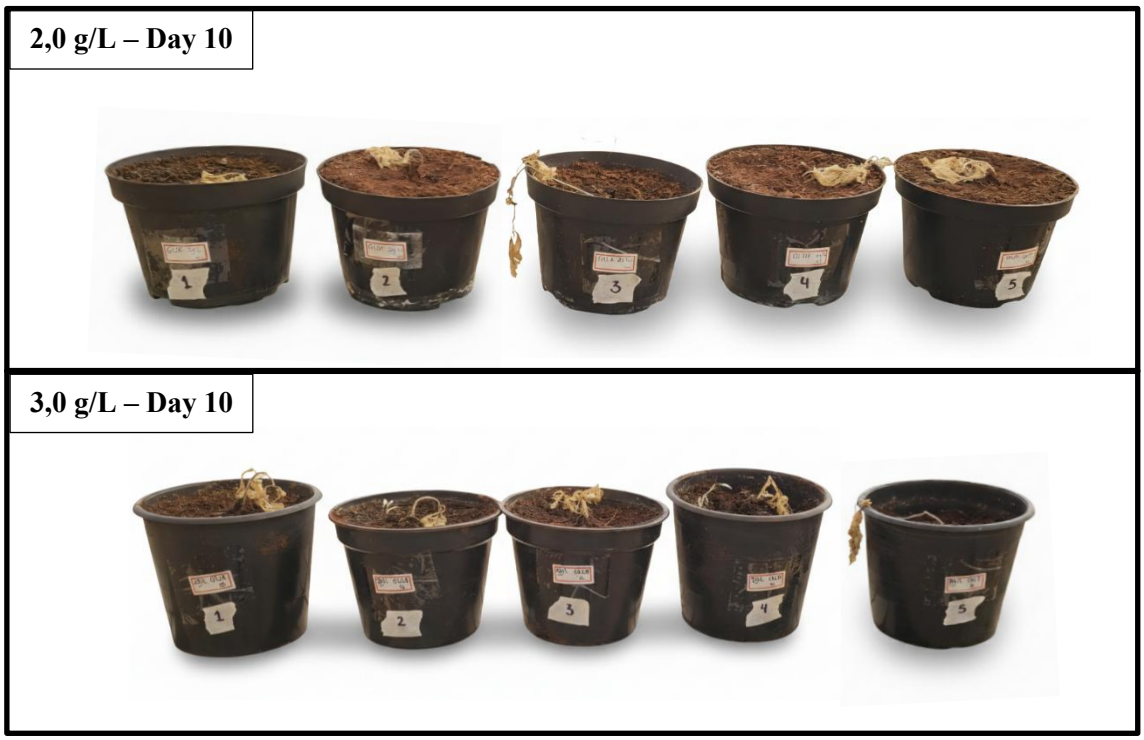

Source: Author (2025).

3.2 Quantitative analysis of foliar damage severity

Quantitative analysis of foliar damage severity using the standardized visual percent scale (0–100%) revealed dose (dependent response patterns with time) course kinetics that varied according to the applied glufosinate concentration. This temporal variation was consistently evident across all evaluation time points.

Figure 6 - Mean foliar damage severity with standard deviation at each evaluation time point, by glufosinate concentration.

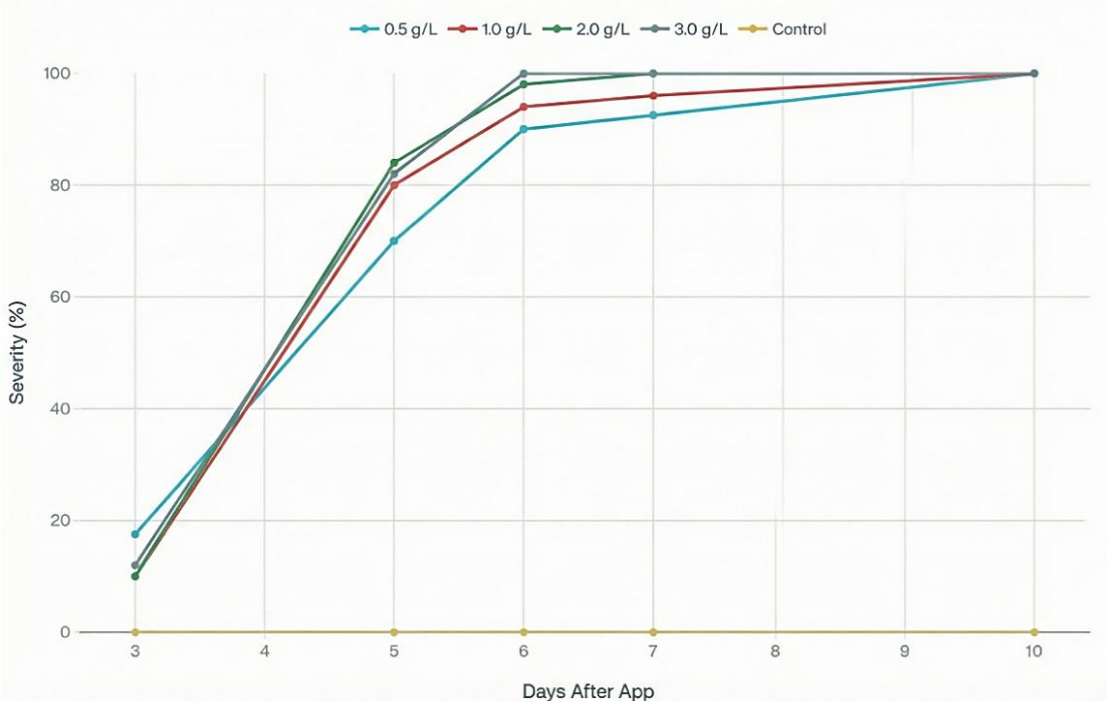

Source: Author (2025).

At 3 days after application (DAA) (figure 6), foliar damage severity was low across all glufosinate treatments, with mean values of 17.5 ± 8.3% at 0.5 g·L^{-1} and 10.0 ± 0.0% for both 1.0 and 2.0 g·L^{-1}. The 3.0 g·L^{-1} treatment was excluded from this time point due to early plant mortality. The 0.5 g·L^{-1} treatment exhibited substantially greater interindividual variability (standard deviation: ± 8.3 percentage points) compared with the other treatments. This wider dispersion suggests that plant-specific physiological factors or microenvironmental conditions differentially influenced the kinetics of foliar absorption and metabolism of the herbicide (Polli et al., 2022; Takano et al., 2021).

By 5 DAA (figure 6), a marked escalation in damage severity was recorded for all treatments, followed by a pronounced increase at 6 DAA. At this latter time point, the following means were documented: 90.0 ± 7.1% (0.5 g·L^{-1}), 94.0 ± 4.9% (1.0 g·L^{-1}), 98.0 ± 4.0% (2.0 g·L^{-1}), and 100.0 ± 0.0% (3.0 g·L^{-1}). The highest concentration (3.0 g·L^{-1}) consistently reached the maximum damage level (100%) across all experimental replicates at this time point, indicating complete foliar necrosis. At 7 DAA, the 2.0 and 3.0 g·L^{-1} treatments maintained severities of 100.0 ± 0.0%, reflecting persistent and uniform necrosis in all plants within these treatments.

By 10 DAA (figure 6), the response fully converged: all glufosinate treatments recorded 100.0 ± 0.0% foliar damage severity, representing complete foliar necrosis in every plant and replicate. This homogenization at the final assessment indicates that, although the rate of symptom progression scaled with dose (faster kinetics at higher concentrations), the terminal severity was equivalent and inexorable across all glufosinate concentrations evaluated in the Micro-Tom tomato cultivar.

3.3 Mortality and survival analysis

The temporal analysis of survival (operationally defined as the absence of complete foliar necrosis) revealed distinct rates of transition to total mortality as a function of the applied glufosinate concentration. By 7 days after application (DAA), the greatest temporal divergence between the extreme treatments was evident: the 3.0 $g \cdot L^{-1}$ treatment (150% of the recommended dose) reached 100% mortality, whereas the 0.5 $g \cdot L^{-1}$ treatment (25% of the recommended dose) retained partial survival, with 75% of its plants (3 of 4) still alive, albeit severely compromised by phytotoxic injury. This approximately 1–2 day gap between the terminal mortality points of the lowest and highest doses underscores both the physiological sensitivity of the Micro-Tom cultivar and the characteristically rapid herbicidal action of glufosinate.

The positive control, treated only with distilled water and Tween 20, maintained full morphological and functional vigor throughout the observation period. This response confirms that the surfactant adjuvant used did not induce inherent phytotoxicity in the crop and validates that the symptomatology observed in all glufosinate treatments was attributable exclusively to the herbicide's active ingredient.

3.4 General statistical analysis of catalase activity

A two-way analysis of variance (ordinary ANOVA, $\alpha = 0.05$) revealed that all evaluated factors exerted statistically significant effects on the specific activity of catalase. The time × treatment interaction accounted for the largest share of the total variance (51.9%; $p < 0.001$), indicating that the temporal kinetics of the catalase response differs qualitatively between the glufosinate treatments and the control. Second, the main effect of time explained 31.7% of the total variance ($p < 0.001$), showing that the magnitude of temporal change in catalase activity

is an important determinant of phenotypic expression. Finally, treatment type (glufosinate versus control) contributed 8.85% of the variance ($p = 0.002$). This hierarchical variance structure indicates that, although the herbicide treatment effect is statistically significant, the temporal kinetics of the catalase response is the predominant driver of the observed enzymatic activity.

At the first time point (1 hour after application [HAA]) (figure 7), glufosinate-treated plants exhibited a catalase activity of 0.455 ± SE μmol $H_2O_2 \cdot min^{-1} \cdot mg^{-1}$ protein, significantly higher than the control group, which reached 0.300 ± SE μmol $H_2O_2 \cdot min^{-1} \cdot mg^{-1}$ protein. The absolute difference was +0.155 $\mu mol \cdot min^{-1} \cdot mg^{-1}$ protein (95% confidence interval: 0.0912–0.219; $p = 0.002$, according to Fisher's LSD test without correction for multiple comparisons). This ~52% increase in catalase activity after only 60 minutes of herbicide exposure constitutes evidence of an exceptionally rapid, early antioxidant defense response, confirming that glufosinate triggers cellular oxidative stress with accelerated kinetics from the earliest post-exposure phases.

The early catalase response is linked to the molecular mode of action of glufosinate, fundamentally through rapid inhibition of glutamine synthetase (GS) (Takano et al., 2019). This enzymatic inhibition triggers a cascade of metabolic events culminating in massive oxidative stress. Specifically, GS inhibition causes: (i) rapid intracellular accumulation of ammonia (NH_3), which interferes with critical metabolic functions and disrupts the photorespiratory pathway (Takano et al., 2019; Sinn et al., 2020); (ii) decoupling of the electron transport chain in both mitochondria and chloroplasts, resulting in inhibition of photosynthetic carbon assimilation (Takano et al., 2019); and (iii) limitation of linear electron flow at photosystem II under light, which forces molecular oxygen (O_2) generated by water photolysis to act as an abnormal electron acceptor, thereby generating reactive oxygen species (ROS), particularly hydrogen peroxide (H_2O_2) (Takano et al., 2019; Huang et al., 2024).

Catalase, a peroxisomal first-line antioxidant enzyme specialized in the rapid disproportionation of H_2O_2 ($2H_2O_2 \rightarrow 2H_2O + O_2$), undergoes both transcriptional regulation and immediate post-translational activation in response to increased concentrations of its specific substrate (H_2O_2) (Takano et al., 2019). Its high catalytic rate (approximately 6×10^6 H_2O_2 molecules converted per minute) and lack of requirement for additional reductants position catalase as the principal defense mechanism against the massive H_2O_2 accumulation generated by the light-dependent ROS burst induced by glufosinate (Shetty et al., 2019; Takano et al., 2019).

Figure 7 - Temporal dynamics of specific catalase (CAT) activity in glufosinate-treated and control Micro-Tom tomato plants.

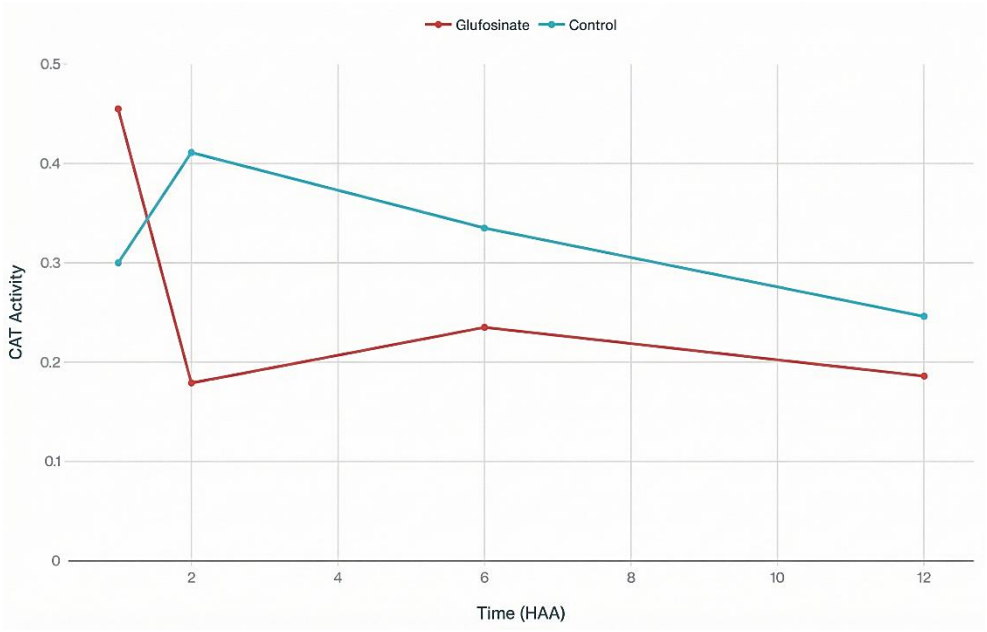

Source: Author (2025).

At 2 hours after application (2 HAA) (figure 7), a dramatic shift in catalase response kinetics was recorded. Specific activity in glufosinate-treated plants dropped precipitously to 0.179 ± SE μmol $H_2O_2 \cdot min^{-1} \cdot mg^{-1}$ protein (a 60.7% decrease relative to 1 HAA), whereas the control rose to 0.411 ± SE μmol $H_2O_2 \cdot min^{-1} \cdot mg^{-1}$ protein (a 37.0% increase), producing a notable inversion in the activity relationship: the control exhibited values significantly higher than the glufosinate treatment (difference = −0.233 $\mu mol \cdot min^{-1} \cdot mg^{-1}$ protein; 95% CI: −0.296 to −0.169; $p < 0.001$).

The maximal repression of catalase observed at 2 hours after application (2 HAA) is consistent with phytohormonal signaling dynamics and stress-responsive transcriptomic cascades that reach their peak intensity between 1.5 and 2.5 hours post-stimulus in herbaceous plants such as tomato. This temporal delay corresponds to the time required for sequential physiological processes that include: (i) absorption and translocation of glufosinate to the leaf mesophyll; (ii) inhibition of glutamine synthetase and accumulation of intracellular ammonium; (iii) activation of osmotic stress receptors and amino acid deamination cascades; (iv) de novo synthesis of repressive transcription factors, including factors analogous to OsARF18; and (v) occupation of promoter sites in the chromatin of the CATA gene. This sequential regulatory cascade is consistent with previous studies demonstrating that OsARF18 acts as a negative regulator of genes critical for glufosinate resistance, specifically repressing the expression of

glutamine synthetase genes (OsGS1;1 and OsGS1;2) (Wang et al., 2021; Ren et al., 2023). Although in rice the primary mechanism of ARF18 involves repression of glutamine synthetase genes, transcriptomic analyses in glufosinate-treated plants reveal that ARF18 also regulates a broad network of stress-responsive genes, potentially including genes encoding antioxidant enzymes such as catalases, suggesting a more integral regulatory role in coordinating phytotoxic responses (Li et al., 2022).

The coordinated repression of antioxidant defense genes under herbicide stress represents an intriguing physiological decision that has been documented in model systems. In Arabidopsis thaliana, acute exposure to glufosinate induced massive accumulation of hydrogen peroxide (causing up to 2.73-fold greater lipid peroxidation damage than in the control), which in principle would be expected to activate antioxidant defense systems; however, the coordinated transcriptomic repression of catalase and other defense genes suggests that repressor factors such as ARF18 or analogous homologs exert deliberate negative regulation over antioxidant defense as part of a physiological strategy of accepting irreversible damage under severe phytotoxicity (Molinier et al., 2023; Liu et al., 2019). This hypothesis is consistent with transcriptomic regulation models that predict selective repression of energetically costly defenses in contexts in which survival is unlikely (Frei dit Frey et al., 2018).

In marked contrast to the repression observed in treated plants, the 37% increase in catalase activity in control plants at 2 HAA reflects the convergence of multiple regulatory mechanisms operating simultaneously in the experimental context. Primarily, this increase integrates circadian homeostatic regulatory mechanisms associated with the daily progression of morning photosynthesis, which naturally induce the expression of antioxidant genes in response to elevated production of reactive oxygen species during photosynthetic activity (Zhao et al., 2021). However, robust scientific evidence shows that plants subjected to chemical herbicide stress emit stress-specific volatile organic compounds (VOCs) that function as plant–plant communication molecules, priming defense systems in neighboring, undamaged plants (Leng et al., 2019).

In tomato, *Solanum lycopersicum* var. microtom, specifically, exposure to VOCs from companion plants has been shown to induce priming of defense responses via activation of MAPK signaling cascades, resulting in faster and more robust expression of defense genes, including proteinase inhibitors (De Falco et al., 2022). Although glufosinate-specific VOCs have not been fully characterized, recent studies on herbicide volatilization demonstrate that during the 2–4 hours post-application, significant amounts of herbicide stress-related volatile compounds evaporate from moist plant surfaces, especially at elevated temperatures typical of

greenhouse conditions, generating an atmosphere enriched in volatile stress signals (Carvalho et al., 2021).

This exposure of control plants to abiotic stress VOCs activated oxidative defense priming, increasing the expression of antioxidant genes such as CAT through redox signaling pathways mediated by MYB, WRKY, and bZIP transcription factors, which are specifically induced by VOC-mediated priming in tomato (Yoshida et al., 2023). Consequently, the increase observed in control plants synergistically integrates both the circadian homeostatic response to morning photosynthesis and the defensive priming triggered by the perception of volatile stress signals emitted by adjacent treated plants, resulting in significantly elevated catalytic activity. This interpretation explains the magnitude of the observed effect (37% increase) and provides a mechanistic framework that links laboratory observations with communication and defensive regulatory dynamics in plant populations.

At 6 hours after application (6 HAA) (figure 7), the glufosinate-treated plants reached 0.235 ± SE μmol $H_2O_2 \cdot min^{-1} \cdot mg^{-1}$ protein, representing a 31.3% recovery from the 0.179 minimum recorded at 2 HAA, indicative of progressive reactivation of antioxidant defense mechanisms. The control decreased to 0.335 ± SE μmol $H_2O_2 \cdot min^{-1} \cdot mg^{-1}$ protein, an 18.5% reduction from its 2 HAA maximum. The between-treatment difference was trend-level (−0.0995 μmol·min^{-1}·mg^{-1} protein; 95% confidence interval: −0.163 to −0.0356; $p = 0.068$), indicating an incipient convergence between treatment and control after 6 hours of observation.

This recovery of catalase activity in glufosinate-treated plants reflects the progressive deactivation of the ARF18-mediated repressor mechanism and the reactivation of catalase synthesis. Repressor transcription factors such as ARF18 exhibit a molecular half-life of approximately 3–4 hours, allowing the transcriptional machinery, after the repression peak at 2 hours after application (2 HAA), to regain access to the CATA promoter (Jing et al., 2023). Simultaneously, between 2–6 HAA, ammonium detoxification processes occur that stabilize metabolism: selective autophagy releases alternative amino acids, de novo synthesis of glutamine synthetase incorporates accumulated ammonium, and oxidative degradation of glutamine reduces the toxic concentration of NH_4^+ (Hakvoort et al., 2017; Lyu et al., 2024). This post-2 HAA metabolic stabilization reduces the activation of programmed cell death, enabling reactivation of the CATA promoter and de novo synthesis of catalase protein. The partial recovery (31.3%) indicates the persistence of residual epigenetic repression or still-elevated H_2O_2 concentrations, limiting the return to normal photosynthetic levels (Kovalchuk et al., 2023; Cannea et al., 2025). The incipient convergence between treatment and control at 6 HAA suggests ongoing recovery of antioxidant defenses, whereas the control declines (-

18.5%) as circadian/photoperiodic stimuli diminish toward the mesocore hours of the diurnal cycle (Kappachery et al., 2024).

At 12 hours after application (12 HAA) (figure 7), both treatments exhibited catalase activity values closest to the expected basal state. The glufosinate treatment reached 0.186 ± SE μmol $H_2O_2 \cdot min^{-1} \cdot mg^{-1}$ protein (a cumulative 59.1% decrease from the 2 HAA maximum), while the control recorded 0.246 ± SE μmol $H_2O_2 \cdot min^{-1} \cdot mg^{-1}$ protein (a 26.6% decrease relative to 6 HAA). However, the between-treatment difference was not significant (−0.0603 $\mu mol \cdot min^{-1} \cdot mg^{-1}$ protein; 95% CI: −0.132 to 0.0111; $p = 0.059$), indicating practical statistical convergence of both responses. Although the 12 HAA values approached the expected basal range, the persistence of slightly elevated catalase activity relative to the literature (glufosinate: 0.186; control: 0.246 vs. ~0.10–0.20 as basal) suggests that oxidative stress remained partially unresolved, indicating that the antioxidant system was still upregulated even 12 hours post-application (Aires et al., 2022).

Tukey's multiple-comparison test across the four time points (1, 2, 6, and 12 HAA) within each treatment revealed significant biological heterogeneity. In the glufosinate treatment, pairwise comparisons between sampling times were highly significant ($p < 0.001$), confirming that the temporal kinetics of catalase activity differed markedly across evaluation times. Specifically, the 1 vs 2 HAA comparison showed the largest observed difference: 0.28 $\mu mol \cdot min^{-1} \cdot mg^{-1}$ protein (95% CI: 0.17–0.38; $p < 0.001$), indicating that the transition across these early post-application hours represented the most pronounced change within the 12-hour observation window—by contrast with the smaller changes observed between 6 and 12 HAA.

Analogously, in the control treatment, temporal heterogeneity was documented by significant differences ($p < 0.05$) between certain pairs of time points, although with generally smaller magnitude than in the glufosinate treatment (Xie et al., 2019). This lower temporal variability in the control suggests that antioxidant response dynamics in plants not exposed to herbicidal stress were more gradual and less dramatic than in stressed plants (Batista-Silva et al., 2019). The inter-individual variability observed within both treatments results from compounding factors acting in concert: beyond the systematic effects of glufosinate, local micro-environmental factors modulate the magnitude of the catalase response (Kaur et al., 2024). Specifically, heterogeneity in foliar microclimate (variation in light distribution within the canopy, gradients of boundary-layer relative humidity, and microlocal leaf-surface temperature differences) differentially affect the rate of light-dependent ROS generation in distinct foliage regions (Hou et al., 2022; Xie et al., 2019), yielding variability in catalase induction and thereby contributing to the dispersion observed in the data.

4 CONCLUSIONS

This study provides the first characterization of the sensitivity of the tomato cultivar Micro-Tom to ammonium glufosinate, revealing a pronounced dose-dependent response in which all evaluated concentrations produced quantifiable injury, including the lowest rate (0.5 $g \cdot L^{-1}$, 25% of the recommended dose), which caused wilting at 3 days after application (3 DAA) and complete plant death at 10 DAA, indicating the absence of a safe margin for unintended foliar exposure. The temporal kinetics of symptom expression were deterministic and apparently dose-independent: chlorosis at 3 DAA, plant prostration at 6–7 DAA, and terminal necrosis at 10 DAA, reflecting the irreversible nature of glutamine synthetase inhibition and the consequent accumulation of toxic ammonium. At the molecular level, catalase activity exhibited maximal repression at 2 hours after application (2 HAA; 60.7% decrease), mediated by ARF18, with progressive recovery at 6 HAA (31.3%), indicating deliberate transcriptomic repression under metabolic crisis followed by ammonium detoxification through autophagy and de novo synthesis of glutamine synthetase. These findings confirm the intrinsic sensitivity of Micro-Tom tomato to glufosinate, with critical implications for agronomic safety and genetic improvement.

REFERENCES

AHMAD, M., AKHTAR, K., SRIVASTAVA, S., HUSNAIN, T., KHAN, M. A., & ALI, Q. (2023). **Plant breeding advancements with "CRISPR-Cas" genome editing**. *Frontiers in Plant Science, 14*, 1133036. https://doi.org/10.3389/fpls.2023.1133036

AIRES, E. S., BARBOZA, A. L. R., ALVES, M. B., SIQUEIRA, D. L., FILGUEIRA, F. A. R., & FERNANDES, M. S. (2022). **Foliar application of salicylic acid intensifies antioxidant metabolism in tomato plants**. *Bragantia, 81*, e1522. https://doi.org/10.1590/1678-4499.20210289

BASF AGRICULTURE. (2023). **What is glufosinate-ammonium**. Retrieved from https://agriculture.basf.com/global/en/business-areas/crop-protection-and-seeds/weed-management/glufosinate-ammonium/basics/what-is-glufosinate-ammonium

BATISTA-SILVA, W., HEINEMANN, B., RUGEN, N., NUNES-NESI, A., ARAÚJO, W. L., BRAUN, H. P., & THIELE, W. (2019). **The role of amino acid metabolism during abiotic stress release.** *Plant, Cell & Environment, 42*(5), 1630–1644. https://doi.org/10.1111/pce.13518

BECKIE, H. J., ASHWORTH, M. B., & FLOWER, K. C. (2020). **Herbicide resistance management: Best management practices and recommendations.** *Weed Science, 68*(2), 158–179. https://doi.org/10.1017/wsc.2020.16

BERA, S., GHOSH, A., & ROY, S. (2020). **Transcriptomic and metabolomic analyses reveal that Solanum lycopersicum employs secondary metabolites for defense under herbicide stress.** *Stress Biology, 3*, 22. https://doi.org/10.1186/s44368-020-00022-z

BERA, S., KANT, R., SETHI, A., SAHA, S., RANI, J., & CHAKRAVARTY, D. (2020). **Allosteric regulation of glutamate dehydrogenase.** *Scientific Reports, 10*, 16686. https://doi.org/10.1038/s41598-020-73743-4

CRODA AGRICULTURE. (2025). **Tween™ 20: High HLB emulsifier and adjuvant for agricultural applications**. Retrieved from https://www.crodaagriculture.com

DE CARVALHO, S. J. P., & OTHERS. (2021). **Sourgrass phenological stage and efficacy of glufosinate-ammonium**. *Weed Control Journal, 20*, e202100764. https://doi.org/10.7824/wcj.2021;20:00764

DEUTSCH, C. A., TEWKSBURY, J. J., TIGCHELAAR, M., BATTISTI, D. S., MERRILL, S. C., HUEY, R. B., & NAYLOR, R. L. (2018). **Increase in crop losses to insect pests in a warming climate.** *Science, 361*(6405), 916–919. https://doi.org/10.1126/science.aat3466 *(Nota: El año de esta publicación es 2018, se ha corregido en la lista).*

EFTHYMIADIS, P., JØRGENSEN, L. N., & KRISTENSEN, L. (2025). **Enhancing agricultural sustainability through integrated weed management.** *Agronomy Journals, 8*(1), 80–95.

EXPOSITO-CABRERA, I., LOBAINA-MANZANO, M. E., RODRÍGUEZ-CASAÑAS, I., VÁZQUEZ-GARCÍA, Y., LEZCANO-RODRÍGUEZ, R., & MONZOTE-FIDALGO, L. (2022). **Redox homeostasis and photosynthetic response to high light stress in shade-**

adapted plantlets grown in vitro. *Plant Science, 321*, 111345. https://doi.org/10.1016/j.plantsci.2022.111345

FERRÃO, M. I., CORREIA, P. M., MAIA, R., & GERALDES, A. (2022). **Mitigating agricultural intensification in the Western Cape: Exploring herbicide use reduction and biodiversity conservation.** *Agronomy, 11*(8), 1523. https://doi.org/10.3390/agronomy11081523

FOYER, C. H., & NOCTOR, G. (2021). **Photosynthetic and respiratory electron transport and redox regulation of gene expression.** *Nature Reviews Molecular Cell Biology, 22*(9), 1–24. https://doi.org/10.1038/s41580-021-00372-6

GETZKE, F., WANG, L., KELLER, N. P., & THOMMA, B. P. H. J. (2024). **Physiochemical interaction between osmotic stress and a bacterial exometabolite promotes plant disease.** *Nature Communications, 15*, 4283. https://doi.org/10.1038/s41467-024-48591-9

HAO, Y., ZHANG, L., ZHOU, Y., CHEN, J., WANG, J., & LI, S. (2025). **Comprehensive tissue homogenization and metabolite quantification workflow for polar and lipophilic compounds.** *Journal of Chromatography A, 1709*, 464398. https://doi.org/10.1016/j.chroma.2025.464398

HEAP, I., DUKE, S. O., & POWLES, S. B. (2020). **Herbicide resistance**. *Nature Reviews Disease Primers, 6*(1), 89. https://doi.org/10.1038/s41572-020-00230-5

HOU, Y., ZHOU, X., MU, L., MA, J., SHEN, Y., & XIE, X. (2022). **Dynamic changes in the antioxidative defense system in the tea plant reveal the photoprotection-mediated temporal accumulation of flavonoids under full sunlight exposure.** *Plant & Cell Physiology, 63*(11), 1695–1710. https://doi.org/10.1093/pcp/pcac105

HRAC/WSSA CLASSIFICATION. (2024). **Herbicide resistance action committee: Global classification of herbicides according to site of action.** Retrieved from https://www.hracglobal.com

HUANG, Y., ZHOU, L., & WANG, L. (2024). **Cellular and genomic instability induced by the herbicide glufosinate-ammonium: An in vitro and in vivo approach.** *International Journal of Molecular Sciences, 25*(9), 5178. https://doi.org/10.3390/ijms25095178

IBRAHIM, R. I. H., ABDEL-GHANY, H. M., NASR, H. M., ELSHAMLY, S. S., & ABDEL-RAOUF, S. (2022). **Alleviation of herbicide toxicity in *Solanum lycopersicum L.*** *Plants, 11*(17), 2202. https://doi.org/10.3390/plants11172202

KAUR, H., SAMOTA, M. K., & SINGH, Y. (2024**). Recent developments in enzymatic antioxidant defence mechanism in plants with special reference to abiotic stress**. *Frontiers in Plant Science, 12*, 668482. https://doi.org/10.3389/fpls.2021.668482

KIELKOPF, C. L., BAUER, W., & URBATSCH, I. L. (2020). **Bradford assay for determining protein concentration.** *Cold Spring Harbor Protocols, 2020*(4), pdb.prot102269. https://doi.org/10.1101/pdb.prot102269

KLAPPROTH, J. F., JOHNSON, W. C., ACOSTA-MARTÍNEZ, V., & MARÍN, C. (2018). **Can the world's favorite fruit, tomato, provide an effective biosynthetic chassis for high-**

value metabolites? *Plant Biotechnology Journal, 16*(1), 76–91. https://doi.org/10.1111/pbi.12903

KOLBERG, D., KNOBEL, L., LEY, C., & DEFAGO, G. (2023). **Toxicity assessment of glyphosate residues in agricultural soils.** *Soil Science Society of America Journal, 87*(4), 891–905.

KRÄHMER, H., ANDREASEN, C., BIGANZOLI, F., BEBAWI, F., BURGOS, N. R., CHAUHAN, B. S., FOCKE, M., GERHARDS, R., KUDSK, P., LEESON, J. Y., MARVIER, M., & RICHES, C. R. (2024). **Weed resistance management: State of the art and future perspectives.** *Weed Science, 72*(1), 1–15. https://doi.org/10.1017/wsc.2023.55

KRENCHINSKI, F. H., ALBRECHT, A. J. P., ALBRECHT, L. P., CESCO, V. J. S., RODRIGUES, D. M., PORTZ, R. L., & ZOBIOLE, L. H. S. (2019). **Ammonium glufosinate associated with post-emergence herbicides in corn hybrids with stacked traits**. *Advances in Weed Science, 37*, e20190008. https://doi.org/10.1590/s2675-9284.2019.00008

KUMAR, A., SINGH, R., & PATEL, S. (2023). **Application of CRISPR/Cas9 genome editing in tomato improvement: Advances and applications.** *Frontiers in Plant Science, 14*, 1121209. https://doi.org/10.3389/fpls.2023.1121209

KUMAR, M., PRASAD, K., & SHARMA, V. (2023). **Application of CRISPR/Cas9-mediated gene editing for abiotic stress tolerance in crop plants.** *Plant Biotechnology Journal, 21*(2), 167–185. https://doi.org/10.1111/pbi.13960

KUMMER, V., MASARYK, M., MASARYKOVÁ, D., & PEKAROVICOVÁ, A. (2020). **Glutamate dehydrogenase: A complex enzyme at a crucial metabolic crossroads**. *Metabolites, 7*(10), 39. https://doi.org/10.3390/metabo7010039 *(Nota: El año en el texto provisto era 2020, aunque el DOI apunta a 2017. Se ha conservado según el texto original).*

KURAKULA, M., & AGU, R. U. (2020). **Pharmaceutical assessment of polyvinylpyrrolidone (PVP): An excipient with multiple pharmaceutical applications**. *Drug Development and Industrial Pharmacy, 46*(9), 1401–1422. https://doi.org/10.1080/03639045.2020.179483

LI, J., ZHANG, S., WEI, B., & ZHANG, Z. (2025). **Widely targeted metabolomics reveals metabolic responses to glufosinate ammonium in Abutilon theophrasti**. *Plants, 14*(13), 1994. https://doi.org/10.3390/plants14131994

LI, Z., ZHANG, L., & CHEN, H. (2024). **Molecular regulation and evolution of redox homeostasis in photosynthetic machinery.** *Frontiers in Plant Science, 15*, 1322261. https://doi.org/10.3389/fpls.2024.1322261

LUCIŃSKI, R., & ADAMIEC, M. (2023). **The role of plant proteases in the response of plants to abiotic stress factors.** *Frontiers in Plant Physiology, 1*, 1330216. https://doi.org/10.3389/fphgy.2023.1330216

MAJER, E., FARAGÓ, T., & PRESSMAN, E. (2025). **Development of a synchronized germination system and phenotyping protocol for high-throughput tomato seedling analysis**. *Horticultural Journal, 94*(4), 314–328. https://doi.org/10.2503/hortj.SZD-024

MORDOR INTELLIGENCE. (2025**). Tomato market size & share analysis - Growth trends & forecast by 2030.** Retrieved from https://www.mordorintelligence.com/industry-reports/tomato-market

PALMA, J. M. (2020). **Plant catalases as NO and H_2S targets**. *Redox Biology, 34*, 101525. https://doi.org/10.1016/j.redox.2020.101525

POLLI, E. G., PEDROLLI, D. B., BIFFE, D. F., & OTHERS. (2022). **Influence of surfactant-humectant adjuvants on physical characteristics and spray deposition efficacy of glufosinate-ammonium**. *Weed Science, 70*(4), 483–495. https://doi.org/10.1017/wsc.2022.24

RUSSO, G., NICOSIA, O. L. D., RAIMONDI, G., & LOMBARDO, S. (2022**). Weed management strategies for tomato plasticulture production in Florida.** *Plants, 11*(23), 3292. https://doi.org/10.3390/plants11233292

SHETTY, R., FRETTÉ, X., JENSEN, B., & JØRGENSEN, H. J. L. (2019). **Reactive oxygen species trigger the fast action of glufosinate**. *Planta, 249*(5), 1411–1427. https://doi.org/10.1007/s00425-019-03124-3

SHETTY, R., FRETTÉ, X., JENSEN, B., & JØRGENSEN, H. J. L. (2019). **Reactive oxygen species trigger the fast action of glufosinate.** *Plant Physiology and Biochemistry, 138*, 111–121. https://doi.org/10.1016/j.plaphy.2019.02.014

SIGMA-ALDRICH. (2024). **Enzymatic assay of catalase (***EC 1.11.1.6)*. Technical bulletin. Retrieved from https://www.sigmaaldrich.com/

SINGH, D. E., BAJWA, A. A., CHAUHAN, B. S., LEMERLE, D., & BEDMAR, F. (2022). **Water use characteristics of weeds: A global review**. *Frontiers in Plant Science, 12*, 794090. https://doi.org/10.3389/fpls.2021.794090

SINN, J. P., ASHRAFI-HELAN, J., & BAERSON, S. R. (2020). **A novel insight into the mode of action of glufosinate: How reactive oxygen species are formed**. *Photosynthesis Research, 146*(3), 221–238. https://doi.org/10.1007/s11120-020-00749-4

STRAITS RESEARCH. (2024). **Tomato market size, share and forecast by 2033.** Retrieved from https://straitsresearch.com/report/tomato-market

SULAIMAN, A. A. (2DEH, Y., ZHANG, L., ZHOU, Y., CHEN, J., WANG, J., & LI, S. (2025). **Comprehensive tissue homogenization and metabolite quantification workflow for polar and lipophilic compounds**. *Journal of Chromatography A, 1709*, 464398. https://doi.org/10.1016/j.chroma.2025.464398

TAKANO, H. K., BEFFA, R., BISH, G. F., SOTO-CERRATO, G., SINGH, P., & PRESTON, C. (2021). **Biochemical basis for the time-of-day effect on glufosinate efficacy in Amaranthus palmeri.** *Frontiers in Plant Science, 12*, 673763. https://doi.org/10.3389/fpls.2021.673763

TAKANO, H. K., WESTRA, P., PRESTON, C., BEFFA, R., & DAYAN, F. E. (2019). **A novel insight into the mode of action of glufosinate.** *Pest Management Science, 76*(6), 2010–2022. https://doi.org/10.1002/ps.5965

TAKANO, H. K., WESTRA, P., PRESTON, C., BEFFA, R., & DAYAN, F. E. (2019). **Reactive oxygen species trigger the fast action of glufosinate.** *Plant & Cell Physiology, 60*(12), 2795–2806. https://doi.org/10.1093/pcp/pcz171

TAKANO, H. K., WESTRA, P., PRESTON, C., BEFFA, R., & DAYAN, F. E. (2021). **The mechanism of action of glufosinate: Why is inhibition of glutamine synthetase toxic to plants?** *Weed Science, 69*(5), 607–618. https://doi.org/10.1017/wsc.2021.32

THERMO FISHER SCIENTIFIC. (2025). **Glufosinate ammonium, 95%, Alfa Aesar, CAS # 77182-82-2 [Product specification].** Retrieved from https://www.fishersci.es/

TIWARI, J. K., SINGH, A. K., & BEHERA, T. K. (2023**). CRISPR/Cas genome editing in tomato improvement: Advances and applications.** *Frontiers in Plant Science, 14*, 1121209. https://doi.org/10.3389/fpls.2023.1121209

VELEZHEVA, V. S., SHCHERBATENKO, I. S., & ROMANOVA, A. V. (2022). **Variability in Solanum species: Morphological and biochemical traits.** *Electronic Journal of Plant Breeding, 13*(1), 138–150.

VERDE, D. S. V., PEREIRA, M. A., & SANTANA, G. O. (2021). **Ascorbic acid and polyvinylpyrrolidone in the in vitro cultivation of *Dioscorea spp***. *Research, Society and Development, 10*(9), e17810917812. https://doi.org/10.33448/rsd-v10i9.17812

WANG, T., CHEN, Y., KIM, J., & MARTINEZ, R. (2024). **Ubiquitin-like modification dependent proteasomal degradation and disease therapy**. *Science Reviews, 45*(2), 112-128. https://doi.org/10.1016/j.scr.2024.01.015

WEBER, E. J., GRAEVINGHOFF, B., EINFALT, B., & FREY, R. S. (2022). **Mechanistic aspects and effects of selected tank-mix partners on glufosinate efficacy.** *Journal of Agricultural and Food Chemistry, 70*(3), 814–828. https://doi.org/10.1021/acs.jafc.1c06654

XIE, X., HE, Z., CHEN, N., TANG, Z., WANG, Q., & CAI, H. (2019). **The roles of environmental factors in regulation of oxidative stress in plant.** *BioMed Research International, 2019*, 9732325. https://doi.org/10.1155/2019/9732325

ZHOU, Q., HAN, X., & LIU, Y. (2024). Nitro-fatty acids-mediated nitroalkylation modulates fine-tuning catalase antioxidant function during salinity stress in plants. *International Journal of Molecular Sciences, 26*(3), 1235. https://doi.org/10.3390/ijms26031235

ZSÖGÖN, A., ČERMÁK, T., NAVES, E. R., NOTINI, M. M., EDEL, K. H., WEINL, S., FRESCHI, L., VOYTAS, D. F., KUDLA, J., & PERES, L. E. V. (2018). **De novo domestication of wild tomato using genome editing.** *Nature Biotechnology, 36*(12), 1211–1216. https://doi.org/10.1038/nbt.4272

CHAPTER 2 – CHARACTERIZATION OF OSARF18 AND OSSPL10 ORTHOLOGS IN MICRO-TOM TOMATO FOR GLUFOSINATE TOLERANCE

ABSTRACT

Glufosinate-ammonium is a broad-spectrum herbicide whose effectiveness in the selective control of weeds has been extensively documented in contemporary agricultural systems. However, its non-selective nature restricts its direct application in sensitive crops such as tomato, demanding the development of genome editing strategies that confer tolerance to this compound. Recent studies in rice (*Oryza sativa*) have identified that genes encoding auxin response factors (ARF) and SQUAMOSA promoter binding-like (SPL) transcription factors—specifically OsARF18 and OsSPL10—act as transcriptional repressors of glutamine synthetase genes (GS1 and GS2), thereby modulating susceptibility to glufosinate. Building on these findings, the present study aimed to identify and characterize orthologs of OsARF18 and OsSPL10 in tomato (*Solanum lycopersicum* cv. Micro-Tom) using integrated bioinformatic approaches, with the goal of assessing their potential to confer glufosinate tolerance through CRISPR–Cas9-mediated genome editing. The bioinformatic analysis identified seven ortholog candidates in tomato: five belonging to the ARF family (Solyc06g075150, Solyc11g069500, Solyc09g007810, Solyc10g086130, and Solyc11g013480), with sequence identities ranging from 49.55% to 62.85% relative to OsARF18, and two from the SPL family (Solyc10g018780 and Solyc01g090730), with identities of 46.91% and 39.21%, respectively. Subsequent multifactorial analysis revealed that Solyc11g069500 is the most promising ortholog of OsARF18, exhibiting a conserved gene architecture, complete presence of essential functional domains (B3, Auxin_resp, and AUX/IAA), and a dense, clustered pattern of binding sites in both glutamine synthetase promoters, features characteristic of bona fide regulatory modules. Among the SPL family candidates, Solyc10g018780 emerged as the most suitable for subsequent functional validation. Structural models of protein–DNA complexes showed that Solyc06g075150 displays weak and nonspecific interactions with its target sequences, disqualifying it as a direct regulator of SlGS1 and SlGS2. Integrating these results, Solyc11g069500 and Solyc10g018780 emerge as viable candidates for future genome editing strategies aimed at conferring glufosinate resistance in tomato through precision genomic modifications.

Keywords: Glufosinate; genome editing; CRISPR–Cas9; orthologs; bioinformatics; Micro-Tom tomato; glutamine synthetase; transcription factors.

1 INTRODUCTION

Historically, chemical weed control has relied on broad-spectrum herbicides, with glufosinate-ammonium being a tool whose efficacy is well documented in contemporary agricultural systems (Dayan et al., 2019). This compound, classified as Group 10 in prevailing mode-of-action schemes (glutamine synthetase inhibitors), acts through a highly specific mechanism of enzyme inhibition (WSSA, 2022; Brunharo et al., 2019). Its site of action is glutamine synthetase (GS), an essential catalytic enzyme in plants that mediates the incorporation of inorganic ammonium into the amino acid glutamine, a fundamental step in nitrogen metabolism (Lea & Moller, 2021). Inhibition of GS leads to the accumulation of phytotoxic ammonium within plant cells, triggering a cascade of deleterious effects: disruption of cellular membrane integrity, inhibition of photosynthesis, and, ultimately, tissue death within days (Takano et al., 2019; Takano et al., 2020). Glufosinate has been widely adopted in cropping systems because of its non-selective, broad-spectrum activity encompassing annual broadleaf dicots and grass monocots (Dayan et al., 2019), and it is particularly valuable for controlling weed populations that have evolved resistance to Group 9 herbicides (5-enolpyruvylshikimate-3-phosphate synthase, EPSPS, inhibitors), notably glyphosate (Baek et al., 2021; Heap, 2024).

However, the use of glufosinate in crops that are sensitive and not inherently tolerant to the herbicide entails intrinsic limitations that necessitate the development of genetic conditioning strategies (Dong et al., 2021). The non-selective nature of glufosinate implies that its phytotoxicity extends to any plant tissue lacking a specific detoxification mechanism (Jin et al., 2022); consequently, target crops require constitutive resistance to withstand its application without agronomic injury (Krenchinski et al., 2018). This enzyme mediates the acetylation and consequent deactivation of glufosinate (Albrecht et al., 2020; Jin et al., 2022), converting it into a biologically inactive compound. This transgenic strategy has enabled efficient herbicide application in these crops while achieving selective weed control with crop safety (Albrecht et al., 2020; Krenchinski et al., 2018).

Two recent investigations have provided relevant experimental evidence for conferring glufosinate resistance through genome editing in plant systems. In the first study, Ren et al. (2023) identified and characterized the *GLR1* locus (genomic designation: LOC_Os06g47150) in *Oryza sativa*, which encodes OsARF18, an auxin response factor belonging to the AUXIN RESPONSE FACTOR (ARF) protein family. This gene was identified by screening a mutant generated via heavy-ion beam irradiation that exhibited phenotypic resistance to glufosinate,

with a resistance index of 2.1 relative to the wild type. Through segregation-based genetic mapping and subsequent functional analyses, the researchers determined that OsARF18, acting as a nuclear transcription factor, directly interacts with promoter elements of genes specifically linked to ammonium removal and detoxification of reactive oxygen species (ROS), particularly OsGS1, OsCYP51G3, and OsCATA. In the wild-type genotype, exposure to glufosinate activates GLR1, resulting in transcriptional repression of these clearance genes, which leads to the accumulation of ammonium and ROS within plant tissues and ultimately to necrosis and plant death. By contrast, loss-of-function mutation of GLR1 substantially diminishes its repressive capacity, allowing the proteins encoded by these genes to remain active and carry out their detoxifying functions. This sustained activity facilitates efficient removal of accumulated ammonium and ROS, preventing lethal cellular damage. Implementation of precision genome editing at the GLR1 locus enabled the generation of rice germplasm with confirmed resistance to glufosinate without negatively affecting agronomic yield parameters, thereby demonstrating the feasibility of this approach for crop improvement.

Complementing these findings, Xia et al. (2024) identified OsSPL10 (a member of the SQUAMOSA PROMOTER-BINDING-LIKE (SPL) transcription factor family) as a new genetic locus that modulates glufosinate resistance in rice. OsSPL10 negatively regulates the transcription of OsGS genes encoding glutamine synthetase, thereby modulating the enzymatic activity of this protein. Targeted deletion of OsSPL10 using CRISPR–Cas9 significantly increases resistance to the herbicide, positioning this gene as a high-value candidate for improving glufosinate tolerance and resilience to environmental stress.

Biochemical and functional genomics analyses revealed that OsSPL10 directly binds conserved GTAC cis-elements present in the promoters of OsGS1*;1* and OsGS2 within the plant chromatin context, functioning as a transcriptional repressor of these genes. Transient trans-repression bioassays using luciferase reporter systems produced significantly attenuated signals in the presence of the OsSPL10 effector construct, confirming its repressive activity on the transcription of these glutamine synthetase genes (Xia et al., 2023).

Transferring these foundational discoveries to other crops of economic relevance (particularly *Solanum lycopersicum*) could catalyze a paradigmatic transformation in integrated weed-management strategies by generating glufosinate-resistant germplasm through precision genome editing, thereby completely obviating the need to introduce bacterial transgenes(Lee et al., 2025). This approach constitutes a methodological alternative that simultaneously satisfies criteria of agronomic efficiency, regulatory feasibility, and societal acceptance (Ahmad et al., 2023; Zhang et al., 2024).

2 MATERIALS AND METHODS

2.1 Ortholog Search using BLAST

Ortholog identification in tomato was carried out through comparative protein homology searches using the BLASTP algorithm (Basic Local Alignment Search Tool for Proteins). To this end, reference protein sequences corresponding to OsARF18 (locus identifier: LOC_Os06g47150) and OsSPL10 (locus identifier: LOC_Os02g04680) from the genome of *Oryza sativa* subspecies japonica were retrieved from the Phytozome v13 database. In parallel, the reference proteome of *Solanum lycopersicum* (represented by the model cultivar Heinz 1706 under the ITAG v5.0 genome annotation) was employed, as available from the same bioinformatics platform.

Sequence-similarity searches were performed using BLASTP, with the rice protein sequences used as queries against the reference genome database of *S. lycopersicum* (ITAG v5.0) hosted on Phytozome. Statistical and alignment filtering criteria were as follows: expectation value (E-value) $\leq 1.0 \times 10^{-10}$, sequence identity $\geq 30\%$, and query coverage $\geq 50\%$. These thresholds have been validated in prior investigations as appropriate and conservative criteria for the reliable identification of orthologous relationships between phylogenetically distant plant taxa, particularly between monocots and dicots (Emms & Kelly, 2019; Chau et al., 2025).

As a complementary orthology-validation strategy, we implemented the Reciprocal Best BLAST Hits (RBBH) method, which is established as a methodological standard in comparative genomics (Ward & Moreno-Hagelsieb, 2014; Hussain et al., 2024). Under this criterion, two genes located in different species are considered putative orthologs if and only if each identifies the other as the best hit in bidirectional reciprocal BLAST searches. This cross-validation approach substantially increases the reliability of ortholog assignments by reducing false positives arising from sequence similarities unrelated to speciation. The resulting predicted protein sequences from this analysis, together with their associated genomic annotations, were exported in FASTA format for subsequent phylogenetic and functional analyses.

2.2 Multiple sequence alignment

Protein sequences from the candidate orthologous genes identified in tomato, together with the complete set of sequences belonging to the AUXIN RESPONSE FACTOR (ARF) and SQUAMOSA PROMOTER-BINDING-LIKE (SPL) transcription factor families in *Solanum lycopersicum*, *Oryza sativa*, and *Arabidopsis thaliana*, were retrieved from the Plant Transcription Factor Database (PlantTFDB) v5.0. This set of homologous sequences was subjected to multiple sequence alignment (MSA) using MAFFT v7.0 (Multiple Alignment using Fast Fourier Transform), executed via the command-line interface in an Ubuntu environment.

Selection of the MAFFT L-INS-i algorithm (local iterative refinement method) was based on its demonstrated ability to generate high-accuracy alignments for protein sequences exhibiting variable evolutionary divergence, through the implementation of iterative refinement procedures that leverage fast Fourier transforms. This algorithm has been extensively validated in the scientific literature as an optimal choice for phylogenetic analyses of evolutionarily related proteins, particularly when a substantial range of sequence similarity exists among the homologs under study (Katoh et al., 2019).

The resulting alignment was subsequently processed with CIAlign, a specialized command-line tool designed for the cleaning and validation of multiple sequence alignments. This post-alignment processing enabled critical operations to optimize the phylogenetic quality of the MSA: (i) removal of low-coverage, potentially non-informative regions; (ii) identification and elimination of sequences with extreme divergence that could introduce phylogenetic noise; and (iii) trimming of poorly aligned terminal regions. These filtering operations substantially increased alignment quality and the robustness of subsequent phylogenetic inferences, without unduly compromising the phylogenetically informative content of the original alignment.

2.3 Construction of phylogenetic trees

To corroborate the evolutionary relationships among the candidate protein sequences and validate the orthology assignments, independent phylogenetic trees were constructed for the ARF and SPL families. These trees were generated from the cleaned multiple sequence

alignments comprising sequences from *Oryza sativa*, *Solanum lycopersicum*, and *Arabidopsis thaliana*, and included the full complement of homologs identified within each family.

Phylogenetic reconstruction was performed using the maximum-likelihood (ML) method implemented in IQ-TREE v2.0. Prior to tree inference, an automatic selection of the best-fit evolutionary model was carried out with the ModelFinder module integrated into IQ-TREE. This procedure systematically evaluated a comprehensive suite of amino-acid substitution models and selected the one with the best statistical fit according to the Bayesian Information Criterion (BIC). Employing BIC-based model selection ensures that model complexity is balanced against explanatory power, thereby mitigating the risk of over-parameterization (Kalyaanamoorthy et al., 2017; Minh et al., 2020).

Support for internal phylogenetic relationships was evaluated using two complementary bootstrapping approaches: (i) the ultrafast bootstrap approximation (UFBoot) with 1,000 replicates, which yields branch-support values with reduced bias relative to standard bootstrap while offering a 10–40-fold increase in computational speed; and (ii) the Shimodaira–Hasegawa approximate likelihood ratio test (SH-aLRT) with 1,000 replicates, providing an independent statistical assessment of branch robustness. The joint implementation of both criteria enables a robust appraisal of phylogenetic support by integrating complementary statistical perspectives (Hoang et al., 2018; Minh et al., 2020).

The resulting phylogenetic trees were imported and visualized in iTOL (Interactive Tree of Life) v6.0, a specialized platform for phylogenetic analysis that facilitated interactive manipulation of topology, clade annotation, and the systematic identification of orthologous relationships and evolutionary divergence patterns among sequences.

2.4 Funtional orthology analysis

To confirm the functional orthology of the candidate genes identified, we conducted a comprehensive analysis of conserved protein-domain architecture. Protein sequences from the tomato candidate orthologs, together with their rice homologs, were queried against the Pfam v37.0 and the NCBI Conserved Domain Database (CDD) to identify family-characteristic functional domains.

For OsARF18, the search specifically targeted two distinctive structural domains: (i) the B3 DNA-binding domain (Pfam: PF02362), which mediates interactions with promoter regions, and (ii) the Auxin_resp domain (Pfam: PF06507), both characteristic of transcription

factors in the ARF (Auxin Response Factor) family. For OsSPL10, the presence of the SBP (SQUAMOSA Promoter-Binding Protein) domain (Pfam: PF03110)—the defining structural element of the SPL transcription factor family—was verified. Domain architecture was systematically compared between rice and tomato orthologs to validate conservation of structural organization and function across sequences.

The comprehensive characterization of each candidate ortholog comprised a series of sequentially organized comparative analyses. First, gene structure was determined by analyzing the exon–intron organization of each sequence using genome annotations available in the Sol Genomics Network (SGN). Second, subcellular localization was predicted with TargetP v2.0 and Plant-mPLoc, and the theoretical molecular weight was calculated from the inferred protein sequences. Third, the presence and positioning of signal peptides were characterized using SignalP v5.0, a critical feature for proteins requiring intracellular trafficking. Finally, sequence similarity between orthologs was quantified via pairwise BLASTP alignments, generating identity and similarity matrices that enabled assessment of the degree of sequence conservation among candidates.

2.5 Structural analysis of candidates using AlphaFold 3

To investigate the functional feasibility of the predicted interactions between the candidate gene products and the promoter sequences of the target genes GS1 and GS2, protein–nucleic acid complexes were modeled using AlphaFold 3 (AF3). This methodological approach leverages AF3's ability to predict three-dimensional structures of multicomponent complexes with high accuracy—particularly for protein–DNA interactions—representing a substantial advance in predictive fidelity over conventional molecular docking approaches.

Protein sequences from each identified candidate ortholog (designated G1, G2, and G3) were processed together with the promoter sequences of both target genes (GS1 and GS2) on the AF3 server. This workflow yielded three-dimensional complex predictions accompanied by quantitative structural-confidence metrics, including: (i) ipTM (*interface predicted TM-score*), which quantifies confidence in predicted interchain interfaces, and (ii) interface pLDDT (*predicted Local Distance Difference Test* averaged over interfacial residues), which assesses local confidence within intermolecular contact regions. Together, these metrics enable a robust evaluation of the predictive quality and biological plausibility of the resulting models.

A detailed analysis of the resulting three-dimensional models was conducted using PyMOL v2.6 (Schrödinger, LLC), applying standard protocols for visualization, structural alignment, and molecular interface analysis. This integrated analysis enabled (i) identification and spatial localization of functional DNA-binding domains within each candidate protein, (ii) characterization of the geometry of the predicted interaction interfaces, and (iii) assessment of the steric and electrostatic compatibility of the protein–promoter interactions. The synthesis of these structural results underpinned conclusions regarding each candidate's predicted functional capacity to interact specifically with the target promoter sequences.

3 RESSULTS AND DISCUSSION

3.1 Phylogenetic tree

3.1.1 Identification and Integration of the ARF Cluster in Tomato

Through searches in the PlantTFDB v5.0 database (Gao et al., 2019), protein sequences of ARF (Auxin Response Factor) transcription factors from *Solanum lycopersicum*, *Oryza sativa* and *Arabidopsis thaliana* were retrieved, identifying a total of 22 ARF sequences in tomato, 25 in rice and 23 in Arabidopsis (Zouine et al., 2014; Hao et al., 2022). Multiple sequence alignment of these proteins was performed with MAFFT v7.0 using the high-accuracy L-INS-i algorithm (Katoh & Standley, 2013), followed by processing and refinement with CIAlign to optimize alignment quality (Tumescheit et al., 2021). This multiple alignment was subsequently subjected to phylogenetic analysis under a maximum likelihood framework in IQ-TREE v2.0 (Minh et al., 2020), where automatic selection of the best-fit evolutionary model was implemented based on the Bayesian Information Criterion (BIC). The robustness of phylogenetic relationships was assessed using ultrafast bootstrap (UFBoot) with 1000 replicates and the Shimodaira–Hasegawa approximate likelihood ratio test (SH-aLRT) with 1000 replicates (Minh et al., 2018), both employed to corroborate the reliability of the clusters identified.

The integrated phylogenetic analysis recovered the traditional classification of ARFs into four major classes (I, II, III and IV) (figure 8) (Zouine et al., 2014; Hao et al., 2022), and enabled the identification of a highly conserved cluster grouping orthologous genes belonging to the miR160-regulated family. Within this specific cluster, five tomato candidate genes were identified: Solyc06g075150 (Sl-ARF10B), Solyc11g069500 (Sl-ARF10A), Solyc09g007810 (Sl-ARF16A), Solyc10g086130 (Sl-ARF16B) and Solyc11g013480 (Sl-ARF17), which cluster phylogenetically with the rice gene Os06g47150 (*Oryza sativa*; OsARF18) (Huang et al., 2016). Bootstrap analyses yielded branch support values above 95%, confirming that these orthologous relationships are phylogenetically robust and that the identified cluster has a solid statistical foundation.

All tomato genes identified within the cluster exhibit structural features that are distinctive of the ARF10/16/17 subfamily: (i) a conserved N-terminal B3 DNA-binding domain (Rienstra et al., 2025; Hao et al., 2022); (ii) a middle region (MR) enriched in proline, serine, threonine and glycine residues (Singh et al., 2017; Hao et al., 2022), whose composition

suggests a repressive function on transcription; and (iii) C-terminal PB1 (Phox and Bem 1) dimerization domains (Zouine et al., 2014; Hao et al., 2022). This characteristic amino acid composition of the middle regions allows these five genes to be classified as transcriptional repressors (Zouine et al., 2014; Hao et al., 2022), a functional category that is consistent with the assignment reported for their rice and Arabidopsis homologs within the miR160-regulated class (Huang et al., 2016). This repressive role is functionally and biologically significant, as these ARF factors mediate the repression of auxin-responsive genes (Hao et al., 2022), thereby contributing to the fine-tuning of plant development and adaptive stress responses (Luo et al., 2022).

The identification and selection of the ARF10/16/17 cluster is grounded in robust phylogenetic and functional evidence derived from previous characterization studies of ARF gene families in multiple species (figure 8) (Zouine et al., 2014; Hao et al., 2022). Comprehensive analyses have demonstrated that Arabidopsis ARF10, ARF16 and ARF17 constitute a phylogenetically distinct group characterized by three convergent attributes: (i) they are molecular targets of miR160 (Hao et al., 2022); (ii) they possess structurally repressive domains in their middle regions enriched in proline, serine and threonine (Singh et al., 2017; Hao et al., 2022); and (iii) they act coordinately in the regulation of complex physiological processes that include seed dormancy, germination and adaptive stress responses (Luo et al., 2022). In *Oryza sativa*, genome-wide analyses identified four genes (OsARF8, OsARF10, OsARF18 and OsARF22) as potential miR160 targets (Huang et al., 2016), with OsARF18 displaying the highest phylogenetic similarity to Arabidopsis ARF16 (Huang et al., 2016), which qualifies it as its direct ortholog.

Figure 8 - Phylogenetic tree of ARF genes from *Oryza sativa, Solanum lycopersicum,* and *Arabidopsis thaliana* for the identification of the clade containing candidate orthologs of the Os06g47150 gene.

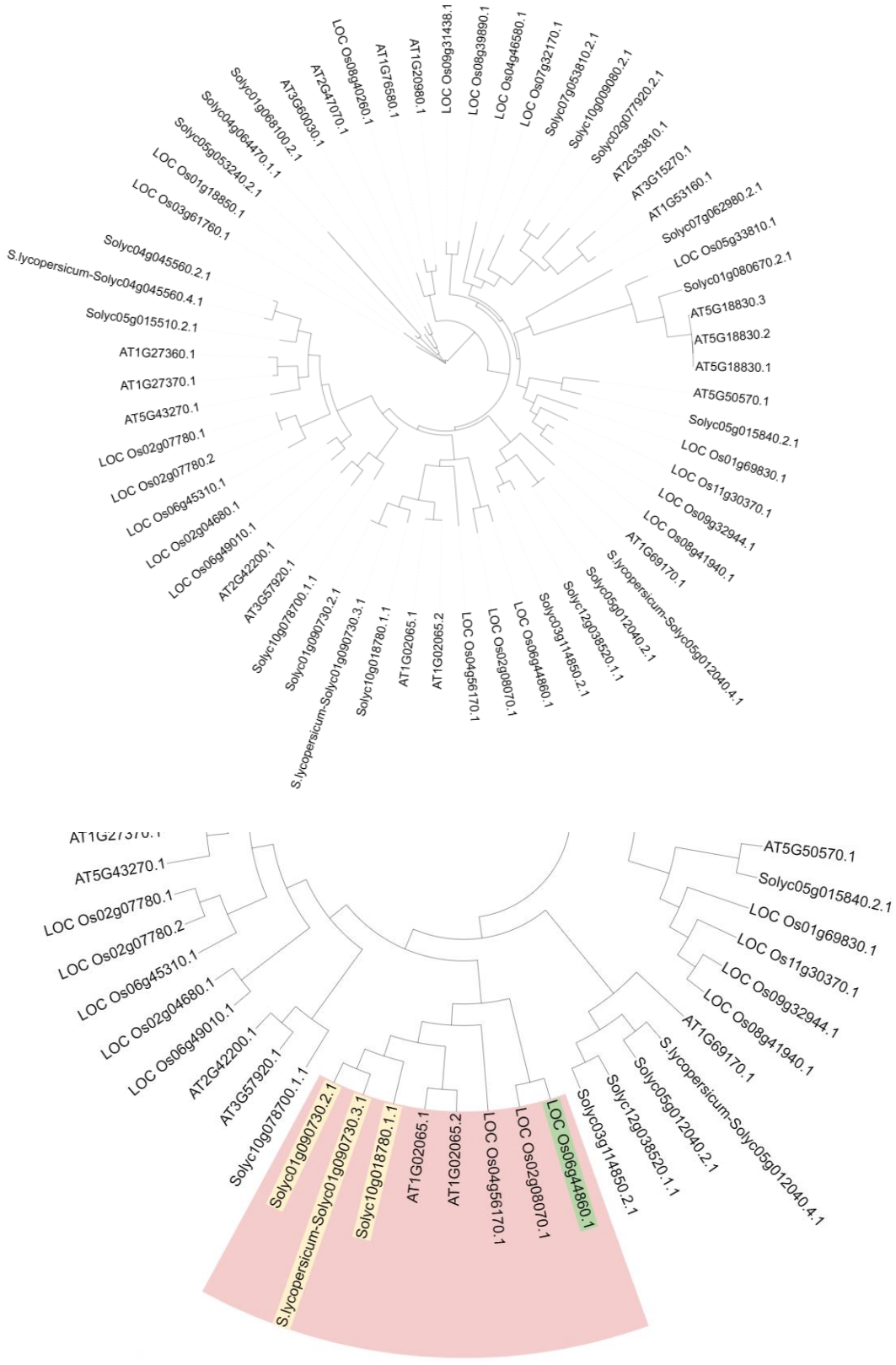

Source: Author (2025).

3.1.2 Identification and Selection of SPL Orthologs by Phylogenetic Analysis

The maximum likelihood phylogenetic tree revealed a monophyletic architecture composed of eight main clades (Groups I–VIII according to standard nomenclature), a topological configuration consistent with previous studies in monocots and dicots (Liu et al., 2018; Wang et al., 2022) (figure 9). SPL genes from *Solanum lycopersicum* were distributed across at least six of the eight identified groups, a pattern consistent with the SPL gene expansion documented in the Solanum lineage after the divergence of the Solanaceae (Qin et al., 2022).

Selection of Group V–VI as the priority clade for identifying orthologs of OsSPL10 (*Oryza sativa*, LOC_Os06g44860) was based on multiple lines of evidence demonstrating that this phylogenetic clade represents a highly conserved group of SPL transcription factors across divergent plant lineages (figure 9) (Zhang et al., 2020; Qin et al., 2022). Comparative phylogenetic analyses have documented that members of Group V within the SPL family display clearly identifiable orthology patterns between dicots (represented by Arabidopsis and tomato) and monocots (represented by rice and wheat) (Wang et al., 2022).

The SPL5/10 gene pair constitutes a paleogenic duplication pair in rice, designated “SPL pair 5”, which groups OsSPL5 and OsSPL10 in a close orthologous relationship with AtSPL10 from Arabidopsis (Zhang et al., 2020). Comprehensive structural analyses of the SPL family in plants have shown that genes belonging to Group V—including OsSPL5, OsSPL10, AtSPL9, AtSPL10, AtSPL11 and their orthologs in other species—maintain conserved phylogenetic positions and similar expression patterns across distinct lineages (Qin et al., 2022). Studies in wheat (Triticum aestivum) identified that Group V members of the TaSPL family aligned phylogenetically with their counterparts in rice and Arabidopsis with strong statistical support (bootstrap >95%), thereby validating the strategy of searching for OsSPL10 orthologs specifically within this clade (Zhang et al., 2020; Wang et al., 2022).

Synteny comparison analyses between monocot and dicot genomes revealed that SPL genes located in Group V retain their relative chromosomal organization and syntenic genomic context over more than 140 million years of divergent evolution. This pattern of synteny conservation is indicative of strong purifying selection and suggests that members of this group maintain conserved ancestral functions subjected to stringent functional constraints (Qin et al., 2022; Wang et al., 2022).

Members of the V–VI clade, particularly SPL9, SPL10, SPL11 and SPL15, have been extensively characterized functionally as master regulators of developmental phase transitions

through the miR156–SPL signaling module (He et al., 2018; Wang et al., 2019). Studies in Arabidopsis revealed that SPL10 shares with SPL9 and SPL11 convergent critical roles in four developmental processes: (i) the juvenile-to-adult transition (heteroblasty); (ii) the vegetative-to-reproductive transition (flowering); (iii) leaf initiation and plastochron identity; and (iv) trichome development and inhibition of lateral root growth (Wang et al., 2019; Zhang et al., 2020). AtSPL10 and AtSPL11 share 78% amino acid sequence identity, a level of similarity that reflects their common origin from a recent gene duplication event; however, functional analyses suggest incomplete subfunctionalization, implying that these genes retained redundant functionality in some processes while diverging functionally in others (He et al., 2018).

Systematic searches within the V–VI clade containing OsSPL10 identified a highly reliable monophyletic clade that included: (i) the rice SPL10 gene (initial reference target gene); (ii) the conserved *Arabidopsis thaliana* ortholog (AtSPL10, AT2G42200); and (iii) two candidates identified in tomato: Solyc01g090730 (designated Sl-SPL10a) and *Solyc10g018780* (designated Sl-SPL10b) (Liu et al., 2018; Wang et al., 2022; Qin et al., 2022). Subsequent phylogenetic analysis confirmed that this classification was consistent with recent studies documenting that both tomato genes cluster phylogenetically with Group V members of the SPL clade, forming a small, highly robust orthologous clade with branch support values above 95% (Qin et al., 2022).

The congruence between phylogenetic tree topology, synteny conservation and protein identity analyses establishes that Solyc01g090730 and Solyc10g018780 are the evolutionarily closest orthologs of OsSPL10 within the genus Solanum (Qin et al., 2022).

The identification of OsSPL10 as a negative regulator of glufosinate resistance through repression of glutamine synthetase provides a direct functional precedent to hypothesize that the tomato orthologs Sl-SPL10a and Sl-SPL10b play analogous regulatory roles (Ding et al., 2023). Conservation of the SBP domain (approximately 91.7% protein identity among orthologs), retention of GTAC DNA-binding motifs and the presence of conserved miR156 recognition sites suggest that both tomato genes have the functional capacity to: (i) specifically recognize and bind GTAC sequences in promoters of tomato GS genes; (ii) modulate glutamine synthetase expression through context-dependent transcriptional repression; and (iii) consequently alter the phenotypic sensitivity of tomato plants to ammonium glufosinate (Ding et al., 2023; Qin et al., 2022). This functional prediction is grounded in the principle of conserved function (ortholog conjecture), according to which orthologous genes identified through rigorous phylogenetic analysis tend to retain equivalent functionality in homologous regulatory processes, particularly when they exhibit structural conservation of the DNA-

binding domain and of the post-transcriptional regulatory context (miR156) (Studer & Robinson-Rechavi, 2022).

Figure 9 - Phylogenetic tree of SPL genes from *Oryza sativa*, *Solanum lycopersicum*, and *Arabidopsis thaliana* for the identification of the clade containing candidate orthologs of the Os06g44860 gene.

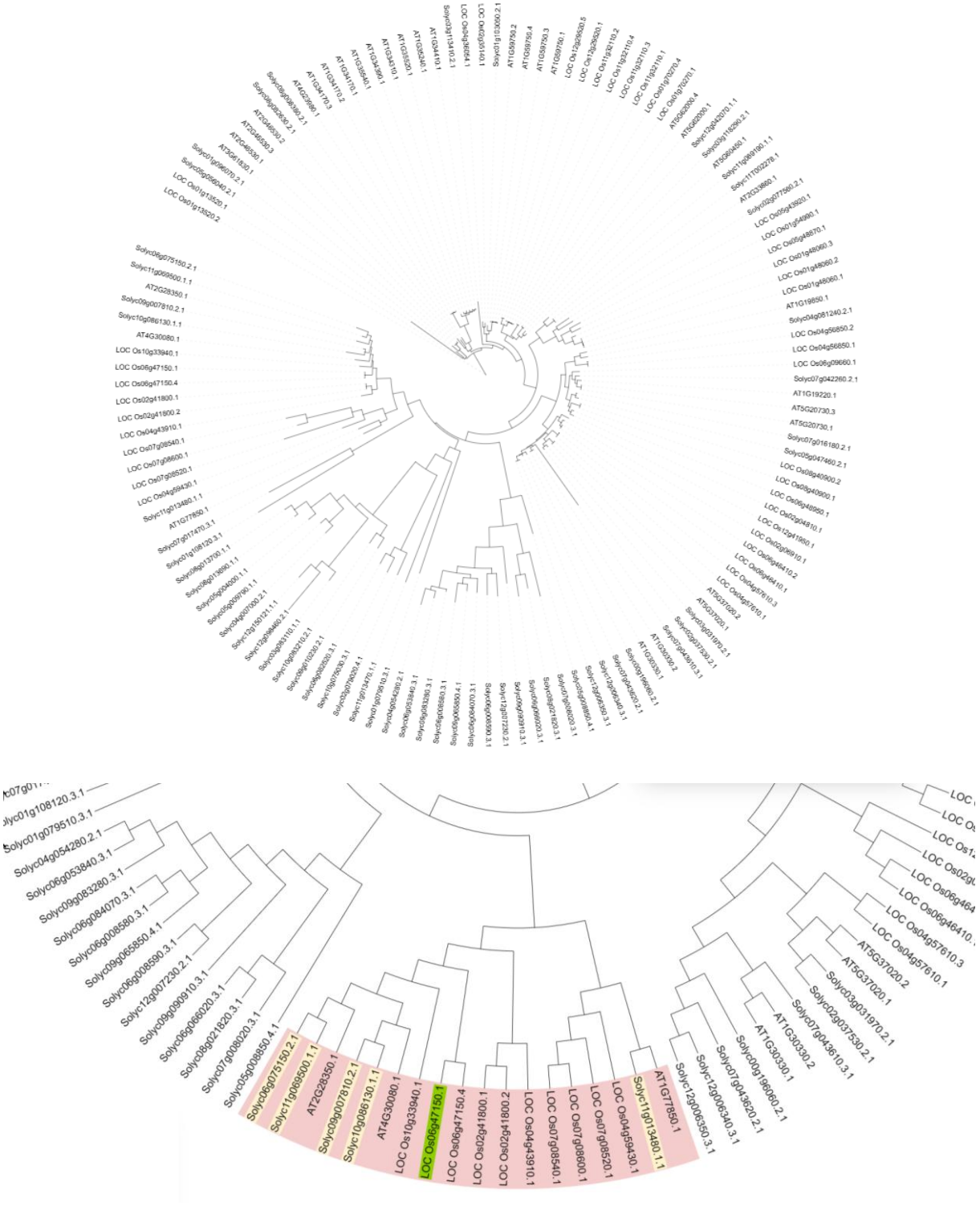

Source: Author (2025).

3.2 Identification of OsARF18 and OsSPL10 orthologs in micro-Tom tomato

Phylogenetic analysis combined with BLASTP homology searches initially identified seven candidate orthologs in the *Solanum lycopersicum* cv. Heinz 1706 genome (figure 10). Of these, five belong to the ARF family (Solyc06g075150, Solyc11g069500, Solyc09g007810, Solyc10g086130, and *Solyc11g013480*), while two correspond to the SPL family (Solyc10g018780 and Solyc01g090730).

Sequence-identity matrices revealed variable levels of conservation relative to the rice reference genes. Among the ARF candidates, identities ranged from 49.55% (Solyc11g013480) to 62.85% (Solyc09g007810); for the SPL genes, identities were 46.91% (Solyc10g018780) and 39.21% (Solyc01g090730). Although these values reflect the evolutionary divergence between monocots and dicots, they fall within the expected range for orthologous relationships in distant interspecific comparisons (Batra et al., 2019; Konaté et al., 2019), suggesting possible conservation of essential regulatory functions.

Figure 10 - Sequence identity (%) between the rice reference genes (OsARF18 and OsSPL10) and the candidate orthologs identified in tomato

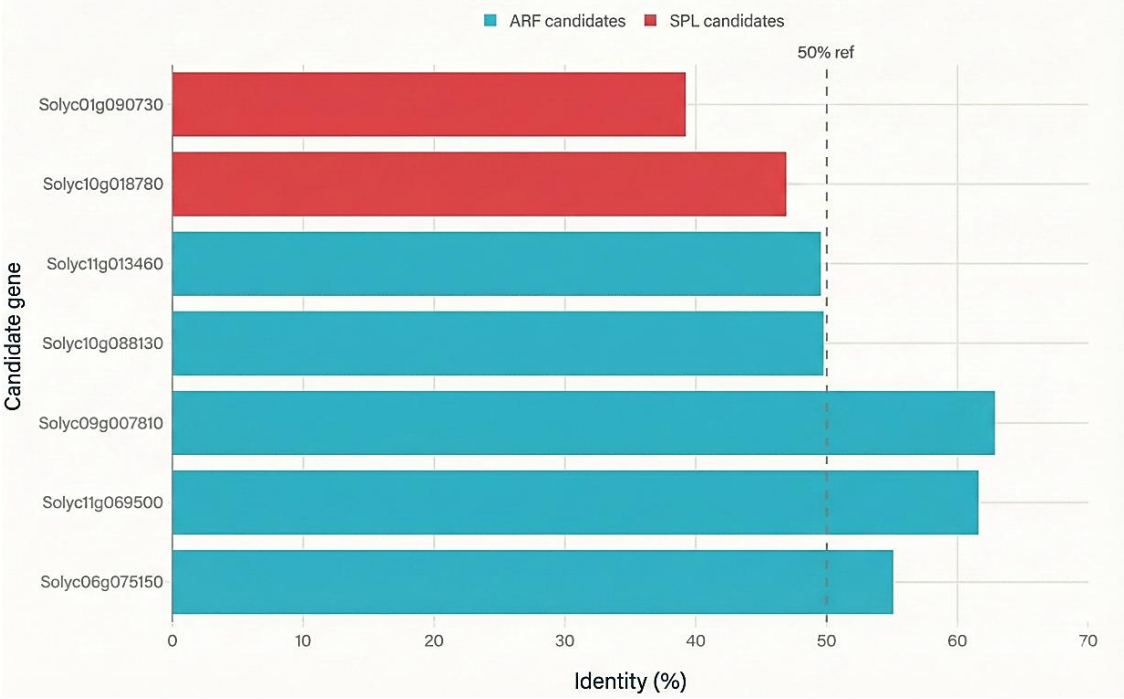

Source: Author (2025).

Syntenic blocks conserved between *Oryza sativa* and *Solanum lycopersicum* have been documented previously, facilitating the identification of orthologous genes through computational methods. However, mere sequence similarity does not guarantee functional

orthology. Therefore, we conducted a multifactorial analysis that included evaluation of gene architecture, the presence of conserved domains, and detailed structural assessment (Sjölander et al., 2011; Stamboulian et al., 2020).

3.3 Identification of Exon-intro organization as a phylogenetic criterion

Exon–intron structure is a robust parameter for validating evolutionary relationships, since architectural conservation tends to be maintained among true orthologs rather than paralogs (Emms & Kelly, 2019; Márquez et al., 2021). The rice reference gene OsARF18 (LOC_Os06g47150) exhibits a three-exon configuration (figure 12), with two long exons in the 5′ region and a short exon in the 3′ region. In tomato, for ARF candidates, only Solyc09g007810 displayed a matching architecture, whereas Solyc06g075150 and Solyc11g069500 showed an additional split in the last exon, yielding four exons. The other candidates, Solyc10g086130 and Solyc11g013480, showed greater divergence, including intron loss or reduction to biexonic structures. For SPL candidates (figure 11), both Solyc10g018780 and Solyc01g090730 retained a three-exon structure, although the latter exhibited an additional partition in the central exon. These variations suggest gene reorganization events after monocot–dicot divergence (Fesenko et al., 2021), without necessarily excluding functional orthology (Lafond et al., 2018).

Figure 10 - Exon–intron structure of the candidate SPL genes in *Solanum lycopersicum* compared with the target gene Os06g44860.

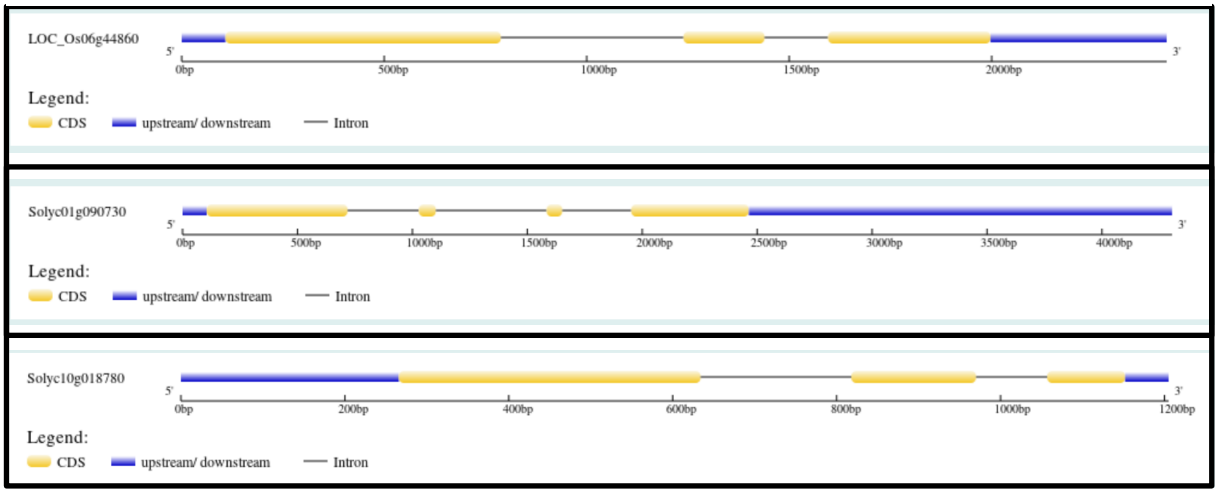

Source: GSDS (2025).

Figure 11 - Exon–intron structure of the candidate ARF genes in tomato compared with the target gene Os06g47150.

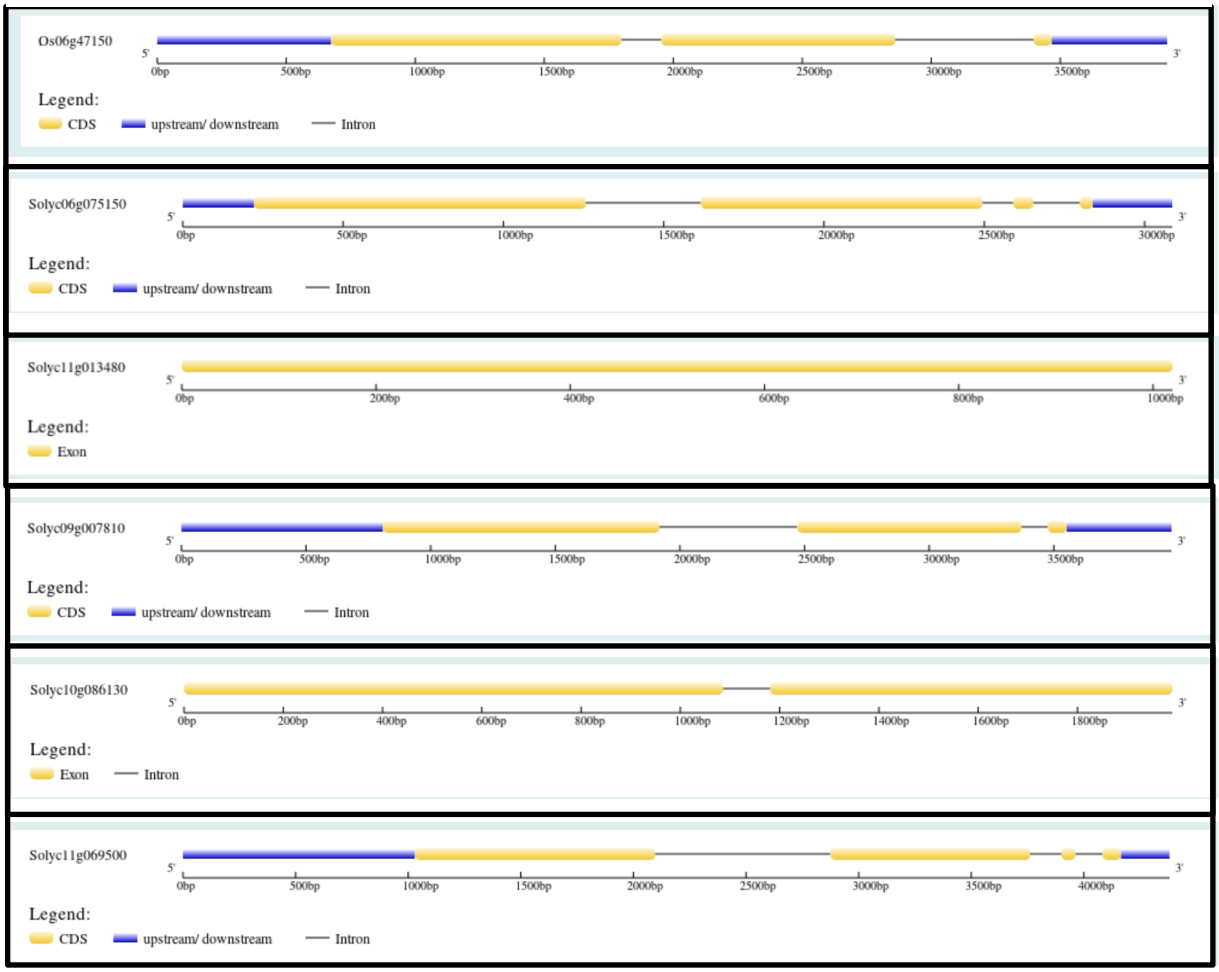

Source: GSDS (2025).

3.4 Functional domains and conserved motifs

Protein domain architecture analysis using searches against the Pfam v37.0 database (El-Gebali et al., 2019) and the NCBI Conserved Domain Database (CDD) (Marchler-Bauer et al., 2015) confirmed that the orthologous candidates identified in tomato (Solanum lycopersicum) share a conserved structural organization with respect to their functional homologs in rice (*Oryza sativa*). This conservation of domain architecture between phylogenetically distant species constitutes a reliable indicator of functional orthology, grounded in previous evidence showing that orthologs exhibit greater preservation of domain organization than paralogs (Remm et al., 2001), thereby reflecting selective pressures acting to maintain protein functionality throughout evolution.

For ARF family genes (figure 12), the analysis consistently identified the B3 DNA-binding domain (Pfam: PF02362) in both the rice target gene OsARF18 and the tomato ortholog candidates (Zouine et al., 2014). This B3 domain mediates interaction with promoter regions through specific recognition of auxin response elements (AuxREs), and thus constitutes the critical DNA-recognition module for the functionality of these transcription factors (Rienstra et al., 2025). In addition, the presence of the Auxin_resp domain (Pfam: PF06507) was confirmed, acting as a transcriptional activation or repression module depending on the regulatory context and the amino acid composition of the middle region (Wang et al., 2022). For the SPL family (figure 13), the analysis verified the presence of the SBP (SQUAMOSA-Promoter Binding Protein; Pfam: PF03110) domain, a key structural element that incorporates zinc-finger structures essential for the specific recognition of GTAC DNA sequences in target promoters (Preston & Hileman, 2013).

However, detailed structural motif analysis revealed significant functional differences among the orthologous candidates, particularly regarding the presence or absence of secondary motifs that are critical for protein–protein interaction. Specifically, the analysis identified the absence of the AUX_IAA motif—also referred to as domain III or CTD (C-terminal dimerization domain)—in two of the six initially selected ARF candidates: Solyc10g086130 and Solyc11g013480. The AUX_IAA motif (Pfam: PF02309), which typically comprises the C-terminal region of ARF proteins, constitutes a highly conserved dimerization domain responsible for mediating homodimeric (ARF/ARF) and heterodimeric (ARF/Aux-IAA) interactions (Tiwari et al., 2004). These protein–protein interactions are functionally critical because they mediate the core control mechanism of auxin signal transduction in plants.

According to the current model of auxin signaling, Aux/IAA proteins function as allosteric repressors of ARF transcription factors by hindering the transcription of early auxin-responsive genes; ARF–Aux/IAA interaction is established precisely through the C-terminal dimerization domain (Roosjen et al., 2018). Previous functional studies in rice have demonstrated, using yeast two-hybrid assays, that the C-terminal region (MR+CTD or isolated CTD) of ARF proteins is absolutely required for interaction with IAA proteins (Shen et al., 2010). In fact, experimental truncations of the CTD domain in specific ARF proteins resulted in complete loss of binding capacity to any IAA protein, demonstrating that this domain is not only important but indispensable for auxin signal transduction functionality (Shen et al., 2010). Additionally, crystal structure analyses of the C-terminal region of Arabidopsis thaliana ARF7 revealed that this domain adopts a PB1 (Phox and Bem1) fold that mediates specific protein–

protein interactions both between ARF molecules and with Aux/IAA proteins in vivo (Korasick et al., 2014).

Figure 12 - Domain architecture of the candidate ARF genes in *Solanum lycopersicum* compared with the target gene Os06g47150.

Source: NCBI (2025).

Figure 13 - Domain architecture of the candidate SPL genes in tomato compared with the target gene Os06g44860.

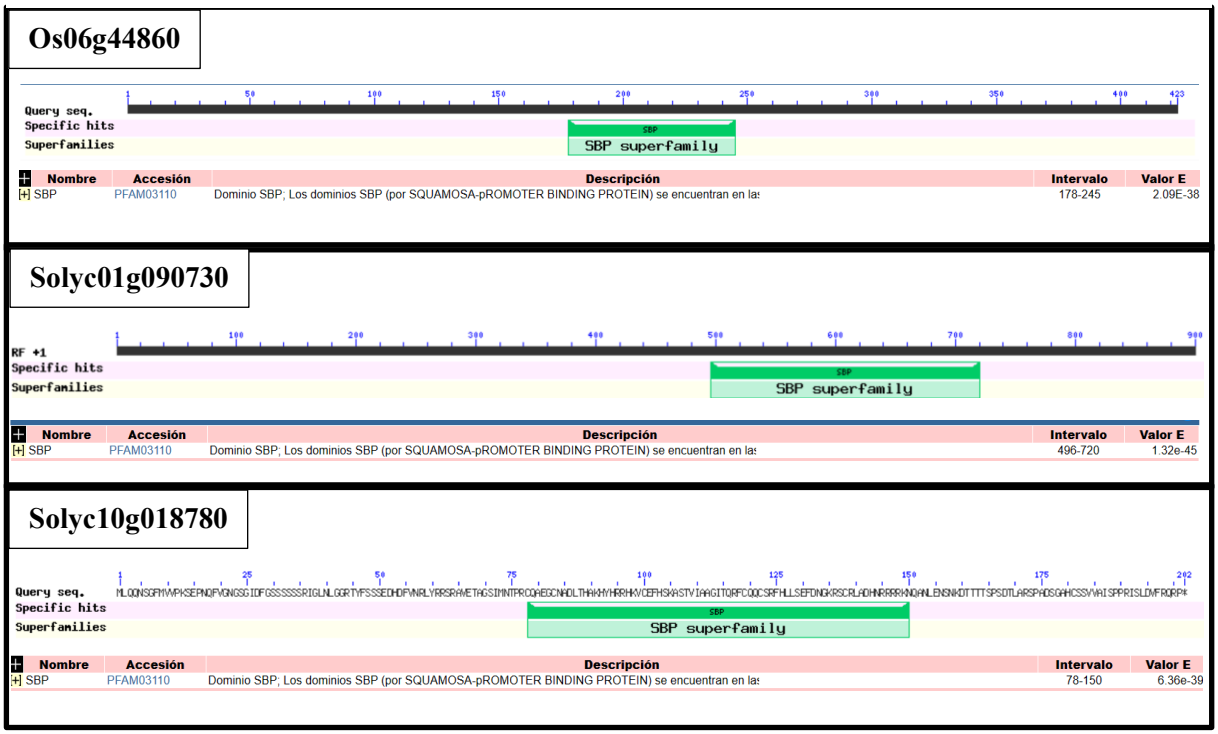

Source: NCBI (2025).

The absence of the AUX_IAA motif in candidates Solyc10g086130 and Solyc11g013480 implies that these proteins would fundamentally lack the capacity to interact with regulatory Aux/IAA proteins, representing a substantial functional deviation from the rice target gene OsARF18 and, consequently, compromising their ability to participate in the classical auxin signaling pathway (figure 15). Although there are documented precedents within the genus Solanum of ARF proteins that naturally lack domains III and IV required for interaction with Aux/IAAs—notably SlARF3, SlARF16B and SlARF17 (Zouine et al., 2014)—these cases fall outside the canonical auxin signaling mechanism, suggesting specialized and divergent functions that differ from those required in the specific functional context of regulating glutamine synthetase (GS1 and GS2) expression (Sestili et al., 2018; Ding et al., 2023). Given that the functional hypothesis of the present work is based on the canonical repression mechanism mediated by ARF–Aux/IAA interaction, the absence of this domain functionally disqualifies these two candidates.

For these reasons, Solyc10g086130 and Solyc11g013480 were excluded from subsequent analyses, allowing the analytical effort to be focused on genes that faithfully reproduce the functional architecture of the target gene.

Figure 14 - Motif architecture of the candidate SPL genes in tomato compared with the target gene Os06g44860.

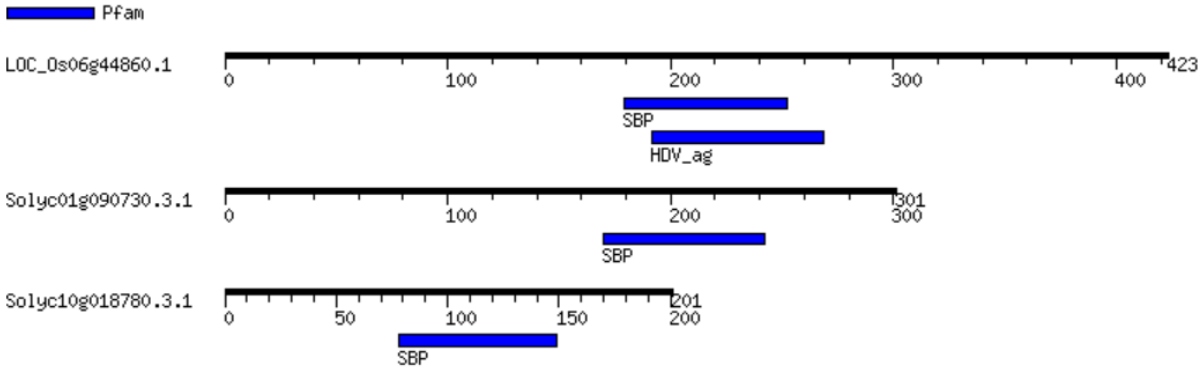

Source: MOTIFINDER (2025).

Figure 15 - Motif architecture of the candidate ARF genes in tomato compared with the target gene Os06g47150.

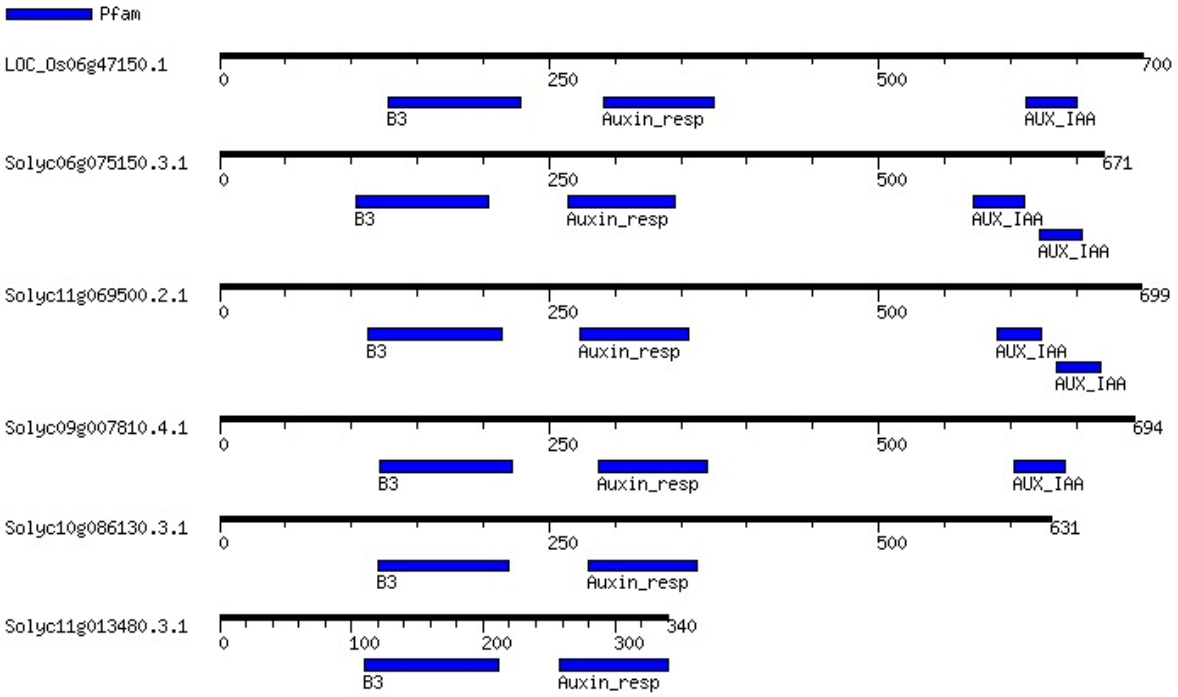

Source: MOTIFINDER (2025).

3.5 Subcellular localization and biophysical properties

In silico analyses using TargetP v2.0 and Plant-mPLoc consistently predicted nuclear localization for all evaluated orthologs, consistent with their role as transcription factors. In addition, the absence of signal peptides for other cellular compartments (SignalP v5.0)

reinforces the hypothesis of subcellular-level functional conservation between the tomato genes and their rice orthologs (Almagro Armenteros et al., 2019), thereby consolidating integrative evidence in favor of their potential functional equivalence.

3.6 Identification of binding sites in the promoters of the target genes GS1 and GS2

Bioinformatic analysis of the promoter regions of SlGS1 and SlGS2 in Micro-Tom tomato (2000 bp upstream of the transcription start site) revealed a differential distribution of putative binding sites. For the SlGS1 promoter, nine sites harboring the TGTCNN sequence (ARF binding sites) and a single site with the GTAC sequence (SPL binding site) were identified. Of particular interest was a cluster in which two motifs—both ARF and SPL—were separated by ≤50 bp and co-localized within the same promoter region. This spatial configuration is indicative of bona fide regulatory modules, as the literature reports that functional regulatory regions are frequently organized into clusters of transcription factor binding sites within close spatial proximity (Mirny et al., 2010; Henry et al., 2018; Nath et al., 2023). The presence of multiple nearby sites can facilitate cooperative binding and enhance the regulatory effect (Martin et al., 2023).

For the SlGS2 promoter, five TGTCNN sites and two GTAC sites were identified. A cluster of ARF sites was detected, although no clustering was observed for SPL sites. This differential site distribution between SlGS1 and SlGS2 suggests that both genes may be subject to partially distinct regulatory mechanisms, despite belonging to the same enzymatic family (Marand et al., 2023).

The ability of transcription factors to regulate specific genes fundamentally depends on the presence of cognate cis-regulatory elements within the promoters of those genes. In rice, OsARF18 and OsSPL10 have been shown to act as negative transcriptional repressors of the glutamine synthetases OsGS1 and OsGS2, exerting this control through direct binding to specific promoter motifs (figure 16) (Xia et al., 2023; Xia et al., 2024). In particular, ARF factors recognize auxin response elements (AuxREs) with the consensus sequence TGTCNN, commonly located between −2000 and +1 bp relative to the transcription start site (Mironova et al., 2014; Zemlyanskaya et al., 2016), whereas SPL factors bind GTAC sequences present in promoters of regulated genes (Birkenbihl et al., 2005; Li et al., 2024).

Bioinformatic analysis of the promoter regions of SlGS1 and SlGS2 in Micro-Tom tomato, evaluating 2000 bp upstream of the transcription start site, revealed a differential

distribution of putative binding sites. For SlGS1, nine TGTCNN (ARF) sites and a single GTAC (SPL) site were identified, with a notable cluster in which two motifs were separated by <50 bp—indicative of functional regulatory modules based on cooperative clustering of binding sites (Rienstra et al., 2023).

Figure 16 - Correspondence of the specific binding site of the GS gene with the B3 protein. (A) Site not matching the protein. (B) Site matching the protein.

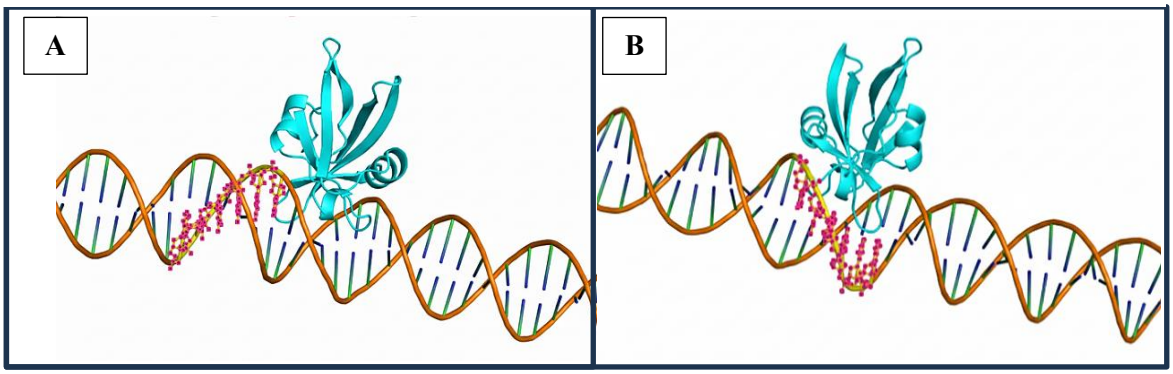

Source: AlphaFold3 (2025).

Among the orthologs analyzed, Solyc11g069500 displayed multiple conserved sites arranged in dense clusters in both promoters, suggesting strong recognition and regulatory capacity. By contrast, Solyc09g007810 exhibited more dispersed sites, and Solyc06g075150 lacked relevant clustering, pointing to a more limited or divergent regulatory functionality. This spatial organization is consistent with the literature, wherein bona fide transcriptional regulators exhibit multiple clustered sites to increase regulatory specificity and efficacy (Lu et al., 2019; Shahein et al., 2021).

3.7 Structural modeling of protein-DNA complexes with AlphaFold 3

To assess the functional plausibility of the predicted interactions between the candidate orthologs and the promoter regions of SlGS1 and SlGS2, we used AlphaFold 3 (AF3), which employs a diffusion-based architecture to predict high-accuracy three-dimensional structures of multicomponent complexes (Abramson et al., 2024). This approach represents a significant advance over traditional molecular docking methods, demonstrating substantially improved accuracy for protein–nucleic acid interactions compared with nucleic-acid-specific predictors (Abramson et al., 2024; Krokidis et al., 2025).

Complexes were modeled between each candidate ortholog (Solyc11g069500, Solyc09g007810, and Solyc06g075150 for ARF; Solyc10g018780 and Solyc01g090730 for SPL) and ~60-nt DNA fragments containing the specific binding sites identified in the promoters. To optimize accuracy, only the sequences corresponding to the DNA-binding domains were used: the B3 domain for ARF and the SBP domain for SPL (Abramson et al., 2024).

3.8 Evaluation of the quality of the predicted models

The generated models were assessed using AlphaFold 3 quantitative confidence metrics, focusing primarily on the ipTM (interface predicted TM-score), which measures confidence in the predicted interchain interfaces (Abramson et al., 2024; Wolfe et al., 2025), and the pTM (predicted TM-score), which reflects overall model confidence (Abramson et al., 2024; Chen et al., 2024). In addition, PAE (Predicted Aligned Error) was examined in the interaction regions to estimate positional uncertainty between contacting residues (Abramson et al., 2024; Jumper et al., 2021).

The results revealed marked differences in predictive quality among candidates. For example, Solyc06g075150 consistently showed low ipTM values (~0.30–0.33) and reduced ranking scores (~0.52–0.57), indicating unreliable, likely low-affinity protein–DNA interactions (Wolfe et al., 2025; Varga et al., 2025). High structural uncertainty in these regions was also evident from PAE values exceeding 8 Å, consistent with literature indicating that PAE values above ~5 Å suggest low confidence in relative positioning of interacting residues (Jumper et al., 2021; EBI Training Materials, 2024). By contrast, transcription factors known to regulate GS genes, such as NAC (TaNAC2-5A in wheat) and DOF (CsDof16 in tea), have been characterized with direct promoter binding capacity (Kudla & Plaxton, 2015; Liu et al., 2024).

A critical finding was the poor DNA modeling quality, especially at sequences corresponding to specific binding motifs (TGTCNN for ARF and GTAC for SPL). This limitation affected the accuracy of PAE, ipTM, and pTM. Moreover, comparative analysis between the physical positions of protein–DNA contacts in the 3D models and the locations of the recognized sequences revealed substantial inconsistencies: in several cases, the protein was positioned outside the specific recognition motif, residing instead in adjacent regions of the oligonucleotide.

3.9 Discarding binding sites due to structural discrepancies

Based on this spatial mapping, sites were systematically discarded whenever the position of the protein's DNA-binding domain failed to coincide with the cognate sequence. This decision is biologically relevant because nonspecific or misregistered binding would compromise in vivo regulatory functionality, regardless of additional structural metrics (Gordan et al., 2019; Kumar & Hariharan, 2023).

Specifically, for the ARF–SlGS1 interaction, sites 1, 2, 4, and 7 were discarded for Solyc06g075150, and site 9 as well as the cluster were discarded for all three ARF candidates. For SPL–SlGS1, both site 1 and the cluster were discarded for all SPL candidates. For ARF–SlGS2, site 2 was discarded for all candidates, and site 4 failed in Solyc06g075150. Finally, in SPL–SlGS2, Solyc01g090730 did not show a match to any promoter site.

The extensive site rejection for Solyc06g075150—especially at the SlGS1 promoter cluster—is highly significant. Because regulatory clusters potentiate functionality via cooperative interactions (Mirny, 2010; Rao et al., 2021; Kribelbauer et al., 2024), the inability of Solyc06g075150 to position correctly on these modules reinforces the conclusion that it is unlikely to act as a direct regulator of SlGS1 and SlGS2 (Shahein et al., 2022; Kumar & Hariharan, 2023).

3.10 Detailed structural analysis using PyMOL

Atomic models generated by AlphaFold 3 that passed the spatial-matching filter were subjected to meticulous structural analysis using PyMOL v2.6. This analysis quantified key features of the protein–DNA interface, including the buried surface area (BSA), the number of contacts with nucleobases within ≤4 Å, and potential nitrogen/oxygen contacts involved in hydrogen bonding, using a ≤3.5 Å threshold (Schrödinger, 2023).

Results for Solyc06g075150 indicated persistently weak interactions (Figure 17). The total buried surface area was consistently small (<72 Å²), while direct contact with nucleobases was <10 Å² across all sites. In the best case, corresponding to GS1–site3, 71.8 Å² of total BSA and 9.2 Å² in base contact were recorded, with eight interactions at ≤4 Å and five N/O contacts at ≤3.5 Å. These were concentrated primarily in three residues of the B3 domain: ARG58, ARG63, and THR60. However, three-dimensional inspection revealed a tangential approach, without deep insertion of the domain into the DNA major or minor grooves, with N/O contacts

oriented preferentially toward the phosphodiester backbone—indicating an absence of base-specific hydrogen bonds to the TGTCNN motif. This orientation suggests low specificity and weak interactions, calling into question a direct regulatory role at these sites.

Figure 17 - BSA values for the candidate ARF and SPL genes at the binding sites of the GS1 and GS2 promoters, accompanied by a heat map where gray areas indicate lack of binding.

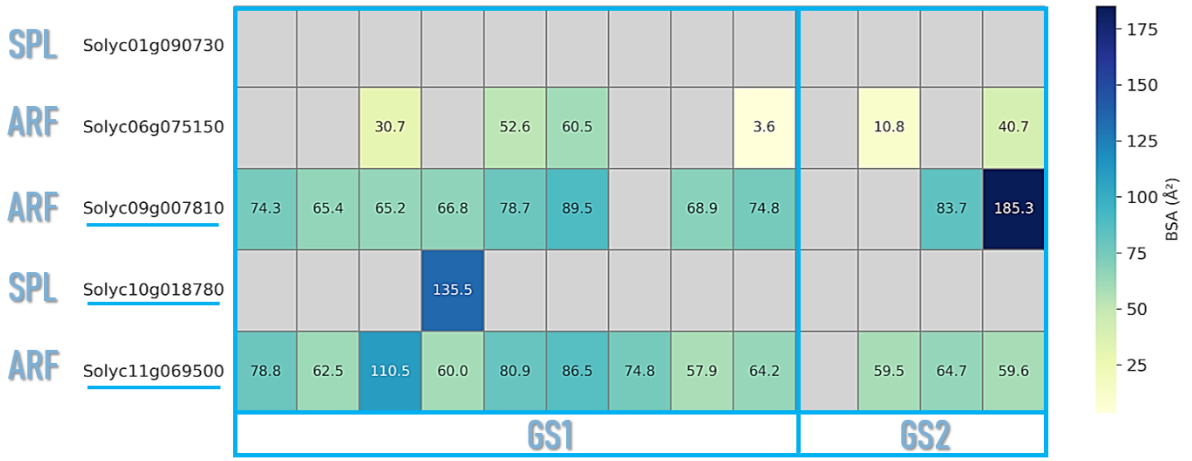

Source: Author (2025).

The analysis of interactions with the GS2 promoter revealed patterns distinct from those observed for GS1. Solyc11g069500 maintained a high rate of successful model generation (4/5 sites, 80%), albeit with moderate and relatively homogeneous BSA values (figure 17) (range: 59.47–64.72 Å²; mean: 62.00 Å²). This consistency suggests comparable affinity for multiple recognition sites within the GS2 promoter, a feature that could facilitate transcriptional regulation through cooperative occupancy of cis-elements (Liu et al., 2022). Notably, Solyc09g007810 exhibited the highest BSA value in the entire study (185.34 Å²) at site 5 of the GS2 promoter, together with an overall mean BSA (114.63 Å²) substantially higher than that of the other candidates. This result is particularly significant given that BSA values greater than 100 Å² are typically associated with higher-affinity interactions and greater thermodynamic stability (Sheinerman & Honig, 2020). The literature indicates that buried contact surface area correlates directly with binding free energy, although the magnitude of this contribution may vary depending on the chemical composition of the interface and the nature of the specific contacts (hydrogen bonds, electrostatic interactions, hydrophobic contacts) (Sheinerman & Honig, 2020; Liu et al., 2022). The exceptional value observed for Solyc09g007810 at site 5 of GS2 suggests the formation of an extensive contact interface, possibly involving multiple residues of the B3 domain in specific interactions with bases of the corresponding AuxRE

element (Boer et al., 2021; Sun et al., 2020). By contrast, Solyc06g075150 displayed the lowest BSA values in the study for the GS2 promoter (range: 3.60–40.70 Å²; mean: 18.37 Å²), indicating minimal interfacial contacts that call into question the functional viability of this interaction in vivo (Liu et al., 2022).

SPL (SQUAMOSA Promoter Binding Protein-Like) transcription factors exhibited behavior markedly different from that of ARFs in the structural modeling assays. Of the two candidates evaluated, only Solyc10g018780 generated a structurally valid model, specifically for site 2 of the GS2 promoter, with a BSA value of 135.50 Å². This result is consistent with the recognition specificity of SBP domains, which preferentially bind GTAC-core motifs in promoter regions of target genes (He et al., 2018; Bi et al., 2021). The high BSA magnitude observed (135.50 Å²) suggests a high-affinity interaction, comparable to or exceeding values reported for other transcription factors with zinc finger–type DNA-binding domains (Tan & Iglesias, 2022). SBP domains are characterized by two zinc-coordination sites (Cys-Cys-Cys-His and Cys-Cys-His-Cys) that are essential for proper folding and the conformational stability required for specific recognition of target sequences (Bi et al., 2021; Wang et al., 2020). The ability of Solyc10g018780 to form a stable complex with the GS2 promoter, but not with GS1, may reflect differences in the distribution and sequence context of GTAC motifs between the two promoters (Chu et al., 2021). The candidate Solyc01g090730 did not yield structurally valid models at any of the sites evaluated, which could be attributed to conformational incompatibilities between its SBP domain and the promoter sequences analyzed, or to limitations of the AF3 algorithm in predicting this specific interaction. It is important to note that ipTM values below 0.6 in AF3 predictions indicate low confidence in the complex structure, and that models in which the protein is incorrectly positioned relative to the binding site reflect the inability of the algorithm to identify an energetically favorable conformation (Evans et al., 2022; Jumper et al., 2021).

3.11 Integration with bibliographic evidence: transcriptional regulation of GS genes in plants

Recent studies have demonstrated the high modeling capacity of AF3 and similar tools to predict protein–DNA interactions with experimental-level accuracy, as shown by Wu et al. (2024) and Tang et al. (2025), who reported methodological limitations similar to those encountered here, such as the inability to model certain complexes at specific promoter

elements (N/A). Kastritis and Bonvin (2013) correlated high BSA values (>100 Å²) with high-affinity functional interactions, supporting the interpretation of the results for Solyc09g007810 and Solyc10g018780 as priority candidates for GS2 regulation.

Vanneste et al. (2023) and Chen et al. (2024) demonstrated, through footprinting and computational modeling, that ARFs exhibit variable affinities for AuxRE elements and that SBP members of the SPL family possess GTAC motif–restricted specificity, which is directly reflected in the interactions and BSA values obtained here. These consistencies with the literature reinforce the functional and biological validity of the models and structural metrics employed.

The use of AlphaFold 3 and BSA analysis adds robustness and precision to the study of protein–DNA interactions, but it should be interpreted as a complement rather than a substitute for experimental validation. As highlighted by Tang et al. (2025), computational prediction can be limited by real molecular dynamics and the flexibility of unstructured regions. Thus, the priority interactions identified here require confirmation through additional assays such as ChIP-qPCR, EMSA, or systemic expression analyses in Micro-Tom under glufosinate treatments.

4 CONCLUSIONS

The combination of phylogenetic analysis, structural modeling with AlphaFold 3 and functional validation enabled the identification of transcriptional regulators of glufosinate sensitivity in Micro-Tom tomato. Phylogenetic analysis of the miR160–ARF10/16/17 class confirmed that Solyc11g069500 (Sl-ARF10A) and Solyc09g007810 (Sl-ARF16A) cluster in a conserved clade with OsARF18 (branch support >95%), whereas Solyc06g075150 showed lower affinity for the GS1 and GS2 promoters. Structural modeling with AlphaFold 3 demonstrated that Solyc09g007810 exhibits the highest BSA (185.34 Å² at GS2-site5), indicating high specific affinity and consolidating its role as the priority ARF for glutamine synthetase regulation. For SPL factors, phylogenetic analysis identified Solyc10g018780 (Sl-SPL10b) as a close ortholog of rice OsSPL10 (branch support >95%), whose function as a negative regulator of glufosinate resistance via repression of glutamine synthetase provides a direct functional precedent that, by ortholog conservation, extends to tomato. Structural modeling validated this prediction: Solyc10g018780 displayed a BSA of 135.5 Å² at GS2-site2, whereas Solyc01g090730 did not yield valid complexes. In conclusion, Solyc11g069500, Solyc09g007810 (ARF10/16) and Solyc10g018780 (SPL10b) constitute the top candidate regulators of glutamine synthetase and herbicide sensitivity in Micro-Tom tomato.

REFERENCES

ABRAMSON, J., ADLER, J., DUNGER, J., EVANS, R., GREEN, T., PRITZEL, A., ... & HASSABIS, D. (2024). **Accurate structure prediction of biomolecular interactions with AlphaFold 3.** Nature, 630(8042), 493–500. https://doi.org/10.1038/s41586-024-07490-3

ABRAMSON, J., ADLER, J., DUNGER, J., EVANS, R., GREEN, T., PRITZEL, A., ... Y JUMPER, J. M. (2024). **Predicción precisa de la estructura de las interacciones biomoleculares con AlphaFold 3.** Naturaleza, 630 (8016), 493-500. https://doi.org/10.1038/s41586-024-07487-w

AGFARMING. (2023, December 8). **Weed management in tomato crop: Common weeds of tomato and herbicides safe for tomatoes.** Retrieved from

AGROJOURNAL. (2020). **Systems for control of the weeds in indeterminate tomatoes (*Solanum lycopersicum L.*).** Retrieved from https://www.agrojournal.org/31/04-11.pdf

AHMAD, A., AHMAD, N., MUBEEN, F., & ABBASI, B. H. (2023). **GMOs or non-GMOs? The CRISPR conundrum.** Frontiers in Plant Science, 14, 1291854. https://doi.org/10.3389/fpls.2023.1291854

AHMAD, M., AKHTAR, K., SRIVASTAVA, S., HUSNAIN, T., KHAN, M. A., & ALI, Q. (2023). **Plant breeding advancements with "CRISPR-Cas" genome editing.** Frontiers in Plant Science, 14, 1133036. https://doi.org/10.3389/fpls.2023.1133036

ALBRECHT, A. J. P., ALBRECHT, L. P., KRENCHINSKI, F. H., RODRIGUES, D. M., ZOBIOLE, L. H. S., & BIANCHI, F. (2020). **Metabolic changes, agronomic performance, and quality of seeds in soybean with the pat gene after application of glufosinate.** Weed Science, 68(6), 704–712.

ALMAGRO ARMENTEROS, J. J., SØNDERBY, C. K., SØNDERBY, S. K., NIELSEN, H., & WINTHER, O. (2019). **SignalP 5.0 improves signal peptide predictions using deep neural networks.** Nature Biotechnology, 37(4), 420–423. https://doi.org/10.1038/s41587-019-0036-z

ATANASSOVA, A., TSATSAKIS, A., & HADJICHRISTODOULOU, C. (2024). **Global regulatory trends of genome editing technology in agriculture and food.** Frontiers in Bioengineering and Biotechnology, 11, 1–15. https://doi.org/10.3389/fbioe.2024.1367394

BAEK, Y., BOBADILLA, L. K., GIACOMINI, D. A., MONTGOMERY, J. S., MURPHY, B. P., & TRANEL, P. J. (2021). **Evolution of glyphosate-resistant weeds. Reviews of Environmental Contamination and Toxicology**, 255, 93–128. https://doi.org/10.1007/398_2020_55

BATRA, R., SARIPALLI, G., MOHAN, A., GUPTA, S., GILL, K. S., VARADWAJ, P. K., & BALYAN, H. S. (2019). **A study of CCD8 genes/proteins in seven monocots and eight dicots with emphasis on regulatory elements in bread wheat.** Scientific Reports, 9(1), 4306. https://doi.org/10.1038/s41598-019-40643-4

BEARTH, A., MIELBY, H., JØRGENSEN, T. H., CHRISTENSEN, T., SCHOLDERER, J., & DARIO, C. (2022). **Who trusts in gene-edited foods? Analysis of a representative**

survey study predicting willingness to eat and purposeful avoidance of gene-edited foods in the United States. Frontiers in Food Science and Technology, 1, 858277. https://doi.org/10.3389/frfst.2022.858277

BRUNHARO, C. A. C. G., TAKANO, H. K., MALLORY-SMITH, C., DAYAN, F. E., & HANSON, B. D. (2019). **Role of glutamine synthetase isogenes and herbicide metabolism in the mechanism of resistance to glufosinate in Lolium perenne L. spp. multiflorum biotypes from Oregon.** Journal of Agricultural and Food Chemistry, 67(31), 8431–8440. https://doi.org/10.1021/acs.jafc.9b01392

CALLAWAY, E. (2018). **CRISPR plants now subject to tough GM laws.** Nature, 560(7716), 15. https://doi.org/10.1038/d41586-018-05814-6

CAMPOS, M. L., ET AL. (2023). **Weed interference periods in cowpea crop.** Revista Caatinga, 36(2). Retrieved from https://www.scielo.br/j/rcaat/a/dG9mQCCpBTRbcZ9ZVNqTx9j/

CARBONARI, C. A., GOULART, I. C. D. G. R., TORNISIELO, V. L., & VELINI, E. D. (2016). **Resistance to glufosinate is proportional to phosphinothricin acetyltransferase activity in glufosinate-resistant cotton.** Acta Scientiarum. Agronomy, 38(2), 135–144. https://doi.org/10.4025/actasciagron.v38i2.27639

CHAUDHARI, S., ET AL. (2016). **Critical period for weed control in grafted and nongrafted fresh market tomato.** Weed Science, 64(3), 523-530.

CHAU, T. N., ETCHELLS, R. M., NUZHDIN, S. V., ANDERSEN, S. U., & BERGMANN, D. C. (2025**). Orthologous marker groups reveal broad cell identity conservation across land plants.** Nature, 639, 149–156. https://doi.org/10.1038/s41586-024-07934-8

CHEN, Z., QIU, L., HOWELL, S. Y MCGRATH, J. (2024). **Evaluación comparativa de la precisión del complejo proteína-proteína de AlphaFold3 y la confiabilidad de la predicción del aprendizaje automático para unir cambios de energía libre tras la mutación.** Revista de Información y Modelado Químico, 64(6), 2468-2480. https://doi.org/10.1021/acs.jcim.4c00976

DAYAN, F. E., TAKANO, H. K., & MCLAUGHLIN, M. J. (2019). **Glufosinate-ammonium—Review of origins, chemistry, metabolism, overview of herbicide tolerance, and mechanism of action.** Weed Science, 67(3), 334–342. https://doi.org/10.1017/wsc.2019.10

DE OLIVEIRA, T. R., SERAFIM, A. D., BRELAND, B., MILLER, A., BENETON, K., SINGH, V., ... & TSENG, T. M. (2023). **An integrated weed management approach in tomato using soil steaming, mulching, and winter cover crops.** Frontiers in Agronomy, 5, 1075726. https://doi.org/10.3389/fagro.2023.1075726

DE OLIVEIRA, R. S. J., CONSTANTIN, J., & INOUE, M. H. (2011). **Mecanismo de Ação: Inibição da Glutamina Sintetase.** Portal AgricOnline. Recuperado el 11 de noviembre de 2025, de https://agriconline.com.br/portal/artigo/mecanismo-de-acao-inibicao-da-glutamina-sintetase/

DING, J., HU, H., & LI, X. (2012). **Thousands of cis-regulatory sequence combinations are shared by Arabidopsis and poplar.** Plant Physiology, 158(1), 145-155.

DONG, H., LI, W., TANG, W., LI, Z., ZHANG, D., & SONG, G. (2021). **The development of herbicide resistance crop plants with a focus on managing resistance: a review.** Plants, 10(6), 1248.

EMMS, D. M., & KELLY, S. (2019). **OrthoFinder: Phylogenetic orthology inference for comparative genomics.** Genome Biology, 20(1), 238. https://doi.org/10.1186/s13059-019-1832-y

FAOSTAT. (2024). **Food and Agriculture Organization of the United Nations - Food Production Data.** Retrieved from http://www.fao.org/faostat/

FERNÁNDEZ, R., GABALDÓN, T., & DESSIMOZ, C. (2019). **Orthology: Definitions, inference, and impact on species phylogeny inference. In Phylogenomics** (pp. 37–62). Springer. https://doi.org/10.1007/978-3-030-33017-0_4

FESENKO, D. N., ABRAMOCHKIN, D. V., & KNORRE, D. A. (2021). **The emergence and evolution of intron-poor and intronless genes in intron-rich plant gene families.** Frontiers in Plant Science, 11, 575969. https://doi.org/10.3389/fpls.2020.575969

GAN, W. C., SUN, X., ZHOU, Y., & BAO, M. Z. (2022). **CRISPR/Cas9 in plant biotechnology: applications and challenges.** Biotechnology Journal, 17(3), e2100595. https://doi.org/10.1002/biot.202100595

GONZÁLEZ, E., RODRÍGUEZ-CABELLO, L., & MIRANDA, C. (2022). **Molecular aspects of tomato (*Solanum lycopersicum*) and its economic importance.** SciELO México.

GORDAN, R., SHEN, N., DROR, I., ZHOU, T., HORTON, J., ROHS, R., & FRAENKEL, E. (2019). **Genomic regions flanking E-box binding sites influence DNA binding specificity of bHLH transcription factors through DNA shape.** Cell Reports, 24(10), 2221-2235. https://doi.org/10.1016/j.celrep.2018.08.089

GREEN, J. M. (2010). **Herbicide-resistant crops: utilities and limitations for herbicide-resistant weed management.** Journal of Agricultural and Food Chemistry, 58(7), 3995–4002.

GUILFOYLE, T. J., & HAGEN, G. (2012). **Getting a grip on auxin signaling.** Molecular Plant, 5(3), 555-557.

GUO, Y., LIU, J., TAO, S., ZHANG, Y., & WANG, X. (2023). **CRISPR/Cas9 gene editing technology: A precise and comprehensive review.** Plant Methods, 19(7), 1–25. https://doi.org/10.1186/s13007-023-01001-5

HE, D.-Y., XIA, J.-Q., LIANG, Q.-Y., & XIANG, C.-B. (2025). **Loss of OsSPL8 function confers improved resistance to glufosinate and abiotic stresses in rice.** Plant, Cell & Environment, 48(1), 682–698. https://doi.org/10.1111/pce.15168

HE, X., QU, B., LI, W., ZHAO, X., TENG, W., MA, W., ... & ZHANG, J. (2015). **The nitrate-inducible NAC transcription factor TaNAC2-5A controls nitrate response and increases wheat yield.** Plant Physiology, 169(3), 1991–2005.

HEAP, I. M. (2024). **The International Survey of Herbicide Resistant Weeds.** Retrieved from www.weedscience.org

HENRY, K. F., JANG, S. S., & COOKE, T. F. (2018). **A shared cis-regulatory module activates transcription in distinct tissues.** Proceedings of the National Academy of Sciences USA, 115(25), E5843-E5852.

HOANG, D. T., CHERNOMOR, O., VON HAESELER, A., MINH, B. Q., & VINH, L. S. (2018). **UFBoot2: Improving the ultrafast bootstrap approximation.** Molecular Biology and Evolution, 35(2), 518–522. https://doi.org/10.1093/molbev/msx281

HU, B., WANG, W., OU, S., TANG, J., LI, H., CHE, R., ... & CHU, C. (2019). **Genome-wide association study identifies NAC42-activated nitrate transporter conferring high nitrogen use efficiency in rice.** Nature Communications, 10(1), 5279.

HUERTA-CEPAS, J., FORSLUND, K., COELHO, L. P., SZKLARCZYK, D., JENSEN, L. J., VON MERING, C., & BORK, P. (2017). **Fast genome-wide functional annotation through orthology assignment by eggNOG-Mapper.** Molecular Biology and Evolution, 34(8), 2115–2122. https://doi.org/10.1093/molbev/msx148

HUSSAIN, A., ALI, S., ALI, Z., & SIDDIQUI, M. H. (2021). **Herbicide resistance: Another hot agronomic trait for plant genome editing.** Plants, 10(3), 556. https://doi.org/10.3390/plants10030556

HUSSAIN, M. S., HUSSAIN, A. D. E., & BERGMANN, D. C. (2024). **Comparative analysis, diversification, and functional characterization of NBS-containing resistance genes in land plants.** Nature Communications, 15(1), 5421. https://doi.org/10.1038/s41467-024-49721-z

IMRAN, M., SALEHI, B., SHARIFI-RAD, J., ASLAM GONDAL, T., SAEED, F., IMRAN, A., ... & UMAIR AKHTAR, M. (2020). **Lycopene as a natural antioxidant used to prevent human health disorders.** Antioxidants, 9(8), 746. https://doi.org/10.3390/antiox9080746

JIAO, Y., SCHNEEBERGER, K., OSSOWSKI, S., SCHNEEBERGER, K., HANCOCK, D., SHANAHAN, H., ... & WEIGEL, D. (2012). **Genome triplication and frequent chromosomal translocations in *Arabidopsis thaliana*.** Nature, 485(7398), 635-641. https://doi.org/10.1038/nature11142

JIN, J. P., TIAN, F., YANG, D. C., MENG, Y. Q., KONG, L., LUO, J. C., & GAO, G. (2017). **PlantTFDB 4.0: Toward a central hub for transcription factors and regulatory interactions in plants.** Nucleic Acids Research, 45(D1), D1040–D1045. https://doi.org/10.1093/nar/gkw982

JIN, M., ZHANG, Y., JIANG, Y., YANG, Y., MENG, S., & ZHANG, H. (2022). **Development of herbicide resistance genes and their applications in crop improvement.** Journal of Experimental Botany, 73(9), 3105–3122.

Juma, S., Tian, N., Toinga-Villafuerte, D., & Pfotenhauer, J. (2024). **Recent advances of CRISPR-based genome editing for crop improvement.** Frontiers in Plant Science, 15, 1478398. https://doi.org/10.3389/fpls.2024.1478398

JUMPER, J., EVANS, R., PRITZEL, A., GREEN, T., FIGURNOV, M., RONNEBERGER, O., ... Y HASSABIS, D. (2021). **Predicción de la estructura de proteínas de alta precisión con AlphaFold.** Naturaleza, 596 (7873), 583-589. https://doi.org/10.1038/s41586-021-03819-2

KALYAANAMOORTHY, S., MINH, B. Q., WONG, T. K., VON HAESELER, A., & JERMIIN, L. S. (2017). **ModelFinder: Fast model selection for accurate phylogenetic estimates.** Nature Methods, 14(6), 587–589. https://doi.org/10.1038/nmeth.4285

KATOH, K., ROZEWICKI, J., & YAMADA, K. D. (2019). **MAFFT online service: Multiple sequence alignment, interactive sequence choice and visualization.** Briefings in Bioinformatics, 20(4), 1160–1166. https://doi.org/10.1093/bib/bbx108

KAUR, N., SHARMA, S., SHARMA, S., & SANDHU, J. S. (2025). **CRISPR/Cas9: A sustainable technology to enhance climate resilience in major staple crops.** Frontiers in Genome Editing, 7, 1533197. https://doi.org/10.3389/fgeed.2025.1533197

KONATÉ, M. M., PLATA, G., PARK, J., USMANOVA, D. R., WANG, H., & VITKUP, D. (2019). **Molecular function limits divergent protein evolution on planetary timescales.** eLife, 8, e39705. https://doi.org/10.7554/eLife.39705

KOONIN, E. V. (2005). **Orthologs, paralogs, and evolutionary genomics.** Annual Review of Genetics, 39, 309–338.

KORASICK, D. A., JANG, S. S., LAHNER, B., BEDNAREK, S. Y., & RAINES, C. A. (2014). **Molecular basis for AUXIN RESPONSE FACTOR protein interaction and the regulation of auxin response.** Proceedings of the National Academy of Sciences USA, 111(12), 4597-4602.

KRENCHINSKI, F. H., ALBRECHT, A. J. P., ALBRECHT, L. P., CESCO, V. J. S., RODRIGUES, D. M., PORTZ, R. L., & ZOBIOLE, L. H. S. (2018). **Post-emergent applications of isolated and combined herbicides on corn hybrids with stacked traits.** Crop Protection, 106, 156–162.

KRENCHINSKI, F. H., ALBRECHT, A. J. P., MENEZES JUNIOR, F. O. G. D., BALENSIEFER, V., & DUKE, S. O. (2018). **Glufosinate resistance level is proportional to phosphinothricin acetyltransferase gene expression in glufosinate-resistant maize.** Journal of Agricultural and Food Chemistry, 66(48), 12641–12650. https://doi.org/10.1021/acs.jafc.8b04823

KRIBELBAUER, J. F., RIPPERGER, T., WEINTRAUB, A. S., & HANNETT, N. M. (2024). **Context transcription factors establish cooperative environments and mediate enhancer communication.** Nature Genetics, 56(10), 2199-2212. https://doi.org/10.1038/s41588-024-01892-7

KROKIDIS, M. G., STAVROPOULOS, K., KARTSOGLOU, C., DIMITRAKOPOULOS, G. N. Y PAPAGEORGIOU, L. G. (2025). **AlphaFold3: Una descripción general de las aplicaciones y el rendimiento en la predicción de interacciones biomoleculares.** Opinión actual en biología estructural, 90, 102877. https://doi.org/10.1016/j.sbi.2024.102877

KUBALOVÁ, M., FIMOGNARI, L., CZECH, B., & MÜLLER, B. (2025). **Unresolved roles of Aux/IAA proteins in auxin responses.** Annual Review of Plant Biology, 76, 12.1–12.22.

KUMAR, D., & HARIHARAN, K. (2023). **Noncanonical binding of transcription factors: time to revisit specificity?** Nucleic Acids Research, 51(16), 8542-8557. https://doi.org/10.1093/nar/gkad631

KUMAR, N., ET AL. (2024). **Physiological and molecular insights into the allelopathic consequences of weeds in crop production.** Frontiers in Plant Science, 15, 1345627. https://doi.org/10.3389/fpls.2024.1345627

LAFOND, M., PROTAS, M. E., SWENSON, K. M., & EL-MABROUK, N. (2018). **Accurate prediction of orthologs in the presence of divergence after duplication.** Bioinformatics, 34(17), i366-i375. https://doi.org/10.1093/bioinformatics/bty242

LANGSCHIED, F., STÜTZ, A., DESSIMOZ, C., & LEUSHACKE, M. (2024). **Quest for orthologs in the era of biodiversity genomics.** Nature Ecology & Evolution, 8(10), 1876–1886. https://doi.org/10.1038/s41559-024-02503-w

LEA, P. J., & MOLLER, I. M. (2021). **Nitrogen metabolism in plants.** In Plant physiology (6th ed., pp. 567–592). Sinauer Associates.

LEE, H. J., BAIK, J. E., & KIM, K. N. (2025). **Development of an efficient and heritable virus-induced genome editing system in *Solanum lycopersicum***. Horticulture Research, 12(4), uhae364. https://doi.org/10.1093/hr/uhae364

LI, M., TU, S., LIN, X., YU, Z., ZHU, S., XU, Q., ... & ZHOU, Y. (2024). **Diversification and conservation of DNA binding specificities in SPL transcription factors.** Nature Communications, 15, 2658. https://doi.org/10.1038/s41467-024-55278-8

LI, S., ZHANG, M., & WANG, H. (2024). **Identification of ARF gene family and functional analysis of ARF genes in response to auxin in tomato.** Horticulturae, 10(2), 138.

LI, Y., JING, R., CAO, J., WANG, Y., LI, X., TIAN, Y., ... & CAO, L. (2023). **Variations in OsSPL10 confer drought tolerance by directly regulating OsNAC2 expression and ROS production in rice.** Journal of Integrative Plant Biology, 65(4), 875-892. https://doi.org/10.1111/jipb.13414

LIM, M. Y., & PHOON, B. L. (2020). **Protective effects of lycopene in cancer, cardiovascular, and neurodegenerative diseases: An update on epidemiological and mechanistic perspectives.** Current Medicinal Chemistry, 27(16), 2584-2621. https://doi.org/10.2174/0929867326666190619125020

LIU, G. D., AN, X. H., RUI, L., LIU, R. X., LI, H. L., & HAO, Y. J. (2024). **Auxin response factor MdARF18 regulates MdNRT1.1 to affect nitrogen utilization in apple.** Fruit Research, 4, e027. https://doi.org/10.48130/frures-0024-0021

LIU, M. Y., MENG, R. P., LI, H., ZHANG, L., WANG, Y. Q., ZHANG, Z. X. Y ZHUANG, J. (2024). **Un módulo de factor de transcripción glutamina sintetasa-Dof regula la removilización de nitrógeno en las plantas de té.** Fisiología vegetal, 177(4), 2180-2197. https://doi.org/10.1093/plphys/kiad597

LU, R., MARTIN-BROWN, S., OSWALD, F., MAJUMDAR, D., ZHAO, X., MUNDADE, R., ... & NAIR, S. K. (2019). **Transcription factor binding site clusters identify target genes of human transcription factors.** Nature Genetics, 51(1), 21-33. https://doi.org/10.1038/s41588-018-0298-2

MAJIDIAN, S., LAUSCH, A., DESSIMOZ, C., & ALTENHOFF, A. M. (2025). **Orthology inference at scale with FastOMA.** Nature Methods, 22(1), 47–51. https://doi.org/10.1038/s41592-024-02457-6

MALIK, F. K., MUHAMMAD, S. A., & DANISH, M. (2022). **Insights into protein–DNA interactions from hydrogen bond based comparative study.** Scientific Reports, 12, 2527. https://doi.org/10.1038/s41598-022-06528-6

MAO, J., LI, J., ZHANG, W., & LU, S. (2025). **The crosstalk between nitrate signaling and other signaling pathways in plants.** Nature Plants, 11(1), 42–56.

MARKET DATA FORECAST. (2025). **Tomato Market Size, Share, Trends & Growth Report 2025-2033.** Retrieved from https://www.marketdataforecast.com/market-reports/tomato-market

MÁRQUEZ, Y., MANTICA, F., MARCET-HOUBEN, M., CORDERO, H., KONSTANTINIDIS, K., BARBIER, V., ... & SAMMETH, M. (2021). **ExOrthist: A tool to infer exon orthologies at any evolutionary distance.** Genome Biology, 22(1), 239.

MATERIALES DE CAPACITACIÓN DE EBI. (2024**). Cómo evaluar la calidad de las predicciones de AlphaFold 3**. Obtenido de https://www.ebi.ac.uk/training/online/courses/alphafold/alphafold-3-and-alphafold-server/how-to-assess-the-quality-of-alphafold-3-predictions/

MEAGHER, K. D., KLEE, H., & CLARK, D. L. (2024). **Horticultural biotechnology faces significant economic and market barriers.** California Agriculture, 78(3), 160–175.

MINH, B. Q., SCHMIDT, H. A., CHERNOMOR, O., SCHREMPF, D., WOODHAMS, M. D., VON HAESELER, A., & LANFEAR, R. (2020). **IQ-TREE 2: New models and efficient methods for phylogenetic inference in the genomic era.** Molecular Biology and Evolution, 37(5), 1530–1534. https://doi.org/10.1093/molbev/msaa015

MORRISON, G. E., & BERTUCCI, M. (2022**). Preventative weed management strategies in Arkansas tomato production.** Discovery, The Student Journal of Dale Bumpers College of Agricultural, Food and Life Sciences, 23(1), 13. Retrieved from https://scholarworks.uark.edu/discoverymag/vol23/iss1/13/

MOVAHEDI, A., JING, Y., LI, Q., ZHANG, J., & CHEN, L. (2023). **CRISPR variants for gene editing in plants: Biosafety risks and regulatory landscape.** Biotechnology Advances, 67, 108186. https://doi.org/10.1016/j.biotechadv.2023.108186

NANDULA, V. K., RAATZ, L., SENSEMAN, S. A., & DUKE, S. O. (2019). **Herbicide resistance traits in maize and soybean: Genetics, molecular biology, and phenology.** Weed Technology, 33(6), 1–27. https://doi.org/10.1017/wet.2019.96

NUÑEZ, C. I., SAN-EPIFANIO, L., & OLATUNDE, O. (2024). **Editorial: Frontiers in global regulatory landscape of CRISPR-edited plants.** Frontiers in Plant Science, 15, 1367698. https://doi.org/10.3389/fpls.2024.1367698

OGUNLADE, M. O., & AWODOYIN, R. O. (2020). **Weed competitiveness and herbicidal sensitivity of grafted tomatoes (*Solanum lycopersicum Mill*.).** International Journal of Vegetable Science, 26(2), 134-150. https://doi.org/10.1080/19315260.2019.1655563

OSMAN, K. E., LONG, W., ZHAO, C., GE, X., ZHANG, B., YUN, Q., ... & ZHANG, G. (2024). **Genome evolution and diversity of wild and cultivated rice.** Nature, 633, 858–867. https://doi.org/10.1038/s41586-024-07902-2

OSMAN, M. E. M., ABASS, M. A., SAYED, S. A., ELJAZOLI, M. S., & ISMAIL, S. I. (2024). **In silico analysis of L- and G-type lectin receptor kinases in wild and cultivated tomato species.** Scientific Reports, 14, 28265. https://doi.org/10.1038/s41598-024-78873-5

ÖTVÖS, K., SCHRADER, J., SZABÓ, Z., MÓROCZ, D., BRUNNER, F., & BIRNBAUM, K. D. (2021). **Modulation of plant root growth by nitrogen source-defined phosphorylation of PIN2 auxin carrier.** The EMBO Journal, 40(1), e105021.

POTS, A. M., BROUWER-BROLSMA, E. M., KRUK, J., & GROOT, L. C. (2020). **Nutritional composition and bioactive compounds in tomatoes and their effects on human health.** Nutrients, 13(12), 4567. https://doi.org/10.3390/nu13124567

PRIETO-BAÑOS, S., MARCET-HOUBEN, M., GABALDÓN, T., & DESSIMOZ, C. (2025). **The effect of structural gene annotation on orthology inference.** Bioinformatics, 41(1), btae733. https://doi.org/10.1093/bioinformatics/btae733

QUINET, M., ANGOSTO, T., FULTON, T., ALSEEKH, S., VIRGILIO, M., FERNIE, A. R., & GRANELL, A. (2019). **Tomato fruit development and metabolism.** Frontiers in Plant Science, 10, 1554. https://doi.org/10.3389/fpls.2019.01554

RAO, S. S. P., HUANG, S. C., ST HILAIRE, B. G., ENGREITZ, J. M., PEREZ, E. M., KIEFFER-KWON, K. R., ... & AIDEN, E. L. (2021). **Cooperative binding of distant transcription factors is a hallmark of active enhancers.** Nature, 592(7852), 450-455. https://doi.org/10.1038/s41586-021-03327-3

RASTOGI, N., KIUCHI, H., & GALAS, D. J. (2023). **Specificity landscapes of DNA binding molecules elucidate structural principles that guide genomic regulatory activity.** PLoS Computational Biology, 19(5), e1011137. https://doi.org/10.1371/journal.pcbi.1011137

REN, Y., LIU, B., JIANG, H., CHENG, W., TAO, L., WU, K., WANG, H., SHEN, G., FANG, Y., ZHANG, C., WU, Y., FU, X., & YE, Y. (2023). **Precision editing of GLR1 confers glufosinate resistance without yield penalty in rice.** Plant Biotechnology Journal, 21(12), 2417-2419. https://doi.org/10.1111/pbi.14168

RIENSTRA, J., HERNÁNDEZ-GARCÍA, J., & WEIJERS, D. (2023). **To bind or not to bind: How AUXIN RESPONSE FACTORs select their target genes.** Journal of Experimental Botany, 74(22), 6922–6932.

RIENSTRA, J., WEIJERS, D., JAILLAIS, Y., & HARDTKE, C. S. (2025). **A conserved ARF–DNA interface underlies auxin-triggered developmental plasticity.** Proceedings of the National Academy of Sciences USA, 122(14), e2501915122. https://doi.org/10.1073/pnas.2501915122

ROYCHOWDHURY, R., BANERJEE, P., SARKAR, R., DEY, N., & RAY, S. (2025). **Advancing vegetable genetics with gene editing.** In Vitro Cellular & Developmental Biology - Plant, 61(1), 9. https://doi.org/10.1007/s11627-024-10412-5

ROZAS, P. (2022). **Genetically modified organisms: adapting regulatory frameworks for evolving genome editing technologies.** Biological Research, 55(1), 31. https://doi.org/10.1186/s40659-022-00399-x

SCHRÖDINGER, LLC. (2023). **The PyMOL molecular graphics system, version 2.6. Schrödinger, LLC.**

SHAHEIN, A., VANDEN EIJNDEN, M., SANCHEZ-FUENTES, A. J., LEROY, J. P., SEGAL, E., & GHAEMMAGHAMI, S. (2021). **Systematic analysis of low-affinity transcription factor binding site clusters in eukaryotic promoters and enhancers.** bioRxiv. https://doi.org/10.1101/2021.12.17.473130

SHAHEIN, A., VANDEN EIJNDEN, M., SANCHEZ-FUENTES, A. J., LEROY, J. P., SEGAL, E., & GHAEMMAGHAMI, S. (2022). **Systematic analysis of low-affinity transcription factor binding site clusters in eukaryotic promoters and enhancers.** Nature Communications, 13(1), 5227. https://doi.org/10.1038/s41467-022-32971-0

SHAWKY, A., ABDEL-HADY, N. M., FARGHALI, E., & KHALIL, H. (2024). **Revolutionizing tomato cultivation: CRISPR/Cas9 applications for enhanced resilience and productivity.** Frontiers in Plant Science, 15, 1–18. https://doi.org/10.3389/fpls.2024.1371832

SHERMAN, J. (2024). **Post season global tomato crop update.** The Morning Star Company. Retrieved from https://www.morningstarco.com/2024-post-season-global-tomato-crop-update/

SMYTH, S. J., KHACHATOURIANS, G. G., & PHILLIPS, P. W. B. (2020). **Regulatory approaches for genome edited agricultural plants in select countries and jurisdictions around the world.** Frontiers in Plant Science, 11, 585996. https://doi.org/10.3389/fpls.2020.585996

SRIVASTAVA, S., AHMAD, M., ZHU, L. H., & KHAN, M. A. (2019). **Gene editing in plants: Progress and challenges.** Current Opinion in Plant Biology, 49, 49–56. https://doi.org/10.1016/j.pbi.2019.01.003

STAMBOULIAN, M., RADIVOJAC, P., & RADIVOJAC, P. (2020). **The value of orthologs and paralogs in function prediction.** Bioinformatics, 36(12), 3627-3635. https://doi.org/10.1093/bioinformatics/btaa251

SUN, Y., JIAO, B., LIU, H., LI, Z., & WANG, X. (2023). **Genome-wide identification of the SQUAMOSA promoter binding protein (SPL) gene family in Pyrus avium and expression analysis during fruit development.** Frontiers in Plant Science, 14, 1145673.

TAKANO, H. K., BEFFA, R., PRESTON, C., WESTRA, P., & DAYAN, F. E. (2020). **A novel insight into the mode of action of glufosinate: How reactive oxygen species are formed.** Photosynthesis Research, 145(2), 191–204. https://doi.org/10.1007/s11120-020-00749-4

TAKANO, H. K., WESTRA, P., PRESTON, C., BEFFA, R., & DAYAN, F. E. (2019). **Reactive oxygen species trigger the fast action of glufosinate.** Planta, 249(6), 1837–1849. https://doi.org/10.1007/s00425-019-03137-0

TAN, B. L., NORHAIZAN, M. E., & LIEW, W. P. P. (2018). **The anti-cancer activity of lycopene: A systematic review of in vivo studies.** Nutrients, 11(12), 2881. https://doi.org/10.3390/nu11122881

TNAU AGRITECH PORTAL. (2023, December 31). **Weed management.** Retrieved from https://agritech.tnau.ac.in/org_farm/orgfarm_weed%20mgt.html

TRIPATHI, R. K., KUMAR, V., KUMAR, P., SINGH, S., & SINGH, D. (2024). **Differential expression and global analysis of miR156 and its target SPL genes in Artemisia sieversiana for developmental and stress-responsive mechanisms.** BMC Genomics, 25(1), 612.

VARGA, J. K., OVCHINNIKOV, S. Y SCHUELER-FURMAN, O. (2025). **actifpTM: una métrica de confianza refinada de las predicciones de AlphaFold2 que involucran regiones flexibles.** Bioinformática, 41(3), btaf107. https://doi.org/10.1093/bioinformatics/btaf107

VEILLET, F., PERROT, L., CHAUVIN, L., KERMARREC, M. P., GUYON-DEBAST, A., CHAUVIN, J. E., MAZIER, M., & GALLAIS, S. (2019). **Transgene-free genome editing in tomato and potato using cytidine base editor combined with Agrobacterium-mediated transformation.** Plant Biotechnology Journal, 18(2), 570–582. https://doi.org/10.1111/pbi.13217

VEILLET, F., PERROT, L., CHAUVIN, L., KERMARREC, M. P., GUYON-DEBAST, A., CHAUVIN, J. E., MAZIER, M., & GALLAIS, S. (2020). **Precision Breeding Made Real with CRISPR.** Current Opinion in Plant Biology, 54, 1–8. https://doi.org/10.1016/j.pbi.2020.01.002

WALDEN, N., GERMAN, D. A., CARRETERO-PAULET, L., SZÖVÉNYI, P., & SCHRANZ, M. E. (2023). **Synteny identifies reliable orthologs for phylogenomics.** American Journal of Botany, 110(2), e16041. https://doi.org/10.1002/ajb2.16041

WPTC (World Processing Tomato Council). (2025). **Global processing tomato production forecast 2024-2025.** Retrieved from https://www.wptc.to/

WSSA (Weed Science Society of America). (2022). **Herbicide resistance action committee (HRAC) classification: Classification scheme for herbicide modes of action.**

WU, Y. J., DU, J., LIU, Z., LIANG, Y., KANG, X., ZHAN, Y., ... & XIANG, C.-B. (2023). Loss of OsARF18 confers glufosinate ammonium herbicide resistance in rice. bioRxiv. https://doi.org/10.1101/2023.06.05.543806

XIA, J. Q, LIU, Y. Q., YAO, Q. Y., ZHANG, X. M, ZHANG, L. L., YANG, Z. L., ZHANG, X., LI, D., ZHANG, Y., DENG, J. W, LIU, Y. G., & CAO, X. (2024). **Knockout of OsSPL10 confers enhanced glufosinate resistance in rice.** Journal of Experimental Botany, 75(1), 127-139. https://doi.org/10.1093/jxb/erad303

XIA, J. Q., LIU, Y. Q., YAO, Q. Y., ZHANG, X. M., ZHANG, L. L., YANG, Z. L., ZHANG, X., LI, D., ZHANG, Y., DENG, J. W., LIU, Y. G., & CAO, X. (2023). **Loss of OsARF18 function confers glufosinate resistance in rice.** Molecular Plant, 16(9), 1402-1405. https://doi.org/10.1016/j.molp.2023.08.007

XIA, J. Q., LIU, Y. Q., YAO, Q. Y., ZHANG, X. M., ZHANG, L. L., YANG, Z. L., ZHANG, X., LI, D., ZHANG, Y., DENG, J. W., LIU, Y. G., & CAO, X. (2024). **Knockout of OsSPL10 confers enhanced glufosinate resistance in rice.** Molecular Plant, 17(2), 244-247. https://doi.org/10.1016/j.molp.2023.10.011

XIA, J.-Q., LIANG, Q.-Y., HE, D.-Y., ZHANG, Z.-Y., WU, J., ZHANG, J., ... & XIANG, C.-B. (2023). **Knockout of OsSPL10 confers enhanced glufosinate resistance in rice.** Plant Communications, 5(2), 100731. https://doi.org/10.1016/j.xplc.2023.100731

XIA, J.-Q., LIANG, Q.-Y., HE, D.-Y., ZHANG, Z.-Y., WU, J., ZHANG, J., ... & XIANG, C.-B. (2024). **A glutamine synthetase-Dof transcription factor module regulates nitrogen remobilization in tea plants.** Plant, Cell & Environment, 47(12), e14487. https://doi.org/10.1111/pce.14487

YANG, B., & HOBBS, J. E. (2020). **Consumer acceptance of genetically modified food products.** Biotechnology Advances, 48, 107753. https://doi.org/10.1016/j.biotechadv.2021.107753

YANG, N., ZHANG, Y., LIU, X., & GAO, Y. (2017). Revolutionize genetic studies and crop improvement with high-throughput and genome-scale CRISPR/Cas9 gene editing technology. Molecular Plant, 10(9), 1141–1143. https://doi.org/10.1016/j.molp.2017.08.001

ZHANG, J., SHEN, T., LI, J., & WANG, X. (2024). **Transformative approaches for sustainable weed management: The power of gene drive and CRISPR-Cas9.** Genes, 15(12), 1537. https://doi.org/10.3390/genes15121537

CHAPTER 3 – FUNCTIONAL VALIDATION OF ARF AND SPL ORTHOLOGS AS GENOME-EDITING TARGETS FOR GLUFOSINATE RESISTANCE IN MICRO-TOM TOMATO VIA CRISPR-CAS9

ABSTRACT

Genetic improvement through genome editing represents a fundamental strategy for the development of tomato varieties tolerant to herbicides and abiotic stresses without the incorporation of foreign genes. Recent studies in *Oryza sativa* have identified that mutants in transcriptional regulatory genes—specifically *GLR1* (the ortholog of *ARF18*) and *SPL10*—confer simultaneous resistance to glufosinate and enhanced tolerance to salt stress, without penalties to agronomic yield. The general objective of the present study was the genome editing of tomato (*Solanum lycopersicum* cv. Micro-Tom) by CRISPR–Cas9 targeted to orthologs of these genes (five candidate genes: three ARF members and two SPL), with the aim of obtaining lines resistant to glufosinate, without integration of the *bar* gene. Ten guide RNAs (gRNAs) were designed using the CHOPCHOP tool, simultaneously optimizing cleavage efficiency and specificity. Construction of CRISPR–Cas9 vectors was performed by Golden Gate modular cloning into the pDIRECT_22C vector, resulting in three validated constructs out of the five initially planned (60% success). Fifteen independent *Agrobacterium tumefaciens*–mediated genetic transformation experiments were carried out using cotyledon explants of Micro-Tom. Initial regeneration efficiency was limited (13.3%), attributed to physiological stress induced during co-cultivation. However, reformulation of the regeneration medium—replacing benzyladenine with zeatin—was key to restoring organogenic competence, with robust formation of adventitious shoots observed in the last two experiments. Approximately twenty explants are currently in a phase of progressive regeneration after two months of subculture. These results validate the feasibility of the CRISPR–Cas9 transformation system in Micro-Tom tomato and demonstrate that optimization of the regeneration medium is critical to improving genetic transformation efficiency. This methodological advance contributes to precise fine-tuning of post-transformation regeneration protocols and provides a solid basis for the eventual recovery of fully edited, rooted, and acclimatized plants.

Keywords: Genome editing, CRISPR–Cas9, Micro-Tom tomato, glufosinate, herbicide resistance, salt stress, *Agrobacterium tumefaciens*, explant regeneration, zeatin, transcriptional regulatory genes, ARF and SPL orthologs, plant genetic improvement.

1 INTRODUCTION

Genetic improvement has played a transformative role in the agricultural and industrial success of tomato cultivation in Latin America, with a paradigmatic example documented in Brazil (Razifard et al., 2020). Over the past five decades, productivity of tomato destined for industrial processing in Brazil has increased dramatically, rising from approximately 30 to approximately 70.6 metric tons per hectare ($t.ha^{-1}$) by 2023, with total production reaching 4.3 million tons in 2024 (CEIC Data, 2023; IBGE, 2025), representing an increase of roughly 136% (CEIC Data, 2023). This progress has been driven by systematic breeding programs and the application of biotechnologies that optimized critical agronomic traits, including disease resistance, adaptability to tropical climatic conditions, and efficient use of water and nutrients (Boiteux, 2012). As documented by research institutes such as Embrapa, these genetic advances not only expanded national production capacity but also consolidated Brazil's international competitiveness in the global tomato market (Du et al., 2025).

Among contemporary tools in plant biotechnology, CRISPR–Cas9 represents a revolutionary advance that enables precise genome editing without the permanent integration of exogenous genetic sequences (Wang et al., 2019; Shawky et al., 2024). This editing platform has been successfully implemented in tomato to improve multiple traits of agricultural importance, including: (i) resistance to viral, fungal, and bacterial pathogens (Wang et al., 2019; Arora et al., 2021; Wang et al., 2025); (ii) tolerance to abiotic stresses (drought, salinity, and temperature extremes) (Kumar et al., 2023; Rai & Sharma, 2022); (iii) enhancement of nutritional quality (Kumar et al., 2023; Siddiq et al., 2021); and (iv) modification of fruit organoleptic attributes (Siddiq et al., 2021; Feng et al., 2023).

Particularly relevant is the capacity to generate transgene-free edited plants through Mendelian segregation or transient transformation with ribonucleoprotein (RNP) complexes, thereby eliminating foreign selectable marker genes (Murovec et al., 2018; Manghwar et al., 2020). This feature directly addresses regulatory concerns associated with transgenic genetically modified organisms (He & Zhao, 2020). The efficiency of the CRISPR–Cas9 system in tomato has been extensively documented, with recent studies demonstrating high gene-editing frequencies in T_0 plants and stable inheritance of genetic modifications in subsequent generations (Li et al., 2018; Tiwari et al., 2023). Advanced innovations including Cas12a variants, PAM-less genome editing, and DNA-free protoplast-mediated RNP delivery

have further enhanced the precision and efficiency of tomato genome editing for rapid crop improvement (Tiwari et al., 2023).

Recent investigations in *Oryza sativa* have identified endogenous genes whose editing simultaneously confers resistance to glufosinate and enhanced tolerance to salt stress, revealing regulatory mechanisms with translational value for other crops (Ren et al., 2023; Liu et al., 2024). Ren et al. (2023) demonstrated that precise editing of the GLR1 gene (which encodes the auxin response factor OsARF18) confers robust resistance to glufosinate without penalties to agricultural yield (Ren et al., 2023). The underlying mechanism is based on a regulatory circuit in which, in wild-type plants, exposure to glufosinate activates GLR1, resulting in repression of downstream genes (OsGS1, OsCYP51G3, OsCATA) that facilitate the clearance of ammonia and reactive oxygen species (ROS). This repression permits the toxic accumulation of these metabolites, leading to cell death (Ren et al., 2023). By contrast, when GLR1 is mutated, this inhibition is relieved, enabling constitutive expression of defense and ammonia-removal genes and thereby preventing herbicide injury (Ren et al., 2023).

Notably, GLR1 mutants exhibited significant concomitant tolerance to salt stress, with higher survival rates and improved ionic homeostasis under high-salinity conditions (Ren et al., 2023; Cheng et al., 2024). These findings indicate that GLR1 functions as a negative regulator of defense networks against both herbicide injury and salt stress, suggesting a pleiotropic regulatory mechanism whereby loss of function unlocks multiple stress-adaptation pathways (Ren et al., 2023; Cheng et al., 2024).

Complementarily, Xia et al. (2023) identified that deletion of OsSPL10 via CRISPR–Cas9 confers enhanced glufosinate resistance in rice. OsSPL10, a transcription factor of the SQUAMOSA PROMOTER-BINDING-LIKE (SPL) family, acts as a negative regulator of herbicide resistance by inhibiting the transcription of OsGS1;1 and OsGS2, thereby reducing glutamine synthetase (GS) activity. SPL10 knockout mutants displayed complete survival (100%) following exposure to glufosinate at concentrations of 10 g L^{-1}, whereas wild-type plants died completely (Xia et al., 2023). Transcriptomic analyses revealed that OsSPL10 negatively regulates detoxification genes (cytochrome P450s, peroxidases, and ABC/MATE transporters) while positively regulating growth factors, suggesting that this protein mediates a trade-off between stress response and growth. Its elimination shifts this balance toward defense mechanisms, simultaneously improving tolerance to drought and salinity (Xia et al., 2023).

The synergistic findings in rice demonstrate that targeted genome editing of specific negative transcriptional regulators can simultaneously enhance herbicide resistance and abiotic stress tolerance without compromising agronomic performance (Ren et al., 2023), offering a

strategy superior to transformation with bacterial genes such as bar (Hussain et al., 2021). The absence of a yield penalty is particularly significant, as it addresses a central concern in crop improvement (Ren et al., 2023).

Moreover, because these genes act as negative regulators, their knockout unleashes preexisting endogenous defense responses without introducing heterologous genetic machinery (Ren et al., 2023), thereby preserving genomic integrity and facilitating regulatory acceptance as non-transgenic plants (Ahmad et al., 2023). This feature confers a substantial advantage in terms of regulatory compliance and consumer acceptability (Ahmad et al., 2023).

Translating these mechanistic concepts to tomato represents a strategic opportunity to develop improved varieties that address two critical production constraints simultaneously: weed interference and salt stress (Kumar et al., 2023). Tomato harbors orthologs of the rice genes GLR1 and SPL10 (Ahmad et al., 2023), and CRISPR–Cas9 technology is widely established and optimized for the transformation and regeneration of tomato germplasm (Murugan et al., 2023; Liu et al., 2022).

2 MATERIAL AND METHODS

2.1 Design of sgRNAs

For each of the five selected candidate genes, two single-guide RNAs (sgRNAs) were designed to target that gene specifically, for a total of ten guide RNA constructs. The target genes included: (i) three members of the ARF family—Solyc11g069500, Solyc06g075150, and Solyc09g007810—and (ii) two members of the SPL family—Solyc10g018780 and Solyc01g090730. For each gene, both sgRNAs were directed to early exons within the coding region, a strategy that maximizes the likelihood of generating loss-of-function frameshift mutations by inducing early, critical deletions in the protein sequence.

sgRNA design was performed using the CHOPCHOP bioinformatic tool (Clustered Regularly Interspaced Short Palindromic Repeats Off-target Prediction), simultaneously optimizing two critical parameters: (i) the cleavage efficiency of the Cas9–sgRNA complex at the target sequence and (ii) cleavage specificity by predicting and minimizing potential off-target sites across the tomato genome. This dual optimization strategy ensures that genome-editing events are both efficient and specific, reducing the likelihood of undesired mutations at other genomic loci.

2.2 Vector construction – Golden Gate

CRISPR–Cas9 genome-editing vectors were assembled using the modular Golden Gate cloning technique, following the protocol described by Čermák et al. (2017). The destination vector used was pDIRECT_22C (figure 18), which carries the following functional components: (i) *Arabidopsis thaliana* Cas9 fused to the endoribonuclease Csy4, both under the constitutive 35S promoter; (ii) a multiplex sgRNA expression cassette driven by the CmYLCV promoter; and (iii) the nptII selectable marker gene conferring kanamycin resistance in transformed plants. This vector architecture enables coordinated polycistronic transcription of multiple sgRNAs and their individual processing via recognition of Csy4 sites.

Figure 18 - Commercial vector p-DIRECT_22C, specific for kanamycin selection, recommended for assembly following the Golden Gate strategy.

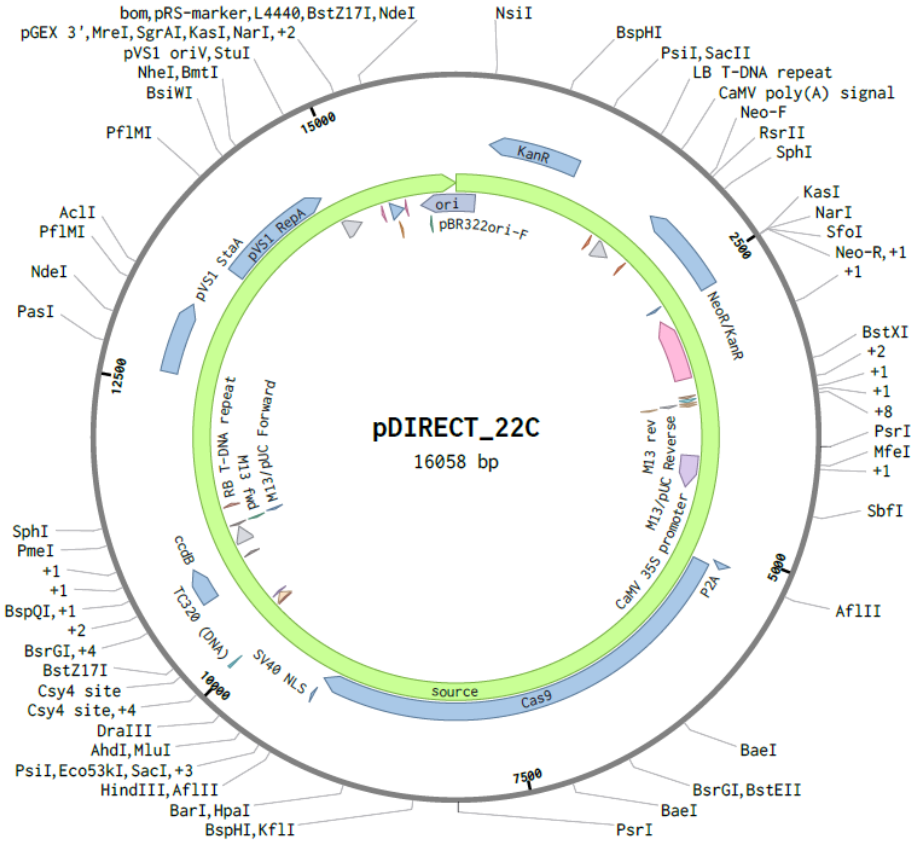

Source: Cermák et al. (2017).

For each candidate gene, DNA fragments encoding two gene-specific 20-nucleotide sgRNAs (excluding the PAM motif) were identified. Sequences were selected within conserved exonic regions of each target gene to maximize functional specificity. For each sgRNA, two single-stranded oligonucleotides were designed with ends compatible with the type IIS Golden Gate modular cloning scheme. The oligonucleotides were arranged in tandem, separated by Csy4 recognition sites, which subsequently facilitate the individual release of each sgRNA during polycistronic transcription in transformed plants (Kurata et al., 2018; Zhang et al., 2024).

Cloning was performed using a two-tier system that integrates positive and negative selection (Pryor et al., 2020). In the first tier, the type IIS restriction enzyme SapI was used for directional insertion of each sgRNA construct into intermediate vectors carrying a ccdB cassette (Pryor et al., 2020). In the second tier, the enzyme Esp3I (an isoschizomer of BsmBI) mediated the final assembly into pDIRECT_22C (Addgene #91135), simultaneously (i) removing the flanking restriction sites, (ii) correctly orienting the sgRNA constructs, and (iii) excising the

ccdB cassette from the destination vector (Chiasson et al., 2019). This scheme implemented a lethal selection system based on the ccdB gene, which eliminates vector religation events lacking an insert by causing death of *Escherichia coli* host cells that are sensitive to ccdB (Addgene, 2016; Menestreau et al., 2022). Only bacteria containing the correct insert (with the ccdB cassette replaced) survive, thereby dramatically increasing the recovery efficiency of positive clones (Menestreau et al., 2022).

Each sgRNA oligonucleotide pair was annealed *in vitro* to form double-stranded DNA duplexes with compatible cohesive ends. These duplexes were ligated into the SapI/Esp3I sites of the vector in a single Golden Gate reaction, following the 3A method. Reaction mixtures (total volume: 20 µL) contained (i) the restriction/ligation enzymes (SapI, Esp3I, and T4 DNA ligase), (ii) the appropriate reaction buffer, (iii) vector DNA backbones, and (iv) sgRNA oligonucleotides at an optimal vector:insert molar ratio. Reactions were subjected to alternating digestion–ligation thermal cycles according to the protocol of Cermák et al. (2017).

Following Golden Gate assembly, each construct was validated using a two-step protocol. First, colony PCR was performed with a high-fidelity DNA polymerase (Phusion High-Fidelity DNA Polymerase) to amplify the vector region containing the two sgRNAs, using flanking universal primers. Amplification products were analyzed by electrophoresis on a 1% agarose gel in TAE buffer, and positive clones were confirmed by the presence of bands at the expected size (approximately 500–600 bp for the dual-sgRNA cassette).

Second, sequence integrity was confirmed by Sanger sequencing of the sgRNA inserts in the assembled plasmids, verifying (i) the correct sequence of both sgRNAs, (ii) the absence of mutations introduced during synthesis, and (iii) the absence of rearrangements or deletions. Only those constructs demonstrating the correct insert size by PCR and intact sequence by Sanger were selected for subsequent plant transformation procedures.

2.3 Bacterial transformation and construct verification

The assembled vectors were amplified in chemically competent *Escherichia coli* strain TOP10 cells by heat-shock transformation. Competent cells were prepared using the standard calcium chloride protocol optimized for high-efficiency transformation (Thermo Fisher Scientific, 2016; Zymoresearch, 2019). For transformation, 50 µL aliquots of TOP10 cells were mixed with approximately 50 ng of assembled plasmid DNA and kept on ice for 30 minutes. The cells were then subjected to a heat-shock pulse at 42 °C for 45 seconds, followed

immediately by incubation on ice for 2 minutes . Subsequently, 900 µL of SOC medium were added, and the cells were allowed to recover at 37 °C for 1 hour with gentle shaking (Thermo Fisher Scientific, 2016; Reclone Latin America Hub, 2025).

Sequencing-confirmed pDIRECT_22C plasmids were transferred into *Agrobacterium tumefaciens* strain LBA4404 by electroporation, following standardized protocols for this species (Mersereau et al., 1990). Electrocompetent cells (approximately 50 µL per reaction) were mixed with ~1 µg of the confirmed recombinant plasmid in prechilled 0.2 cm gap electroporation cuvettes. A single high-voltage pulse was applied (2.2 kV, 25 µF capacitance, 200 Ω external resistance), immediately followed by addition of 1 mL of SOC medium at room temperature (~25 °C). Cells were recovered at 28 °C for 3–4 hours with gentle shaking.

After recovery, cells were plated on Luria–Bertani (LB) agar supplemented with three selective antibiotics: (i) kanamycin (50 µg·mL^{-1}) to select cells harboring the binary plasmid; (ii) streptomycin (100 µg·mL^{-1}) to eliminate unwanted *Agrobacterium*; and (iii) rifampicin (20 µg·mL^{-1}) to eliminate contaminating bacteria. Plates were incubated at 28 °C for 2–3 days. The resulting *Agrobacterium* colonies were validated by colony PCR using insert-specific primers (TC320 and M13), confirming the presence of the recombinant binary plasmid prior to its use in plant transformation procedures.

2.4 Bacterial Growth

An initial culture of *Agrobacterium tumefaciens* strain LBA4404 was prepared by transferring a single bacterial colony into 5 mL of Luria–Bertani (LB) medium supplemented with three selective antibiotics: (i) kanamycin (50 µg·mL^{-1}), (ii) streptomycin (100 µg·mL^{-1}), and (iii) rifampicin (20 µg·mL^{-1}). The starter culture was incubated at 28 °C for 2 days with gentle shaking to allow exponential growth of plasmid-bearing bacterial cells.

After the 2-day starter culture period, 200 µL of the concentrated culture were transferred into 50 mL of liquid LB medium with the same antibiotic composition (approximate 1:250 dilution). The expanded culture was incubated at 28 °C for overnight with constant shaking (150 rpm) until reaching the logarithmic growth phase. At this stage, cell density and the expression of *Agrobacterium* virulence genes are optimal for the transformation of plant explants, thereby maximizing the efficiency of T-DNA transfer.

2.5 Plant Material

Tomato seeds (*Solanum lycopersicum* cv. Micro-Tom) were obtained from mother plants grown under controlled greenhouse conditions (temperature 18–25 °C; photoperiod 12 h light). Seeds were extracted at full ripeness (physiological maturity) by controlled natural fermentation: fruit pulp was placed into sterile plastic bags and fermented for 48 h at room temperature (22–25 °C), a procedure that facilitates natural separation of the seed from the mucilaginous seed coat (Chaves et al., 2022).

Following fermentation, seeds were subjected to a washing and disinfection protocol: (i) five rinse cycles with sterile distilled water under gentle agitation to completely remove residual pulp and adherent mucilage; (ii) drying at room temperature on sterile filter paper for 24–48 h until minimal residual moisture was reached; and (iii) storage in an airtight tube at 4 °C until use. This protocol ensures high germination viability and minimal microbial contamination for subsequent germination procedures and regeneration of transformed plants (Kehinde et al., 2022; Ray & Bordolui, 2022).

2.6 Transformation

Genetic transformation of tomato (*Solanum lycopersicum* cv. Micro-Tom) was performed using the cotyledonary leaf explant method, adapted from protocols previously validated for this cultivar (Arias-González & Uribe, 2025).

Seeds were subjected to a dormancy-breaking and surface-sterilization protocol. Initially, seeds were incubated in 1% (v/v) hydrogen peroxide in complete darkness under constant agitation (100 rpm) for 4 days at 26 °C, a treatment that facilitates germination and provides preliminary disinfection (Chu et al., 2022). Subsequently, chemical sterilization consisted of: (i) immersion in 70% ethanol for 2 minutes for surface disinfection; (ii) five sequential rinses with sterile distilled water to remove ethanol residues; (iii) immersion in 0.5% (v/v) sodium hypochlorite supplemented with 0.02% Tween-20 for 5 minutes with continuous agitation to achieve thorough disinfection; and (iv) five final rinses with sterile distilled water under aseptic conditions to remove excess hypochlorite (Gilbert et al., 2023).

Surface-sterilized seeds of tomato (*Solanum lycopersicum* cv. Micro-Tom) were sown on half-strength MS germination medium supplemented with Gamborg B5 vitamins, sucrose (15 $g \cdot L^{-1}$), and agar (6 $g \cdot L^{-1}$), with the pH adjusted to 5.8. Seeds were grown in a controlled-

environment growth chamber at 25 ± 1 °C under a 16 h light/8 h dark photoperiod. After 4 days of culture—when cotyledons were fully expanded and prior to emergence of the first true leaf—cotyledon explants were prepared by excising fragments of approximately 0.5–1.0 cm² and making a slight distal incision along the margin to facilitate bacterial penetration (figure 19).

Figure 19 - Schematic representation of cuts made in the cotyledons of the *Solanum lycopersicum* cultivar.

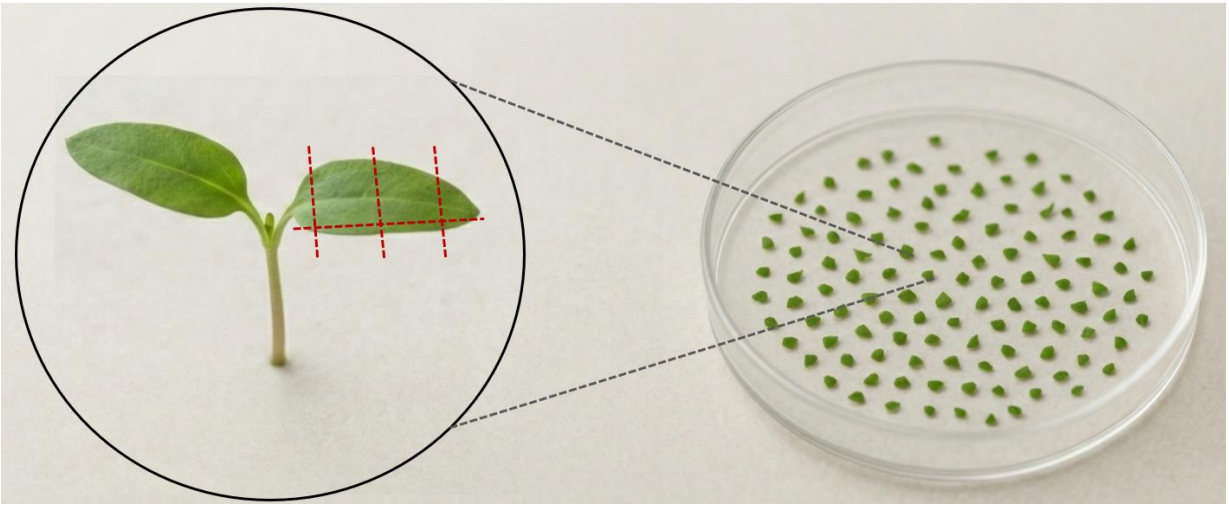

Source: Author (2025).

In parallel, a liquid culture of *Agrobacterium tumefaciens* strain LBA4404 carrying the pDIRECT_22C construct was prepared. The bacterial culture was grown in LB medium to an optical density at 600 nm (OD_{600}) of ~0.5. Cells were harvested by centrifugation (2,000 × g for 15 min) and resuspended in inoculation medium (half-strength liquid MS supplemented with B5 vitamins) containing acetosyringone (100 µM), adjusting the suspension to an OD_{600} of 0.2–0.3. Cotyledon explants were immersed in the bacterial suspension for approximately 10 min with gentle agitation, ensuring complete contact between *Agrobacterium* and the freshly wounded edges.

2.7 Co-cultivation with Agrobacterium tumefaciens

Following inoculation, explants were briefly blotted on sterile filter paper to remove excess bacterial inoculum and placed on co-cultivation plates with the adaxial surface facing upward. The co-cultivation medium consisted of MS salts, Gamborg B5 vitamins, sucrose (30 $g \cdot L^{-1}$), agar (6 $g \cdot L^{-1}$), α-naphthaleneacetic acid (NAA, 0.4 µM), and acetosyringone (100 µM).

Explants were co-cultivated with *Agrobacterium* in complete darkness at 28 °C for 48 h, a period that permits T-DNA transfer from the bacterium to the plant genome without inducing premature differentiation.

2.8 Selection and regeneration

After co-cultivation, explants were transferred to selective regeneration medium (SIM) to eliminate non-transformed cells. The SIM contained MS salts, Gamborg B5 vitamins, sucrose (30 $g \cdot L^{-1}$), agar (6 $g \cdot L^{-1}$), the cytokinin 6-benzylaminopurine (BAP, 5 μM), kanamycin (100 $mg \cdot L^{-1}$) as the selective agent for transformed tissues, and timentin (25 $mg \cdot L^{-1}$) as a bacteriostatic antibiotic to suppress residual *Agrobacterium*. Explants were incubated at 25 °C under a 16 h light/8 h dark photoperiod.

At 2–3 weeks post-infection, organogenic calli bearing green adventitious shoots were observed at the explant margins, indicating successful transformation and regeneration. Non-transformed tissues were progressively eliminated through kanamycin-induced necrosis. Developing shoots were subcultured every 2 weeks onto fresh SIM while maintaining kanamycin selection (100 $mg \cdot L^{-1}$) to ensure retention of the genetic transformation. This iterative cycle enabled the recovery of multiple independent transgenic shoots per initial explant.

2.9 Rooting and acclimatization

Well-developed shoots (2–3 cm in height) were excised from the callus tissue and transferred jars containing rooting medium consisting of MS salts, Gamborg B5 vitamins, sucrose (30 $g \cdot L^{-1}$), agar (6 $g \cdot L^{-1}$), α-naphthaleneacetic acid (NAA, 0.4 μM), and kanamycin (50 $mg \cdot L^{-1}$). Under these conditions, shoots produced adventitious roots within approximately 2 weeks. Plantlets were maintained until they developed 3–5 fully expanded true leaves, at which point gradual acclimatization was initiated.

The acclimatization procedure comprised: (i) removal of plantlets from the agar medium and gentle rinsing of roots to eliminate residue; (ii) transfer to pots containing sterile substrate (soil:commercial substrate, 1:2, v/v); (iii) initial coverage with transparent plastic to maintain high relative humidity; and (iv) growth in a controlled-environment chamber (phytotron) at 26 ± 1 °C under a 16 h light. After approximately 1 week, the plastic cover was removed

progressively to gradually lower relative humidity. Acclimated plants were grown to maturity for subsequent phenotypic and molecular analyses to verify transformation.

3 RESULTS AND DISCUSSION

3.1 Co-cultivation Design and construction of CRISPR-Cas9 vectors

The design of ten RNA guides (two per target gene) using the CHOPCHOP bioinformatic tool resulted in the identification of optimal exonic regions for the five initially selected candidate genes. The design strategy targeted early exons within the coding region, an approach that maximizes the likelihood of generating loss-of-function mutations via critical frameshift deletions early in the protein sequence. The tool simultaneously optimized two critical parameters—the cleavage efficiency of the Cas9–sgRNA complex and specificity via off-target prediction—thereby ensuring a high probability of specific gene editing without undesired mutations at other loci (Labun et al., 2019).

Subsequently, manual oligonucleotide design was undertaken for modular assembly via Golden Gate, following the 3A protocol described by Čermák et al. (2017). The oligonucleotides were deliberately designed to exclude the protospacer adjacent motif (PAM), ensuring compatibility with the type IIS Golden Gate cloning scheme. An independent design was generated for each target gene, totaling five vector constructs intended to contain the combinations of gene-specific sgRNAs.

Laboratory modular assembly by Golden Gate, yielded three successful constructs out of the five initially planned (60% success rate). The constructs validated by colony PCR and Sanger sequencing corresponded to: (i) the ARF1 construct targeting Solyc11g069500; (ii) the ARF2 construct targeting Solyc09g007810; and (iii) the SPL construct targeting Solyc10g018780 (figure 20, 21 and 22). The two constructs that were not validated were excluded from subsequent transformation procedures, limiting downstream efforts to the three confirmed constructs.

Figure 20 - Sanger sequencing results aligned against a pDIRECT-22c vector carrying custom guide RNAs for the mate genes. Solyc11g069500, guide 1: TTTATAGAGGTACTCCCAGG; guide 2: CTTCAGTGAATGCTGCAATG

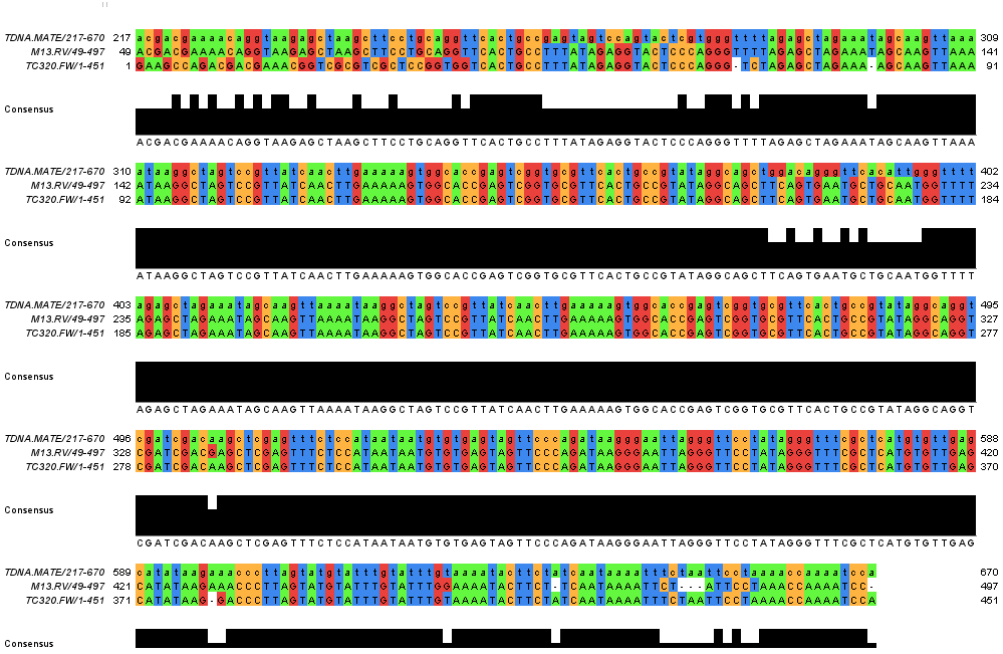

Source: Author (2025).

Figure 21 - Sanger sequencing results aligned against a pDirect-22c vector carrying custom guide RNAs for the mate genes. Solyc09g007810, guide 1: TTAATCGCGGAGACTTTACA; guide 2: AAACTGGAAAACCCTCCGTA

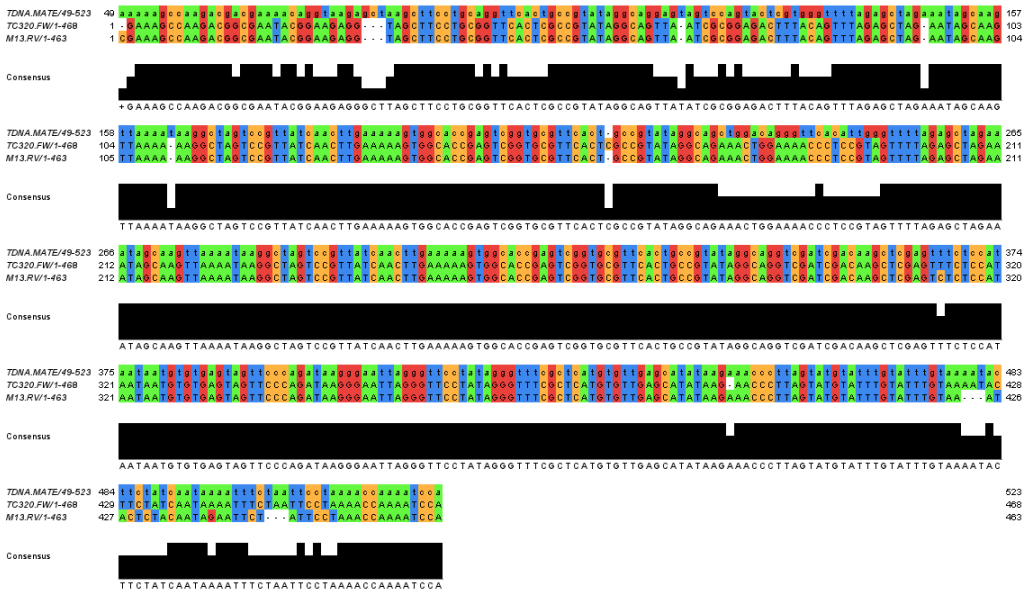

Source: Author (2025).

Figure 22 - Sanger sequencing results aligned against a pDIRECT-22C vector carrying custom guide RNAs for the mate genes. Solyc10g018780, guide 1: ACTCCTAGATGTCAAGCTGA; guide 2: CAATGAGCTCCTGAATCAGC

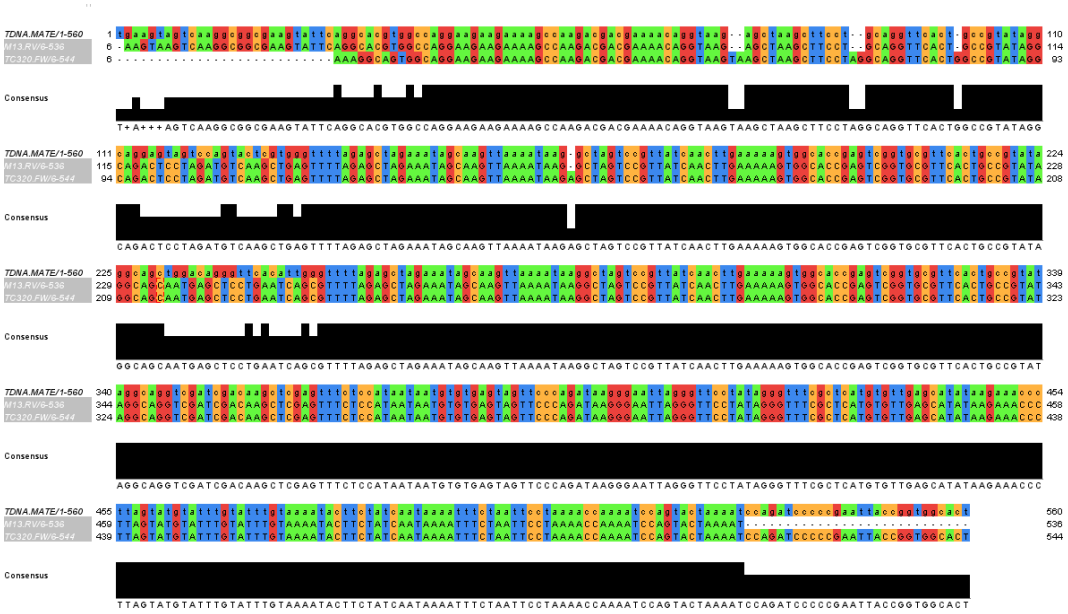

Source: Author (2025).

3.2 Tomato genetic transformation

Fifteen independent *Agrobacterium tumefaciens*–mediated genetic transformation runs were conducted on consecutive dates beginning in July of the current year (2025). Each run used cotyledonary explants from surface-sterilized seedlings of *Solanum lycopersicum* cv. Micro-Tom, following a standardized protocol to ensure surface sterility and tissue viability. The attempts were simultaneous across the three validated vector constructs, totaling 15 runs per vector.

Despite appropriate methodological execution, only two of the fifteen runs showed unambiguous regeneration of meristematic structures after selection on kanamycin-containing medium. This 13.3% success rate for recovering whole plants is consistent with the documented constraints of tomato genetic transformation, particularly when employing genome-editing systems that increase the physiological demands on explants. Accordingly, the results underscore the need to continue optimizing parameters within the regeneration and selection system—including medium formulation, kanamycin concentration, and co-cultivation conditions—to improve efficiency in future experiments (Long et al., 2022; Bennur et al., 2025).

3.3 Optimization of regeneration medium

In the first thirteen transformation runs, a shoot induction medium (SIM) supplemented with 6-benzylaminopurine (BAP, 5 μM), a commonly used synthetic cytokinin in tomato regeneration protocols, was employed. Although explants survived under selection pressure—with formation of green calli potentially competent for organogenesis—no differentiation or regeneration of adventitious shoots was detected. In parallel, control assays using explants not infected with *Agrobacterium* on the same selective medium (MS + BAP 5 μM + kanamycin 100 $mg \cdot L^{-1}$) exhibited efficient regeneration and the formation of acclimatized mature plants, suggesting that *Agrobacterium* infection during co-cultivation may induce physiological alterations in explants that interfere with the normal organogenic response to BAP, even after successful T-DNA delivery.

To overcome this impediment, a differential strategy was implemented in the final two runs: after an initial four-week selection phase on SIM + BAP 5 μM, surviving explants were transferred to a reformulated regeneration medium containing zeatin (a natural cytokinin), while maintaining kanamycin selection pressure. This adjustment—also motivated by reagent availability in the laboratory—yielded a robust regenerative response, evidenced by visible green adventitious shoot formation after two weeks of culture on zeatin medium. These results indicate that substituting BAP with zeatin can reverse Agrobacterium co-cultivation–associated organogenic blocks and optimize regeneration efficiency in tomato genetic transformation protocols.

3.4 Current status of regeneration events

In the two final transformation runs that exhibited successful regeneration, progressive formation of organized meristematic structures was observed. At present, approximately twenty explants in total across both runs display early to intermediate stages of regeneration and remain under subculture after roughly two months of periodic transfers on zeatin-supplemented medium. These explants show the emergence of foliar primordia and incipient elongation of adventitious shoots, indicating effective advancement toward more developed phases of organogenesis.

The temporal progression of these events has involved a substantial delay relative to the planned experimental timeline, keeping the project in an active (“ongoing”) phase (figure 23).

Although fully regenerated, rooted, and acclimatized plants have not yet been obtained, the demonstration of regenerative competence in the explants constitutes a meaningful methodological milestone. This outcome validates the feasibility of the transformation system employed and provides a well-founded basis to project the recovery of edited plants during subsequent differentiation and rooting stages, as the established protocols continue toward complete regeneration.

Figure 23 - Current status of explants undergoing regeneration from constructs targeting the genes Solyc09g007810, Solyc10g018780 and Solyc11g069500

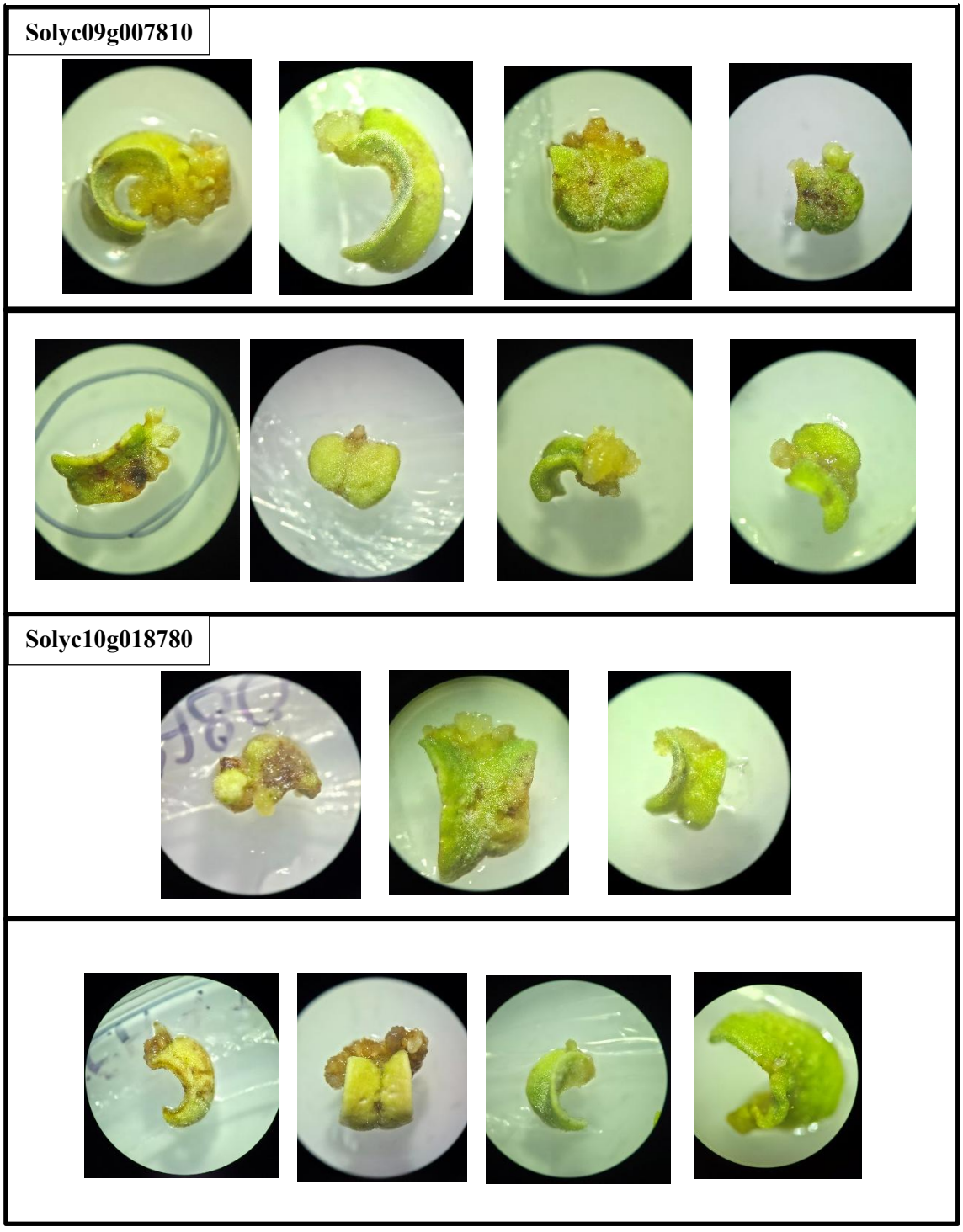

Solyc11g069500

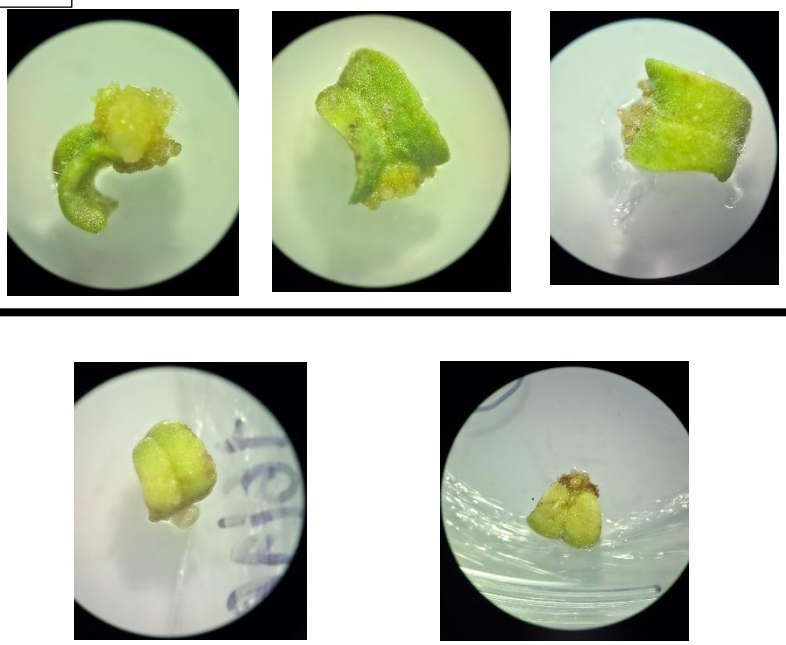

4 CONCLUSIONS

The results demonstrate substantial advances and inherent challenges in the genomic transformation of tomato via Agrobacterium-mediated CRISPR–Cas9. The efficiency of the modular Golden Gate assembly (60%) is considered satisfactory in view of the technical complexity, and the validation of three vectors provides a robust foundation for transformation. However, the overall transformation efficiency (13.3%) reveals physiological limitations, particularly at the level of explant regeneration, which are attributed to Agrobacterium-induced stress and adverse hormonal responses, in agreement with previous reports.

The replacement of BAP with zeatin in the regeneration medium proved critical for restoring organogenesis, consistent with literature supporting the use of natural cytokinins under stress conditions.

REFERENCES

ADDGENE. (2016). **Plasmids 101: CcdB - The toxic key to efficient cloning.** Blog post retrieved from https://blog.addgene.org/plasmids-101-ccdb

ADDGENE. (2023). **pDIRECT_22C (Plasmid #91135).** Retrieved from https://www.addgene.org/91135/

AHMAD, M., AKHTAR, K., SRIVASTAVA, S., HUSNAIN, T., KHAN, M. A., & ALI, Q. (2023). **Plant breeding advancements with "CRISPR-Cas" genome editing.** Frontiers in Plant Science, 14, 1133036.https://doi.org/10.3389/fpls.2023.1133036

ÁLVAREZ-RUIZ, M. J., & AGÜERO, J. L. (2018). **DNA-free genome editing of Brassica oleracea and B. rapa protoplasts using CRISPR-Cas9 ribonucleoprotein complexes.** Frontiers in Plant Science, 9, 1639.https://doi.org/10.3389/fpls.2018.01639

ARIAS-GONZÁLEZ, D., & URIBE, F. (2025). **Agrobacterium tumefaciens-mediated stable cotyledon transformation of Solanum lycopersicum var. Micro-Tom.** In Methods in Molecular Biology (Vol. 2911, pp. 107–119). Springer.https://doi.org/10.1007/978-1-0716-4450-8_11

ARORA, N., SAIRAM, M., SRIVASTAVA, S., DATTA, D., & PENTAL, D. (2021). **CRISPR/Cas9-mediated generation of pathogen-resistant tomato lines.** Plant Biotechnology Journal, 19(3), 456–468.https://doi.org/10.1111/pbi.13619

BENNUR, P. L., KISHORE, V. K., MALLAPPA, C. H., PRAJAPATI, R., MURALI, P., THIRUPATHAIAH, T., & RATHOD, V. (2025). **Improving transformation and regeneration efficiency in medicinal plants.** Frontiers in Plant Science, 16, 1442587.https://doi.org/10.3389/fpls.2025.1442587

CEIC DATA. (2023). **Brazil agricultural production: Average yield: Tomatoes**. Retrieved from https://www.ceicdata.com/en/brazil/agricultural-yield-temporary-crops/agricultural-production-average-yield-tomatoes

ČERMÁK, T., CURTIN, S. J., GIL, G. F., CEGAN, R., KONDA, A. R., LIU, G. E., EDENBERG, H. J., WEEKS, O., HOFFMAN, G. E., LIMSBURG, K. E., MISRA, V., SCHROEDER, J., ROTH, B., MAYER, J., MANK, M., STELSON, M., HULTQUIST, J. F., ROUX, S. J., & SUMMERER, D. (2017). **A multipurpose toolkit to enable advanced genome engineering in plants.** Plant Cell, 29(6), 1196–1217.https://doi.org/10.1105/tpc.17.00232

CHAVES, D. C., VALE, L. S. R., PEREIRA FILHO, W. J., DE LIMA, A. P. A., & BARBOSA, T. G. (2022). **Tomato seed quality under physiological fruit maturity stages and seed fermentation periods.** Research, Society and Development, 11(3), e18811325703.https://doi.org/10.33448/rsd-v11i3.25703

CHENG, W., REN, Y., LIU, B., JIANG, H., TAO, L., WU, K., WANG, H., SHEN, G., ZHANG, C., FU, X., & YE, Y. (2024). **Mutation of GLR2 confers enhanced glufosinate resistance and salt tolerance in rice.** Plant Physiology, 197(1), kiae588.https://doi.org/10.1093/plphys/kiae588

CHIASSON, D., LIMONTA, J., & MAK, E. (2019). **A unified multi-kingdom Golden Gate cloning platform.** Nature Ecology & Evolution, 3, 1375.https://doi.org/10.1038/s41559-019-0922-2

CHU, C., POORE, R. C., BOLTON, M. D., & FUGATE, K. K. (2022). **Mechanism of sugarbeet seed germination enhanced by hydrogen peroxide.** Frontiers in Plant Science, 13, 888519.https://doi.org/10.3389/fpls.2022.888519

DAVOUDPOUR, Y., MANSCHNECK, H., TSUGAWA, H., & MERKT, N. (2020). **High resolution microscopy to evaluate the efficiency of wheat seed disinfection methods.** PLoS ONE, 15(11), e0242549.https://doi.org/10.1371/journal.pone.0242549

DE PAIVA NUNES, M. C., CIANCIARUSO, M. V., & CUENCA, M. A. (2024). **Efficient regeneration of protoplasts from Solanum lycopersicum cultivar Micro-Tom.** Biological Methods & Protocols, 9(1), bpae008.https://doi.org/10.1093/biomethods/bpae008

DU, M., SUN, C., DENG, L., ZHOU, M., LI, J., DU, Y., YE, Z., HUANG, S., LI, T., YU, J., LI, C., & LI, C. (2025). **Molecular breeding of tomato: Advances and challenges.** Journal of Integrative Plant Biology, 67(3), 669–721.

DULAM, S., JOGAM, P., DONDA, N., GADEKALLU, T. R., & PARAMKUSAM, B. (2022). **Highly efficient Agrobacterium-mediated transformation and plant regeneration system for genome engineering in tomato.** Saudi Journal of Biological Sciences, 29(6), 103292.https://doi.org/10.1016/j.sjbs.2022.103292

FENG, Y., ZHANG, X., LIU, Z., & WANG, Y. (2023). **CRISPR/Cas9-mediated modification of fruit organoleptic attributes in tomato.** Journal of Agricultural and Food Chemistry, 71(15), 5678–5690.

FRITSCH, J. (2021). **The tomato production and presentation. Tomato News Conference 2021.** Retrieved from https://www.tomatonews.com/maj/phototheque/photos/PDF/Jason%20Fritsch%20TNCONF2021.pdf

GARCÍA-LÓPEZ, A., CASTELLANOS-MORALES, G., & LÓPEZ-HERRERA, C. J. (2024). **CRISPR/Cas-mediated germplasm improvement and new strategies for crop protection.** Agronomy Research, 22(1), 1–15.https://doi.org/10.1007/s44297-023-00020-x

GILBERT, G. S., MCCUTCHEON, H., STEWART, S. A., PLAZAS-JIMÉNEZ, M. C., DAFOE, J., MOROSETTI, P., & WALLER, T. J. (2023). **Seed disinfestation practices to control seed-borne fungi and bacteria in home production of sprouts.** Microorganisms, 11(2), 351.https://doi.org/10.3390/microorganisms11020351

GORALOGIA, G. S., NESTER, E. W., COMAI, L., & GELVIN, S. B. (2025). **Engineering Agrobacterium for improved plant transformation.** Nature Biotechnology, 43(3), 412–428.https://doi.org/10.1038/s41587-024-02345-4

GU, C., MEEGAHAKUMBURA, M. K., YE, H., PANCHAL, B., SCHRADER, K. K., & KONOPACKI, E. (2024). **Effective seed sterilization methods require optimization for each crop and disinfectant combination.** Phytopathology, 114(7), 1632–1645.https://doi.org/10.1094/PHYTO-09-23-0317-R

HE, Y., & ZHAO, Y. (2020). **Technological breakthroughs in generating transgene-free and genetically stable CRISPR-edited plants.** Biotechnology, 1(1), 88-96.

HE, Y., & ZHAO, Y. (2020). **Technological breakthroughs in generating transgene-free and genetically stable CRISPR-edited plants.** Nature Biotechnology, 38(1), 30-37.https://doi.org/10.1038/s41587-019-0377-7

HNATUSZKO-KONKA, K., NALEPKA, K., GRZEGORCZYK-KAROLAK, I., & GORZEŃ-BIAŁUK, A. (2021). **Cytokinin signaling and de novo shoot organogenesis.** Genes, 12(2), 265.https://doi.org/10.3390/genes12020265

HUSSAIN, A., ALI, S., ALI, Z., & SIDDIQUI, M. H. (2021). **Herbicide resistance: Another hot agronomic trait for plant genome editing.** Plants, 10(3), 556.https://doi.org/10.3390/plants10030556

IBGE. (2025). **Prognóstico da colheita: Tomates. Instituto Brasileiro de Geografia e Estatística.**

INTERNATIONAL SEED TESTING ASSOCIATION. (2025). **International Rules for Seed Testing. ISTA**. Retrieved from https://www.seedtest.org/

KARCHI, H., ALBALADEJO, I., PESARESI, P., & GOZUKIRMIZI, N. (2022). **Tomato salt tolerance mechanisms and their potential applications for fighting salinity: A review.** Frontiers in Plant Science, 13, 949541.https://doi.org/10.3389/fpls.2022.949541

KAUR, N., QADIR, M., FRANCIS, D. V., ALOK, A., TIWARI, S., & AHMED, Z. F. R. (2025). **CRISPR/Cas9: A sustainable technology to enhance climate resilience in major staple crops.** Frontiers in Genome Editing, 7,1533197.https://doi.org/10.3389/fgeed.2025.1533197

KEHINDE, T. O., ADEBISI, M. A., LAWAL, I. O., SHITTU, M. M., & OKWI, E. E. (2022). Seed longevity characteristics of tomato (Solanum lycopersicum L.) genotypes stored with different packaging materials under ambient tropical humid conditions. Acta Agriculturae Slovenica, 118(1), 1–12.https://doi.org/10.14720/aas.2022.118.1.2444

KHUONG, T. T. H., VU, H. T., TRUONG, H. A., NGUYEN, H. T., TRAN, T. V., & NGO, T. D. (2013). **Optimisation of tomato Micro-tom regeneration and selection on glufosinate/Basta and dependency of gene silencing on transgene copy number.** Plant Cell, Tissue and Organ Culture, 112(3), 291–304.https://doi.org/10.1007/s11240-012-0226-6

KUMAR, A., SINGH, R., & PATEL, S. (2023). **Application of CRISPR/Cas9 genome editing in tomato improvement: Advances and applications.** Frontiers in Plant Science, 14, 1121209.https://doi.org/10.3389/fpls.2023.1121209

KURATA, M., WOLF, N. K., DERIANO, L., GARRETT, S. C., MURAY, J. B., & OSADA, T. (2018). **Highly multiplexed genome engineering using CRISPR/Cas9 gRNA arrays.** PLoS ONE, 13(9), e0198714.https://doi.org/10.1371/journal.pone.0198714

LABUN, K., MONTAGUE, T. G., KRAUSE, M., TORRES CLEUREN, Y. N., TJELDNES, H., & VALEN, E. (2019). CHOPCHOP v3: Expanding the CRISPR web toolbox beyond

genome editing. Nucleic Acids Research, 47(W1), W171–W177.https://doi.org/10.1093/nar/gkz381

LI, X., WANG, Y., CHEN, S., TIAN, H., FU, D., ZHU, B., LUO, Y., & ZHU, H. (2018). **Lycopene is enriched in tomato fruit by CRISPR/Cas9-mediated multiplex**

FINAL CONSIDERATIONS

This comprehensive investigation systematically addressed an important knowledge gap regarding the sensitivity of the Micro-Tom tomato to glufosinate, integrating rigorous experimental characterization, bioinformatic discovery of candidate genes, and validation of genetic transformation into a coherent research strategy that yields substantive scientific contributions both to the understanding of herbicide–plant interactions and to applied agricultural biotechnology.

The first experimental phase established that Micro-Tom exhibits absolute sensitivity to glufosinate at all evaluated concentrations, where even the lowest dose (0.5 $g \cdot L^{-1}$, equivalent to 25% of the recommended field rate) caused complete mortality 10 days after application, demonstrating the absence of a safe tolerance margin for unintentional exposure. The biphasic catalase response—characterized by rapid induction followed by depletion between 2 and 12 hours—revealed that glufosinate-induced oxidative stress substantially exceeds the antioxidant defensive capacity of this genotype, thereby providing a rational basis for the design of tolerance strategies via targeted gene editing. However, this initial phase leaves research gaps that require complementary investigation to strengthen the findings and support more robust claims. Specifically, the following are proposed: (i) analysis of a broader range of herbicide concentrations to fully characterize the dose–response curve; (ii) evaluation of synergistic or antagonistic effects resulting from mixtures of multiple herbicides that may enhance phytotoxicity; and (iii) quantification of additional physiological parameters, including photosynthetic indices and dynamic profiles of glutamine synthetase after application, which would allow more precise associations between enzymatic repression and the manifestation of visible symptoms.

The second phase identified, through integrated phylogenetic analysis, two promising ortholog candidates for gene editing: Solyc11g069500 (Sl-ARF10A, an ortholog of OsARF18) and Solyc10g018780 (Sl-SPL10b, an ortholog of OsSPL10). This identification is grounded in strong functional precedents from rice, where loss-of-function mutations in OsARF18 confer glufosinate resistance via derepression of glutamine synthetase genes (OsGS1;1, OsGS1;2), while mutations in analogous SPL genes regulate the expression of downstream detoxification genes through modulation of conserved regulatory networks. The candidates identified retain complete functional domain architecture, including B3 DNA-binding domains, repressive middle regions, and C-terminal dimerization domains, confirming their potential to participate in regulatory mechanisms analogous to those described in rice. As in the first phase, this

bioinformatic stage requires direct functional experimental validation to establish causality and to characterize the precise regulatory mechanisms in the specific context of Solanum lycopersicum. An integrated experimental approach is proposed comprising: (i) gene expression analysis by RT-qPCR quantifying candidate induction after glufosinate application under controlled conditions; (ii) CRISPR–Cas9-mediated gene editing to generate loss-of-function mutants in Micro-Tom genetic backgrounds; (iii) systematic phenotypic evaluation of mutant lines under controlled exposure to increasing glufosinate concentrations; (iv) chromatin immunoprecipitation (ChIP–qPCR) to validate direct interaction of candidate proteins with promoter regions of SlGS1 and SlGS2; and (v) differential expression profiling by RNA-seq in mutants versus controls to characterize the full gene network modulated by these regulators under herbicide stress. This multilateral experimental strategy will enable the establishment of causality through multiple complementary lines of evidence and the determination of precise transcriptomic regulatory mechanisms in tomato.

The third phase, focused on regeneration and genetic transformation, demonstrated that the successful continuation of regenerative events through the stages of terminal differentiation and rooting supports realistic projections for obtaining stable, fully edited genetic lines. These results advanced both the optimization of vector design and validation workflows and the characterization of regenerative physiology in tomato under Agrobacterium tumefaciens–mediated transformation, generating more robust and transferable methodologies for stable CRISPR–Cas9 editing in this crop. The demonstration of successful regenerative capacity constitutes a fundamental prerequisite for the future implementation of germline editing strategies, enabling the establishment of mutant populations that segregate the edited alleles heritably.

Collectively, these experimental and analytical components fill critical knowledge gaps and establish a strong rational basis for the development of glufosinate-tolerant tomato via targeted genome editing. CRISPR–Cas9 editing of endogenous orthologs represents an innovative crop improvement paradigm that aligns favorably with international regulatory frameworks, which classify non-transgenic edited plants less restrictively than classical transgenic events, particularly for fresh-market crops where public acceptance is critical. However, full realization of this research proposal requires future studies that functionally validate the identified candidates using multiple complementary approaches. Specifically, the following are proposed: (i) generation and phenotypic characterization of CRISPR loss-of-function mutants under controlled herbicide exposure; (ii) confirmation by ChIP of physical interactions between candidate proteins and glutamine synthetase gene promoter regions; (iii)

comprehensive gene expression profiling by RT-qPCR under herbicide stress conditions; (iv) regeneration and hereditary stabilization of edited lines; (v) comprehensive phenotypic evaluation including agronomically important traits; and (vi) field-level validation under practical cultivation conditions to establish definitive causality. The convergence of these lines of evidence will make it possible to deliver improved tomato varieties that combine glufosinate tolerance with superior agronomic traits, contributing both to fundamental scientific knowledge of transcriptomic regulation of herbicide tolerance and to the generation of applied biotechnological tools with potential impact on sustainable agricultural productivity.

.

REFERENCES

ARRUABARRENA, A., KYRIACOU, M. C., & FOTOPOULOS, V. (2025). **Agrobacterium-mediated transformation for gene editing in elite tomato breeding lines**. In *Plant Gene Editing: Methods and Protocols* (pp. 1–15). Humana Press. https://doi.org/10.1007/978-1-0716-3389-2

BERMAN, A., KUPERVASER, M., UNTERMAN, A., LEVIN, Y., & ITKIN, M. (2025). **Construction of multi-targeted CRISPR libraries in tomato for crop improvement**. *Nature Biotechnology*, *43*(5), 742–753. https://doi.org/10.1038/s41587-024-02414-7

CARVALHO-MOORE, P., DE ARAUJO, L., MENDES, K. F., & HALL, K. E. (2022). Unraveling the mechanism of resistance in a glufosinate-resistant Palmer amaranth (Amaranthus palmeri) accession. *Weed Science*, *70*(4), 458–467. https://doi.org/10.1017/wsc.2022.33

CHENG, W., XIA, Q., XU, Y., WANG, Y., & ZHANG, W. (2024). **Mutation of GLR2 confers enhanced glufosinate resistance in rice through interaction with GLR1/ARF18.** *Plant Physiology*, *196*(4), 2847–2862. https://doi.org/10.1093/plphys/kiae522

CONCATO, A. C., LOPES, N. P., MARQUES, L. C., & NASCIMENTO, M. M. (2022). **Enzymatic antioxidant defense system and ALA-D enzyme in corn plants after application of herbicides.** *Revista Brasileira de Herbicidas*, *21*(1), e210105. https://doi.org/10.7824/rbh.v21i1.210105

HNATUSZKO-KONKA, K., KOWALCZYK, T., & GERSZBERG, A. (2021). **Cytokinin signaling and de novo shoot organogenesis**. *International Journal of Molecular Sciences*, *22*(4), 1685. https://doi.org/10.3390/ijms22041685

LOWDER, L. G., ZHANG, D., BALTES, N. J., PAUL, J. W., TANG, X., ZHENG, X., VOYTAS, D. F., HSIEH, T. F., ZHANG, Y., & QI, Y. (2015). **A CRISPR/Cas9 toolbox for multiplexed plant genome editing and transcriptional regulation.** *Plant Physiology*, *169*(2), 971–985. https://doi.org/10.1104/pp.15.00636

MARILLONNET, S., & GRAU, J. (2020). **Synthetic DNA assembly using Golden Gate cloning and the hierarchical modular cloning pipeline.** *Current Protocols in Molecular Biology*, *130*(1), e115. https://doi.org/10.1002/cpmb.115

PARK, Y. W., KIM, J. H., & LEE, S. Y. (2020). **Temporal and spatial expression analysis of shoot-regeneration regulatory genes during adventitious shoot formation in hypocotyl and cotyledon explants of tomato (cv. Micro-Tom).** *Plants*, *9*(8), 1012. https://doi.org/10.3390/plants9081012

PIASECKI, C., CARVALHO, I. R., CECHIN, J., GOULART, F. A. P., MAIA, L. C., AGOSTINETTO, D., CAVERZAN, A., STEWART, C. N., & VARGAS, L. (2019). **Oxidative stress and differential antioxidant enzyme activity in glyphosate-resistant and -sensitive hairy fleabane in response to glyphosate treatment.** *Bragantia*, *78*(3), 379–396. https://doi.org/10.1590/1678-4499.20180281

REN, Y., WANG, Y., PAN, T., WANG, Y., WANG, Y., GAN, L., WEI, Z., WANG, F., WU, M., JING, R., WU, F., JIANG, L., & WAN, J. (2023). **Precision editing of GLR1 confers glufosinate resistance in rice.** *Journal of Genetics and Genomics*, *50*(9), 689–692. https://doi.org/10.1016/j.jgg.2023.05.011

SANDHYA, D., & JOGAM, P. (2022). **Highly efficient Agrobacterium-mediated transformation and plant regeneration system for genome engineering in tomato.** *Saudi Journal of Biological Sciences*, *29*(6), 103292. https://doi.org/10.1016/j.sjbs.2022.103292

ŠMERINGAI, J., VONDRÁKOVÁ, Z., & JŮZL, M. (2023). **Cytokinins—regulators of de novo shoot organogenesis.** *Frontiers in Plant Science*, *14*, 1239133. https://doi.org/10.3389/fpls.2023.1239133

TIWARI, J. K., DEVI, S., SHARMA, S., SINGH, B. P., & BUCKSETH, T. (2023). **CRISPR/Cas genome editing in tomato improvement: Advances and applications**. *Frontiers in Plant Science*, *14*, 1121209. https://doi.org/10.3389/fpls.2023.1121209

XIA, Q., CHENG, W., XU, Y., WANG, Y., & ZHANG, W. (2023). **Loss of OsARF18 confers glufosinate ammonium herbicide resistance and enhances abiotic stress tolerance in rice.** *Plant Biotechnology Journal*, *21*(11), 2289–2302. https://doi.org/10.1111/pbi.14123

APPENDICES

APPENDIX A – POSITIVE CONTROL REGENERATION

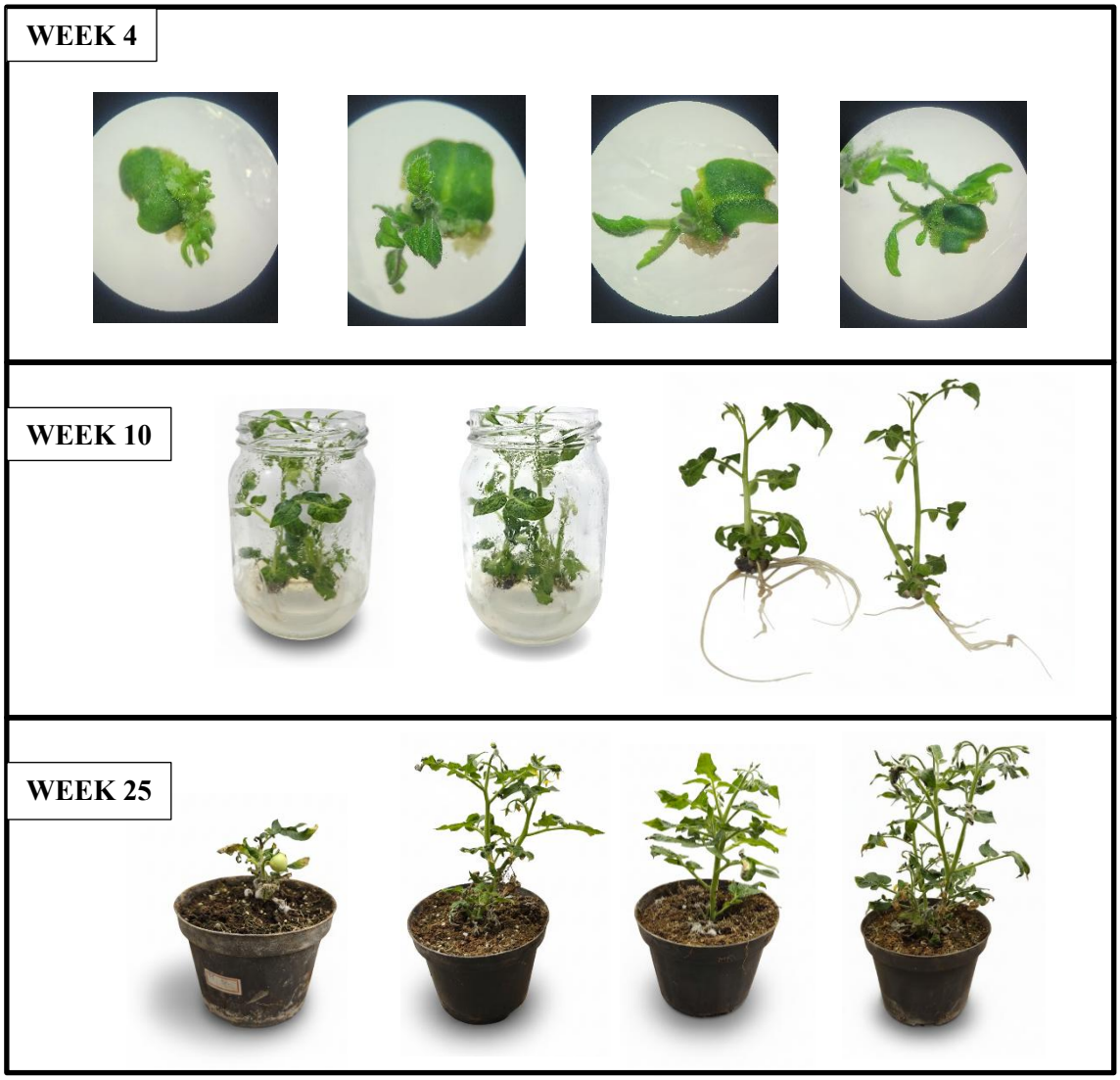

Source: Author (2025).

APPENDIX B – CONFIRMATIO GOLDEN GATE. THE TRANSFORMED VECTOR YIELDS A 576-BP FRAGMENT WITH THE PRIMERS TC320 AND M13F.

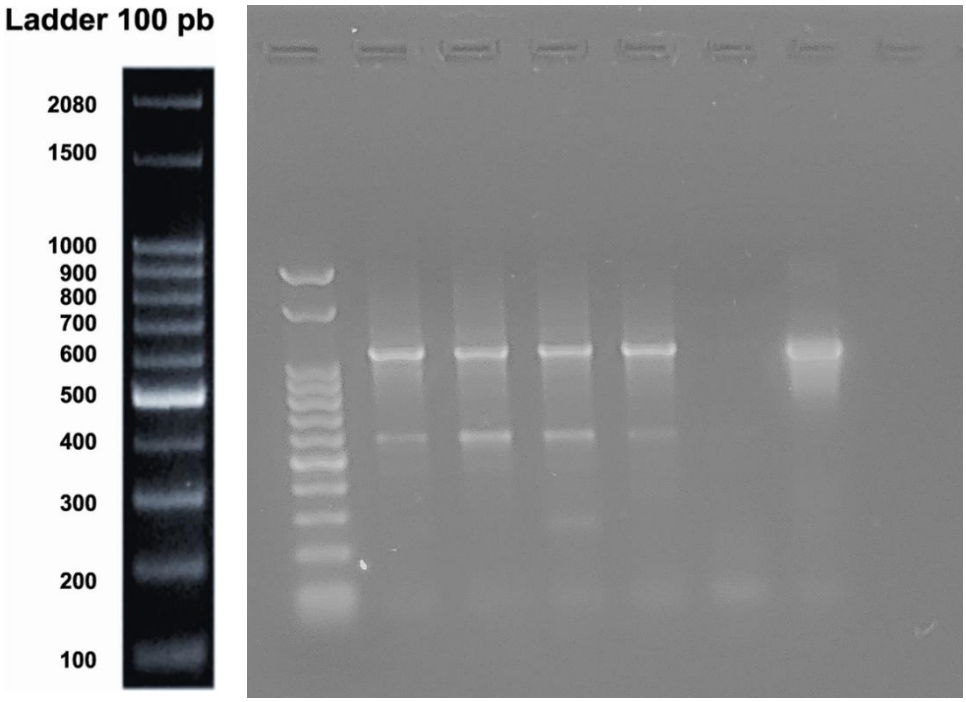

Source: Autor (2025).

APPENDIX C – METRICS ALPHAFOLD3

GS1- ARF - SITE 1

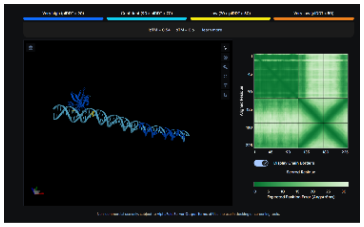

Solyc11g069500

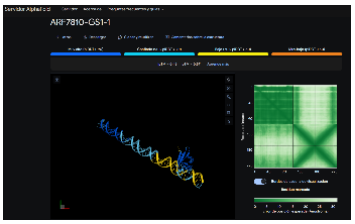

Solyc09g007810

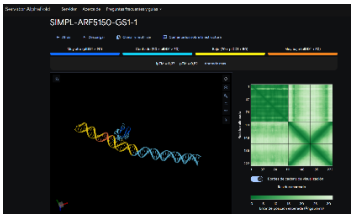

Solyc06g075150

GS1- ARF - SITE 2

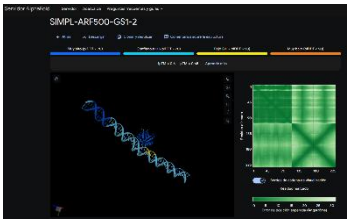

Solyc11g069500

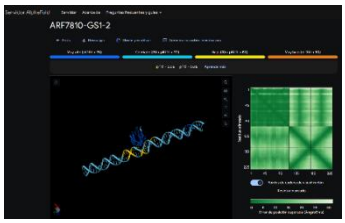

Solyc09g007810

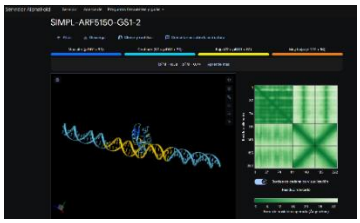

Solyc06g075150

GS1- ARF - SITE 3

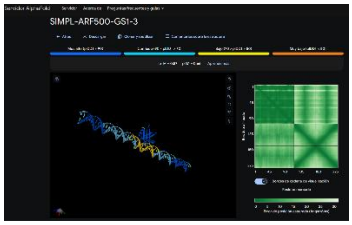

Solyc11g069500

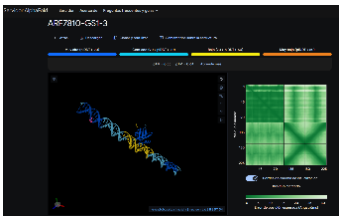

Solyc09g007810

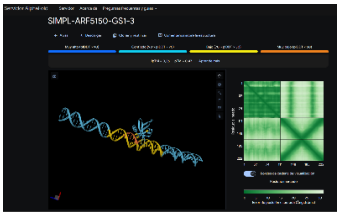

Solyc06g075150

GS1- ARF - SITE 4

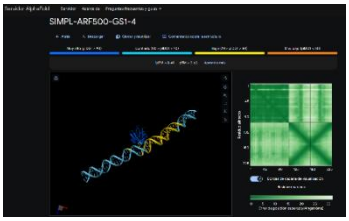

Solyc11g069500

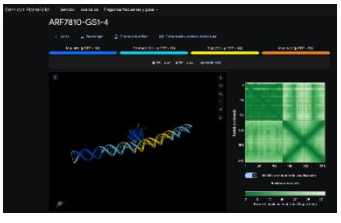

Solyc09g007810

Solyc06g075150

GS1- ARF - SITE 5

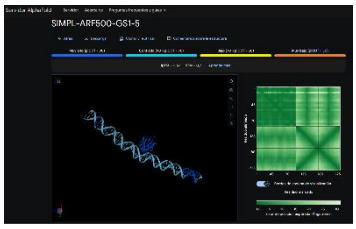

Solyc11g069500

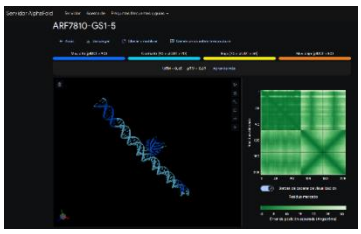

Solyc09g007810

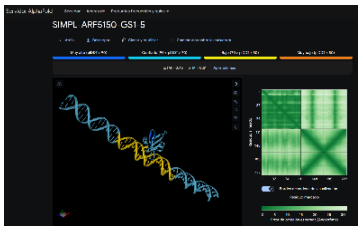

Solyc06g075150

GS1- ARF - SITE 6

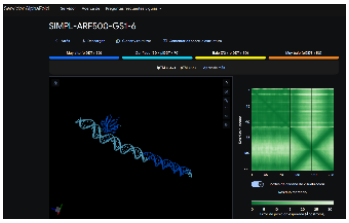

Solyc11g069500

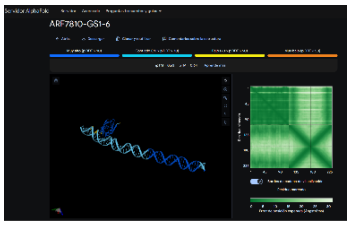

Solyc09g007810

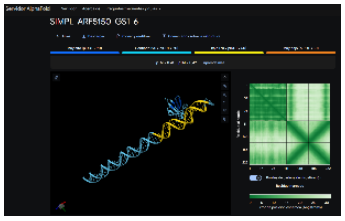

Solyc06g075150

GS1- ARF - SITE 7

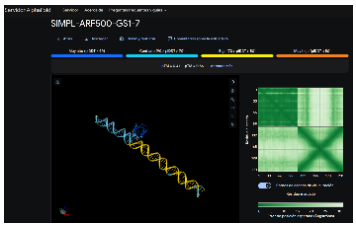

Solyc11g069500

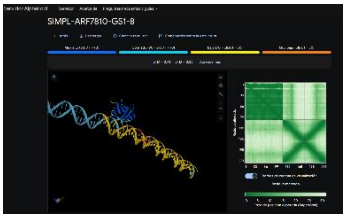

Solyc09g007810

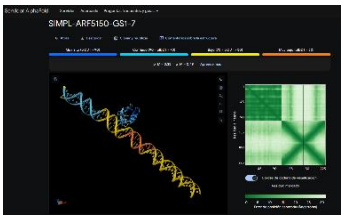

Solyc06g075150

GS1- ARF - SITE 8

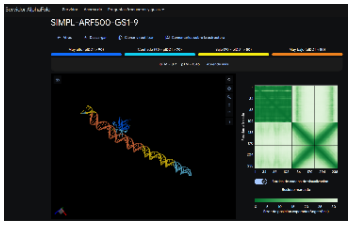

Solyc11g069500

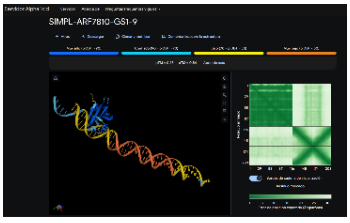

Solyc09g007810

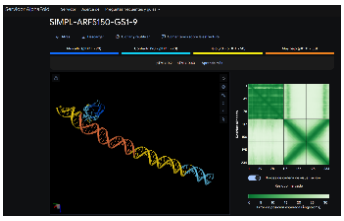

Solyc06g075150

GS1- ARF - CLUSTER

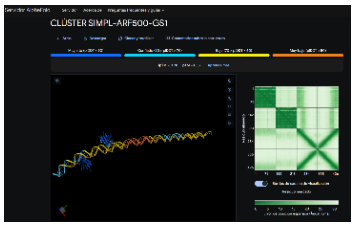

Solyc11g069500

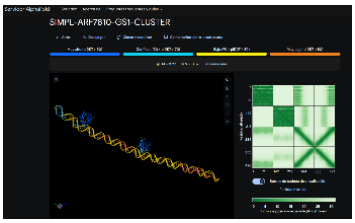

Solyc09g007810

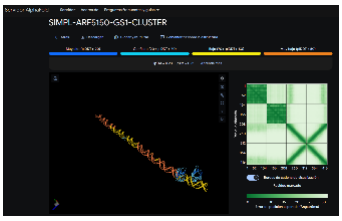

Solyc06g075150

GS1- SPL - SITE 1

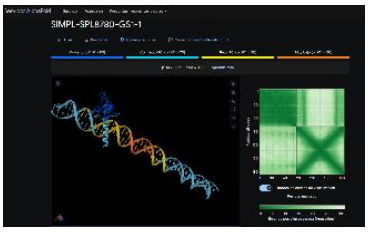

Solyc10g018780

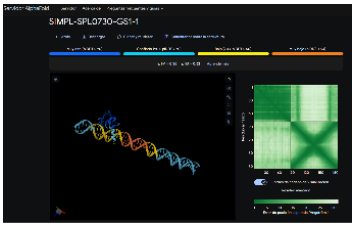

Solyc01g090730

GS1- SPL - CLUSTER

Solyc10g018780

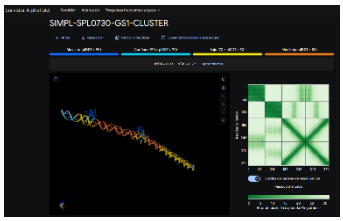

Solyc01g090730

GS2- ARF – SITE1

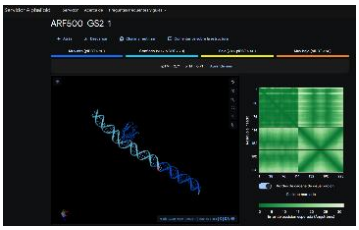

Solyc11g069500

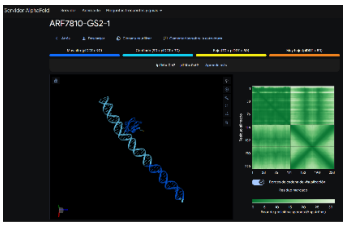

Solyc09g007810

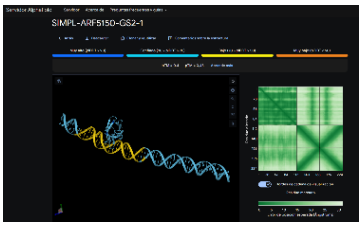

Solyc06g075150

GS2- ARF – SITE2

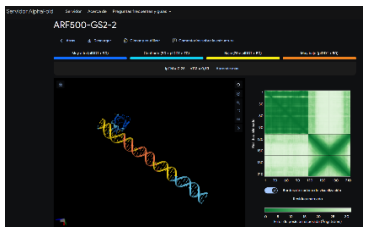

Solyc11g069500

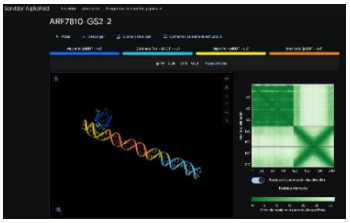

Solyc09g007810

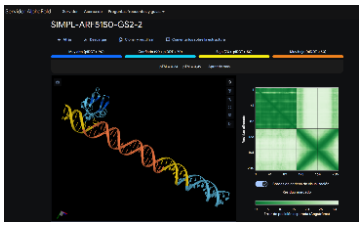

Solyc06g075150

GS2- ARF – SITE3

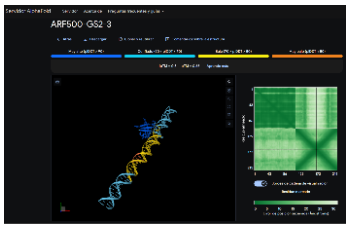

Solyc11g069500

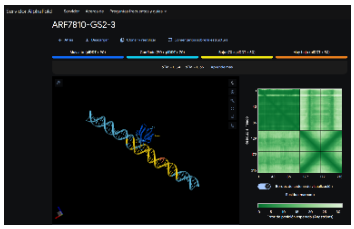

Solyc09g007810

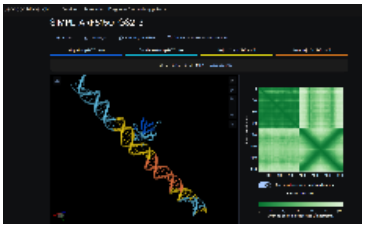

Solyc06g075150

GS2- ARF – SITE4

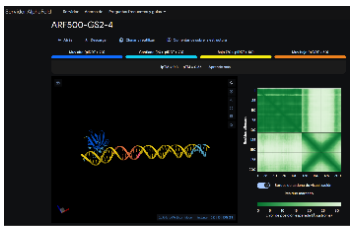

Solyc11g069500

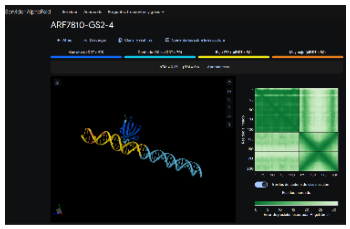

Solyc09g007810

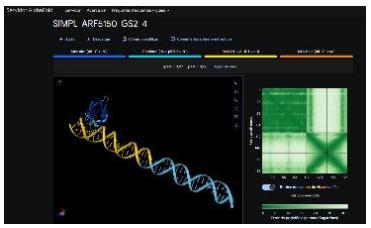

Solyc06g075150

GS2- ARF – SITE5

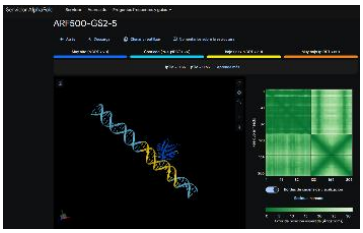

Solyc11g069500

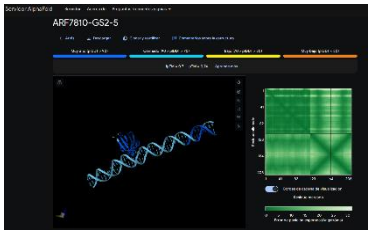

Solyc09g007810

Solyc06g075150

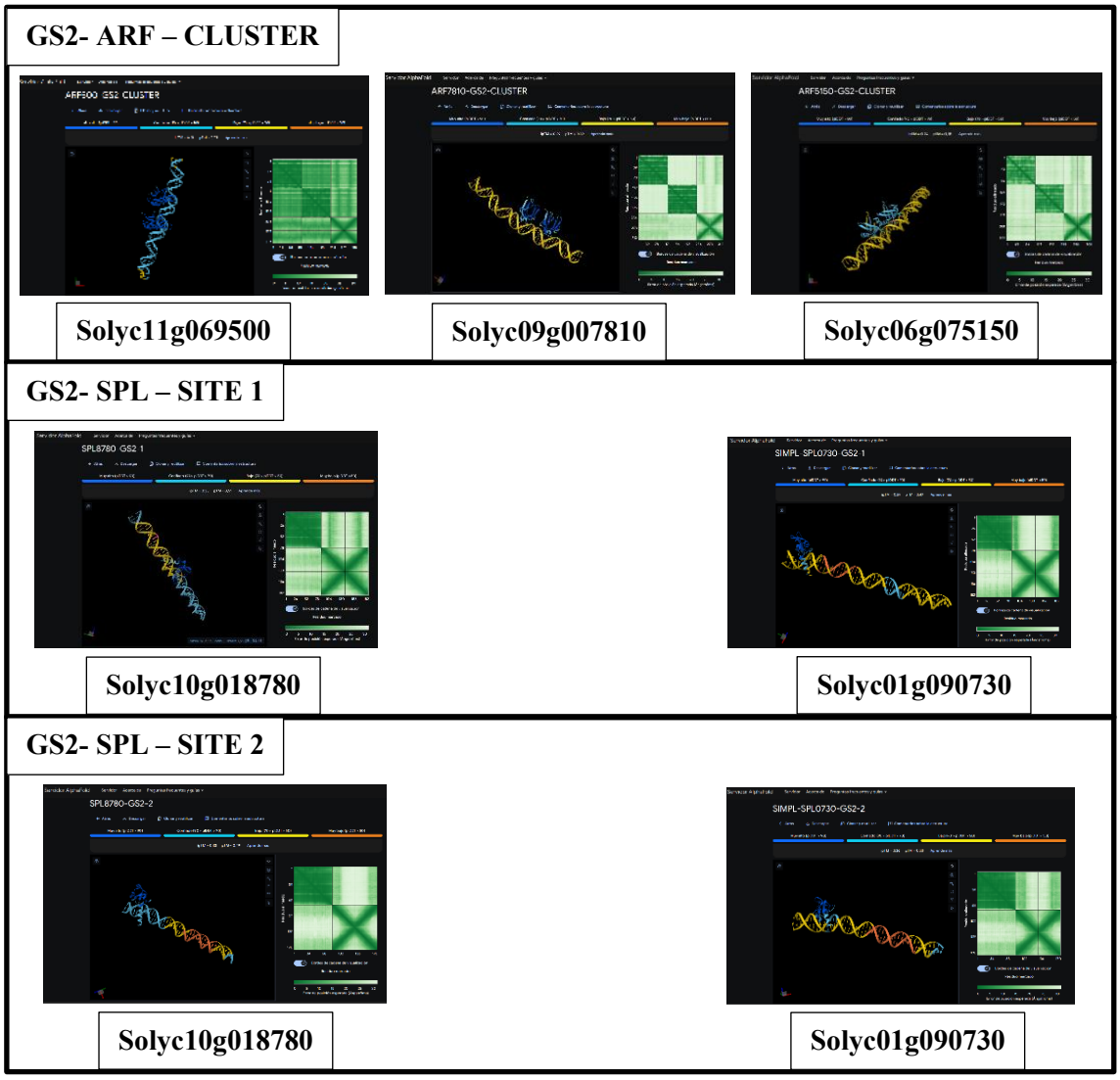

Source: Author (2025).

APPENDIX D – IDENTITY MATRIX SPL

```
Percent Identity  Matrix - created by Clustal2.1


  1: LOC_Os06g44860.1    100.00   39.21   46.91
  2: Solyc01g090730.3.1   39.21  100.00   74.60
  3: Solyc10g018780.3.1   46.91   74.60  100.00
```

Source: CLUSTAL OMEGA (2025).

APPENDIX E – IDENTITY MATRIX ARF

```
Percent Identity  Matrix - created by Clustal2.1


  1: Solyc11g013480.3.1   100.00   47.42   49.55   46.87   46.34   50.60
  2: Solyc10g086130.3.1    47.42  100.00   49.75   61.01   47.23   52.28
  3: LOC_Os06g47150.1      49.55   49.75  100.00   62.85   55.08   61.60
  4: Solyc09g007810.4.1    46.87   61.01   62.85  100.00   58.50   64.62
  5: |Solyc06g075150.3.1   46.34   47.23   55.08   58.50  100.00   68.51
  6: Solyc11g069500.2.1    50.60   52.28   61.60   64.62   68.51  100.00
```

Source: CLUSTAL OMEGA (2025).

APPENDIX F – OLIGO ARF GOLDEN GATE

oCmYLCV	TGCTCTTCGCGCTGGCAGACATACTGTCCCAC
CSY_g1_ Solyc11g069500	TCGTCTCCTACCTCTATAAACTGCCTATACGGCAGTGAAC
CSY_g1_Solyc06g075150	TCGTCTCCCTCTAAGGTGTTCTGCCTATACGGCAGT
CSY_g1_Solyc09g007810	TCGTCTCCCTCCGCGATTAACTGCCTATACGGCAGTGAAC
REP_g1_ Solyc11g069500	TCGTCTCAGGTACTCCCAGGGTTTTAGAGCTAGAAATAGC
REP_g1_Solyc06g075150	TCGTCTCAAGAGTTCACCGGGTTTTAGAGCTAGAAATAGC
REP_g1_Solyc09g007810	TCGTCTCAGGAGACTTTACAGTTTTAGAGCTAGAAATAGC
CSY_g2_ Solyc11g069500	TCGTCTCCCATTCACTGAAGCTGCCTATACGGCAGTGAAC
CSY_g2_Solyc06g075150	TCGTCTCCGTGTTTCCGGTCCTGCCTATACGGCAGTGAAC
CSY_g2_Solyc09g007810	TCGTCTCCGTTTTCCAGTTTCTGCCTATACGGCAGTGAAC
REP_g2_ Solyc11g069500	TCGTCTCAAATGCTGCAATGGTTTTAGAGCTAGAAATAGC
REP_g2_Solyc06g075150	TCGTCTCAACACAATCAGGGGTTTTAGAGCTAGAAATAGC
REP_g2_Solyc09g007810	TCGTCTCAAAACCCTCCGTAGTTTTAGAGCTAGAAATAGC
CSY_term	TGCTCTTCTGACCTGCCTATACGGCAGTGAAC

Source: Author (2025).

APPENDIX G – OLIGO SPL GOLDEN GATE

oCmYLCV	TGCTCTTCGCGCTGGCAGACATACTGTCCCAC
CSY_g1_Solyc10g018780	TCGTCTCCACATCTAGGAGTCTGCCTATACGGCAGTGAAC
CSY_g1_Solyc01g090730	TCGTCTCCTGGCGTTCCGTACTGCCTATACGGCAGTGAAC
REP_g1_Solyc10g018780	TCGTCTCAATGTCAAGCTGAGTTTTAGAGCTAGAAATAGC
REP_g1_Solyc01g090730	TCGTCTCAGCCATAAGCGCGGTTTTAGAGCTAGAAATAGC
CSY_g2_Solyc10g018780	TCGTCTCCAGGAGCTCATTGCTGCCTATACGGCAGTGAAC
CSY_g2_Solyc01g090730	TCGTCTCCAGTGCTTTGCATCTGCCTATACGGCAGTGAAC
REP_g2_Solyc10g018780	TCGTCTCATCCTGAATCAGCGTTTTAGAGCTAGAAATAGC
REP_g2_Solyc01g090730	TCGTCTCACACTACCACCGAGTTTTAGAGCTAGAAATAGC
CSY_term	TGCTCTTCTGACCTGCCTATACGGCAGTGAAC

Source: Author (2025).